A PROCESS INVESTIGATION OF THE BIOSOLUBILISATION OF LOW RANK COAL IN SLURRY SYSTEMS

Bilainu Obozokhai OBOIRIEN
BSc. Chemical Engineering (OAU, Ile-Ife, Nigeria)

Half dissertation submitted in fulfillment of the requirement for the degree of
MASTER OF SCIENCE IN ENGINEERING

Department of Chemical Engineering
University of Cape Town
Cape Town, South Africa.

March 2006

ABSTRACT

The coal biosolubilisation processes may be used to convert low rank coal to either a clean, cost-effective energy source or to value-added products. This can lead to increased utilisation of low rank coal. Low rank coal is currently under-utilised because of its low calorific value, high moisture and sulphur content.

Most research on coal biosolubilisation has centered on pre-treated coal. Little work is reported on native coal. Low yields of solubilised coal products are currently reported in the literature. This may be due to further degradation of the soluble products or to limitation of solubilisation step. These products have potential as starting materials for biotransformation to value-added products. However, to date, small volumes of solubilised coal products are available to assess their potential for further biotransformation owing to current biosolubilisation of low rank coal being widely carried out at a small scale in Petri dishes or Erlenmeyer flask of moderate volume.

This dissertation presents the results of the investigation of biosolubilisation of low rank coal in slurry systems using *Trichoderma atroviride*. Its main objectives were to investigate key operating variables influencing untreated low rank coal biosolubilisation and degradation of soluble products, and to study different reactor configurations for coal biosolubilisation. A factorial experiment was used to investigate particle size fraction and coal loading as key process variables. The highest degree of coal biosolubilisation obtained in the factorial experiment was at 5% (w/v) coal loading using particle size fractions of 600-850 μm. The fungal growth was inhibited at 10% (w/v) coal loading. Coal biosolubilisation was enhanced by increased availability of surface area achieved either by increased loading (up to the critical value) or reduced particle size. Decreasing the particle size fraction from 600-850 μm to 150-300 μm resulted in an increase in surface area with an associated increase in the degree of coal solubilisation of 4-fold.

An empirical relationship developed from the coal weight loss results of the factorial experiments showed that particle size fraction is the key-operating variable. Further statistical analysis, such as the F-test, showed that coal loading and particle size are significant at 99% confidence level. However the interaction between coal loading and particle size was not significant.

Particle size fraction and coal loading do not affect the amount of soluble phenolic production. The highest concentration of phenolic obtained in the factorial experiment was 97 mg l^{-1} and was present before the coal was added. This suggests that the growth medium was the major source of phenolics in the study. The change in pH was independent of the quantity of coal used and the pH change was not caused by coal solubilisation.

Biomass formed was estimated by mass balance approach based on off- gas analysis. The estimated biomass was used for the evaluation of process yield. Product yield was 0.087 g g^{-1} propionic acid and 0.007 g g^{-1} phenolic compounds. The performance of the coal solubilisation process was determined by comparing the maximum stoichiometric yield with experimental yield. The experimental process yield indicated that production of these value added products may not be economically feasible with the *Trichoderma atroviride* biological system investigated in this thesis. Potential exists to arrive at an improved biological system through associated microbial and biochemical studies.

Degradation of soluble products was investigated by measuring carbon dioxide production in a stirred tank bioreactor. Concentration of soluble organic products in cell-free extract and fungal biomass was also investigated. This study also demonstrated that enzymatic and fungal mediation of phenolic accumulation was not significant. No subsequent degradation of soluble phenolic product was observed, rather there was a low yield of multiple products. The rate of carbon dioxide production in the slurry bioreactor was was 0.05 mmole l^{-1} hr^{-1}which was 20-fold less than CPR value predicted from stoichiometry for complete mineralisation of phenolics to CO_2. The maximum phenolic concentration was 106 mg l^{-1} while the TOC concentration was 528 mg l^{-1} after 2 weeks of incubation. Direct comparison of the phenolic concentration and the TOC concentration further supports the low yield of phenolic compounds. Furthermore, an HPLC analysis of the resulting solution of coal biosolubilisation showed the presence of some organic acids. The organic acids identified were acetic acid and propionic acid. The concentration of these organic acids was 35 mg l^{-1} and 176 mg l^{-1} for acetic acid and propionic acid respectively. This further supports that other products were being formed.

Coal biosolubilisation was investigated in the stirred tank reactor, the fluidised bed and the fixed bed bioreactor. The advantages and shortcomings of each of these reactor configurations were assessed. Higher coal weight loss was observed in the stirred tank slurry bioreactor in comparison to the fluidised bed slurry bioreactor at 5% (w/v) coal loading and 600-850 μm coal fractions. This is postulated to be as a result of increased agitation and shear. Higher degree of aeration was required in the fluidised bed bioreactor than in the stirred tank bioreactor because aeration was also used for mixing. The analysis of supernatant from coal biosolubilisation in the packed bed bioreactor showed a maximum absorbance of 0.140 and dry weight of coal showed 0.5% coal weight loss. The low performance was attributed to the large coal particle size fraction (1.5-2 mm) used. Minimal damage to the fungal culture was observed. However, clogging of bed by fungi resulted in channelling or misdistribution that ultimately leads to poor and unpredictable internal mass transport. In addition reduction of bed porosity led to an increase in retention time.

In conclusion, the study has demonstrated that efficient coal biosolubilisation requires a good mass transfer environment, provided in the slurry bioreactor. Further, it is governed by surface area availability, defined by particle size and coal loading. A methodology has been provided to allow biomass estimation for study of process kinetics. However work to date with the *Trichoderma atroviride* biosystem and sub-bituminous coal supplied by SASOL illustrates inadequate accumulation of soluble products. Overcoming this is currently being studied from a microbial and biochemical perspective in associated research.

ACKNOWLEDGEMENTS

All praises and adoration are due to Almighty Allah for seeing me through this study. I thank Him for the strength, good health and courage that He bestowed on me; to Him belongs all praise.

My appreciation and gratitude goes to the following people and organisations:

Prof. Sue Harrison, for her assistance and guidance throughout the course of this project. The advice and assistance provided by Professor Hansford have been invaluable.

Members of the bioprocess research unit for the knowledge, skill and support shared throughout the course of this work; a good working and human relation were established.

The social and administrative support of members and staff of the chemical engineering department. It will be unfair not to acknowledge the friendship among students both within and outside the department.

To all my family members: my wife and my boy for their support and prayers. My parents, brothers and sisters and in-laws for their consistent support, morally and financially, May the Almighty continue to be your guide. Thank you.

To all my friends, especially members of the Nigerian Students Association for their encouragement and making my stay at all time a memorable one.

Finally, I wish to acknowledge the financial support from the Department of Chemical Engineering, UCT.

LIST OF FIGURES

LIST OF TABLES

NOMENCLATURE

Symbol	Description	Units
A	The inverse of the growth yield coefficient $1/Y_{O2}$	g O_2 g biomass^{-1}
B_i	Baffle width	mm
B	Yield coefficient for cell maintenance	g O_2 g biomass $^{-1}$ h^{-1}
C_i	Fractional volumetric concentration of particle species i	
C	Impeller clearance above the vessel base	mm
d	Density of lignite	g cm^3
D_p	Average particle diameter	cm
D_i	Dispersion coefficient of particles	
D	Impeller diameter	mm
F_{in}	Inlet aeration rate	l h^{-1}
g	Acceleration of gravity	cm s^2
H	Height of liquid in the vessel	mm
K_La	Mass transfer coefficient	s^{-1}
L	Length of impeller blade	mm
l_f	Volume of the bed	m^3
P_g/V	Power input	W m^{-3}
T	Tank diameter	mm
t	Time	days
$\bar{t}$	Mean residence time	s
u_s^{α}	Superficial gas flow rat	ms^{-1}
U_i	Velocity of particle	m s^{-1}

V_G	Gas volume in the reactor	cm^3
V_L	Liquid volume in the reactor	cm^3
v_o	Volumetric feed rate	$m^3 s^{-1}$
W	Width of impeller blade	mm
X	Biomass concentration	$g l^{-1}$
X_0	Initial biomass concentration	$g l^{-1}$
$(YCO_2)_{in}$	Inlet mole fraction of carbon dioxide	
$(Y CO_2)_{out}$	Outlet mole fraction of carbon dioxide	
$(YN_2)_{in}$	Inlet mole fraction of Nitrogen	
$(Y O_2)_{out}$	Outlet mole fraction of oxygen	
Z	Distance along the mixing region in the bed	m

Greek Letters	**Description**	**Units**
ρ	Density of the solid particles of species	$kg m^{-3}$
μ	The specific growth rate	h^{-1}
ε	Overall gas hold-up	
γ	Shear rate	s^{-1}
τ	Shear stress	$N m^{-2}$
μ_L	Apparent viscosity	$Ns m^{-2}$
ε_{mf}	Minimum fluidised bed voidage	
ε_f	Voidage	
Φ_s	Shape factor	

ABBREVIATIONS

ANOVA	Analysis of variance
CPR	Carbon dioxide production rate
GAE	Gallic acid equivalent
LiP	Lignin peroxidase
OUR	Oxygen utilisation rate
STR	Stirred tank reactor
TDS	Total dissolved solids.
TOC	Total organic carbon
v/v	Volume by volume
w/v	Weight by volume

CHAPTER 1
INTRODUCTION

1.1 INTRODUCTION

Fossil fuels remain the primary source of energy, with renewable energy sources providing an increasing, but small, contribution to the world's energy needs. Coal represents one of the world's most abundant fossil energy resources. It is estimated that the world's coal reserves stand at $1.53x10^{20}$ Btu, or 71.4% of the world's fossil fuel resource (Hagan, 1989).

Thermal and chemical processes currently dominate conversion of coal to liquid and gaseous products, as well as energy. These generally require extreme conditions of temperature, pressure and chemical environment with efficient processing being limited to coals of high calorific value (Faison, 1993). High rank coal is used for electricity generation and steam generation for industrial uses, transportation, residential heating, conversion to liquid fuels and metallurgical processes. The use of low rank coal for electricity generation and residential heating is limited. This is due to its low heating value and high sulphur content. The potential of microbial systems to process coal, converting low rank coal at ambient temperature and pressure has been demonstrated (Scott *et al.* 1986). Owing to the highly heterogeneous structure of coal, the scale up and commercialisation of the microbial process may not be easy. Microbial solubilisation of coal has been studied with several fungi and bacteria using surface and submerged culture (Cohen and Gabriele, 1982; Fakoussa, 1981; Gokacy *et al.* 2001). The organic material of low rank coal can be converted to valuable oxidised products by coal biosolubilisation. These oxidised products can serve as substrates for further biotransformation to yield various value-added compounds as antioxidants.

The mechanism of microbial solubilisation of coal is not yet understood. It has been postulated that several compounds produced by microorganisms, including alkaline substances, oxidative and hydrolytic enzymes and chelators may be involved in solubilisation of the coal matrix. For a microbiological approach to coal solubilisation to be economical and feasible, mechanisms involving production of extracellular non-stoichiometric agents like enzymes, which are non specific and stable, are required

(Fakoussa and Hofricher, 1999). The alkaline substances produced chemically are cheaper than microbially generated alkaline substances. Further, there is a danger that combustion of alkaline solubilised coal will emit NO_x into the air. Chelators are also classified as uneconomical.

Most filamentous fungi have a saprophytic way of life. They degrade macromolecules from the environment and can take up the simple molecules produced as an energy source for growth. To achieve this, fungi secrete degradative enzymes into the extracellular medium. Coal, as a product of plant fossilisation, preserves some molecules derived from lignin. This is especially prevalent in low rank coals. The lignin is susceptible to degradation by some extracellular fungal enzymes, including lignin peroxidase, manganese-peroxidase and laccase (Larboda *et al.* 1999).

The desired products are primarily a mixture of polar organic compounds of moderate to high molecular weights with a high degree of aromaticity. These are water soluble and can be used directly as fuel or can serve as raw materials for fine chemical manufacture. Microbial metabolism may proceed to degrade the coal and its products completely to carbon dioxide (CO_2) and other low-value products within a non-optimised system, resulting in the loss of the valuable intermediate products and their calorific value.

1.2 RESEARCH OBJECTIVES AND SCOPE

This research forms part of a coordinated multi-disciplinary project in the field of biotechnology under the umbrella of the Advanced Research Centre for Applied Microbiology (ARCAM). The goal of the composite project is to develop a suitable technology for the conversion of low-value phenolic polymeric waste, specifically low rank coal, into high value chemical products. Hence collaborative interactions for this research include screening for novel microorganisms for coal biosolubilisation, process engineering aspects of coal biosolubilisation, biotransformation of polyphenolics to value added compounds and separation technology. Aromatic compounds derived from the biosolubilisation of low rank coal have been postulated to provide a reservoir of substrates for biotransformation to value added compounds with various potential applications including provision of antioxidants for the food industry and catechols for the pharmaceutical industry. Prior to their biotransformation, sufficient volumes of polyphenolic molecules must be produced. Recovery, separation and characterisation of

these molecules is required prior to and post biotransformation. This study contributes to the composite project through its focus on bioprocess engineering aspects of coal biosolubilisation. The objectives of this MSc dissertation are:

- To investigate the role of fungal biomass and extracellular enzymes in both coal biosolubilisation and subsequent degradation of phenolics intermediates.
- To identify key operating variables influencing coal biosolubilisation.
- To compare the stirred tank slurry bioreactor, fluidised bed bioreactor and fixed bed bioreactor configuration for the fungal biosolubilisation of coal.
- To provide process kinetic data on the biosolubilisation and biodegradation of coal for bioreactor design.
- To provide methodology by which to quantify fungal growth in the slurry reactor system.

1.3 PROBLEM STATEMENT

In order to ensure the economic commercialisation of coal biosolubilisation to provide intermediates for synthesis of value-added products such as antioxidants, dyes, catechols, napthols and other chemical derivatives or to be used directly as fuel, it is necessary to achieve a critical rate of biosolubilisation and product yield. This requires both understanding and optimisation of the solubilisation and depolymerisation steps as well as the prevention of subsequent degradation of the biosolubilised products. The key questions and hypotheses of this study, centering on these, are given below.

1.3.1 Key questions

The following questions are addressed through this research:

- What contact is needed between the fungus and the coal for efficient biosolubilisation and depolymerisation?
- Is further decomposition or degradation of the soluble polyphenolic products attributed to extracellular enzymes or to a whole cell process?
- What are the optimum coal loading and particle size fraction conditions for the coal biosolubilisation process?
- Do the process kinetics suggest that coal biosolubilisation is feasible commercially?

1.3.2 Hypotheses

- Coal biosolubilisation is enhanced by increased availability of coal surface area.
- A stoichiometric approach based on off-gas analysis can be used to quantify biomass growth in the presence of coal.
- Contact between whole fungal cells and coal is required to release solubilised organic compounds from coal. To prevent their further degradation, a reactor configuration is required to remove soluble products from the fungi on their formation.

1.4 STRUCTURE OF THE THESIS

Chapter 2 summarises the current status of knowledge with respect to coal biosolubilisation. An overview of the properties of low rank coal that make it more susceptible to microbial attack than hard coals or high rank coals is presented in Section 2.2. A critical appraisal of the microorganisms involved in coal modification, the preferred species and their effectiveness is summarised in Section 2.3. The mechanisms postulated for coal biosolubilisation and depolymerisation were assessed in Section 2. 4. Thereafter factors previously identified to affect coal solubilisation, as well as potential reactor configuration for large scale coal biosolubilisation processes are reviewed in Sections 2.5 and 2.6

Chapter 3 presents the experimental materials and procedures used in this study. All analytical methods used are detailed and their limitations highlighted. Further, the reactor configurations studied for coal biosolubilisation are specified. Reproducibility of the experiments was investigated and findings are presented.

In Chapter 4, results obtained from factorial experimental design used to investigate key operating variables in coal biosolubilisation are presented. Coal loading and the particle size fraction distribution are studied to determine optimum conditions for coal biosolubilisation.

A mass balance approach based on off-gas analysis for the quantification of fungal biomass is validated in Chapter 5. This is then used for the evaluation of product yield. Possible reasons for the low yield of phenolics were investigated and other potential products investigated are presented.

In Chapter 6, reactor configuration is considered. Results obtained from coal solubilisation from the stirred tank slurry reactor, fluidised bed bioreactor and fixed bed bioreactor are compared in order to assess advantages and shortcomings of these reactor configurations for coal solubilisation. Based on the findings, conclusions are drawn and recommendations are put forward in Chapter 7.

CHAPTER 2
LITERATURE REVIEW

2.1 INTRODUCTION

Coal is the most abundant fossil fuel in the world (Osborne, 1988); however its consumption for energy production is the cause of environmental concerns. Most of the coal used as fuel for electricity and steam production is classified as high rank coal (bituminous coal and anthracite) because of its high heating value. Here presence of sulphur in coal is undesirable, causing SO_x emissions. However, reserves of low rank coal (lignite and sub bituminous coal) are quite substantial (Faison, 1993). The utilisation of coal depends on its physical properties (Kirk-Othmer, 1964). High rank coal has higher calorific value and lower sulphur and ash content than low rank coal. To meet a specific energy demand a greater quantity of low rank is required and this leads to a higher SO_x emissions.

Present coal conversion technologies include gasification and liquefaction. Coal gasification is a chemical reaction of coal with air or oxygen and steam which results in the production of either a gas with high calorific value like CH_4 and H_2 or low calorific value like CO and CO_2 (Faison, 1993). The efficiency of coal gasification is a function of the char reactivity. Char is formed from devolatilization of coal which is the first step in gasification process; subsequently the volatiles and char are further converted to gaseous products (Tsai, 1982). The char reactivity is a function of the parent coal and the conditions under which the char was prepared, like heating rate and maximum temperature.

Coal liquefaction is a process of converting solid coal into a liquid fuel under high pressure and temperature. To produce the liquid fuel efficiently, hydrogen and a catalyst must be added. For direct coal liquefaction, hydrogenation of coal occurs in solvent slurry at high temperature and pressure. Direct coal liquefaction involves three basic steps: coal slurrying in solvent, coal dissolution under high temperature and pressure, and transfer of hydrogen to the dissolved-coal products (Perry and Green, 1984).

The present technologies of coal conversion are not currently used for low rank coal conversion because of increased environmental pollution due to its physical properties, including low calorific value, high moisture content and high sulphur content. New coal

conversion technologies are urgently required to increase coal utilisation while ensuring its environmentally responsible use. One possible approach is the utilisation of biotechnological processes to convert lignite either to a clean, cost effective energy source or to value added products which can be used by further biotechnological or chemical syntheses (Fakoussa and Hofricther, 1999).

In order to evaluate the potential of this technology and contribute to its development, it is necessary to first review the nature of the coal substrate and the microorganisms that degrade it.

2.2 COAL ORIGIN AND CLASSIFICATION

Coal is a complex heterogeneous mixture of macromolecular organic compounds with an irregular chemical structure. It is formed from fossilised plant remains through a process involving compaction, hardening, chemical alteration and metamorphism by heat and pressure over geological time (Elliott, 1981). Coal diagenesis and metamorphism result in the gradual increase in rank from lignite, through sub-bituminous coal and bituminous coal to anthracite. This increase in rank is associated with a change in the chemical composition and molecular structure of the organic component of the coal. Inherent moisture and oxygen content decrease consistently throughout the coalification process (Faison, 1993). These changes cause an increase in the heating value, aromatic content and carbon content with a decrease in oxygen, hydrogen and volatile content, seen in Table 2.1. Coal structure has been reported to be a function of the rank of coal i.e. the chemical structure changes with the rank of coal. From the coal models presented in Figure 2.1, it is seen that the transition from low rank coal to high rank coal is accompanied with a loss of aliphatic structures, oxygen content and an increase in aromatic ring content. Hard coal (bituminous coal) is much more resistant towards microbial attack than low rank coal because of its hydrophobicity, the high proportion of condensed aromatic rings and the lower oxygen content (Fakoussa, 1990). Low ranking lignite resembles the virgin lignin from which the coal is derived more closely than highly condensed bituminous coals; hence it is expected to be more susceptible to biological attack by lignin degrading microorganisms (Gokacy *et al.* 2001).

Coal is located worldwide, with big reserves in USA, Russia, China and India. This is illustrated in Figure 2.2. However, the largest coal producing countries are China, the USA,

India, Australia and South Africa. Much of global coal production is used in the country in which it was produced; only around 18% of coal production is destined for the international coal market. The total reserves of low rank coal account for about 47% of the total recoverable reserves of high and low rank coal, while the total low rank coal production accounts for about 28 % (World Coal Institute, 2005). Countries which have significant production and utilisation of low rank coal include the USA, Germany, Australia, Indonesia, Russia, Turkey, Czech Republic, Poland, Canada, India and Thailand. Germany is the largest consumer of low rank coal. In 1998, 28% of its electricity was generated from low rank coal. Over 90% of low rank coal mined world wide is consumed in power stations close to the mine, 4% by the industry, and 3% by households and the rest in other applications (Rheinbraun, 2000). Based on the information above, it is evident that there are abundant reserves of low rank coal and it is under-utilised. The problem of low utilisation of low rank coal is a worldwide issue, but of less importance in South Africa where coal reserves are mostly high rank coal.

Table 2.1: Characteristics of different ranks of coal (Faison, 1993).

Characteristics	**Lignite**	**Sub bituminous**	**Bituminous**	**Anthracite**
Age(x 10^6 year)	20-60	60-100	>100	>200
Carbon (wt %)	70-75	75-85	85-90	90-97
Hydrogen (wt %)	4-6	4-6	4-5	3-5
Oxygen (wt %)	20-25	10-20	5-10	1-3
Aromatic carbon content (wt %)	30-50	60-70	70-80	80-95
Volatile content (wt %)	40-50	35-50	10-45	>5
Moisture content (wt %)	20-45	5-25	1-5	<1
Heating value (x10^3 Btu/lb)	6.3-8.3	8.3-11.5	10.5-14	>14

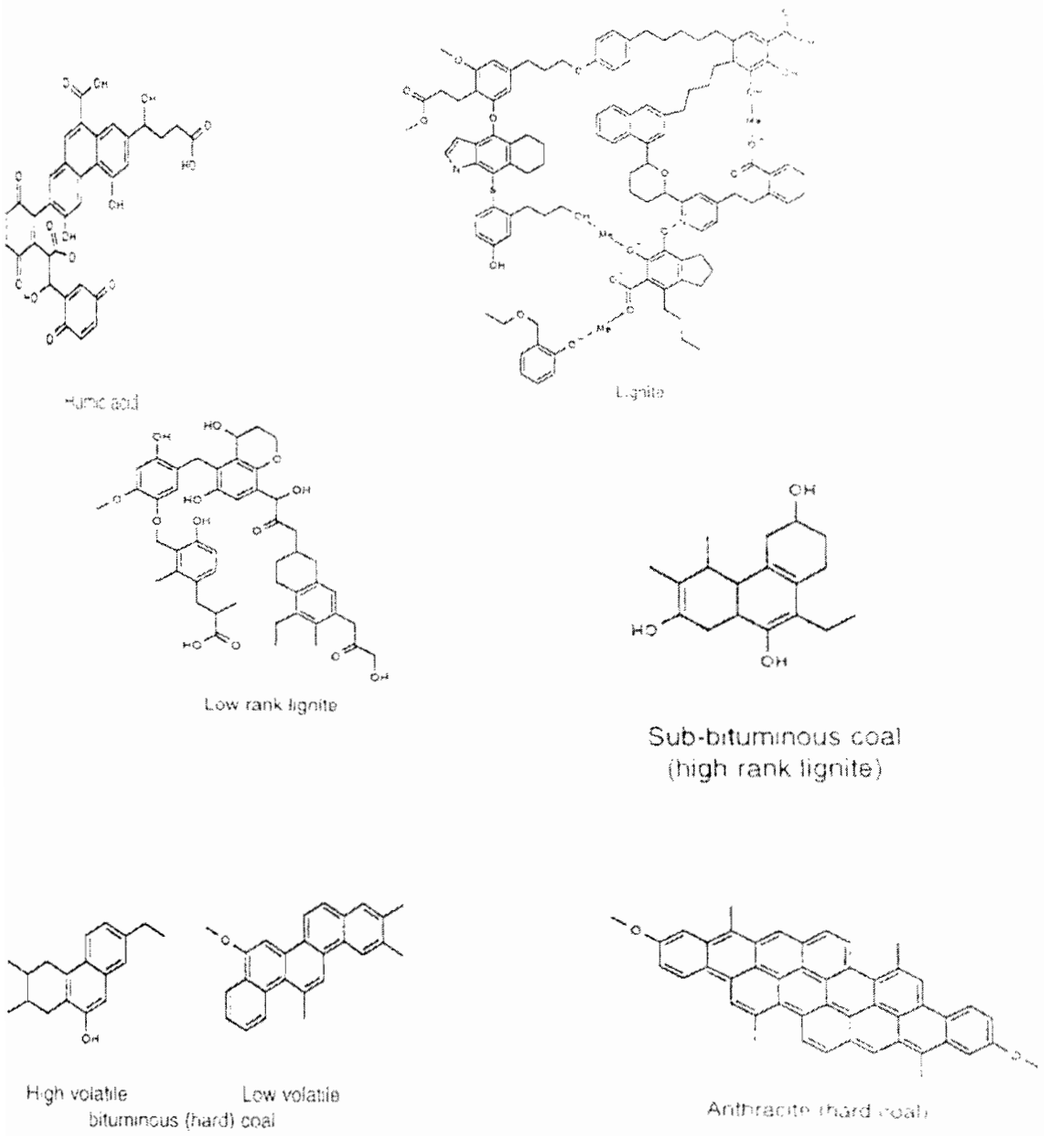

Figure 2. 1: Typical coal models for coal substances of different rank (Fakoussa and Hofrichter, 1999).

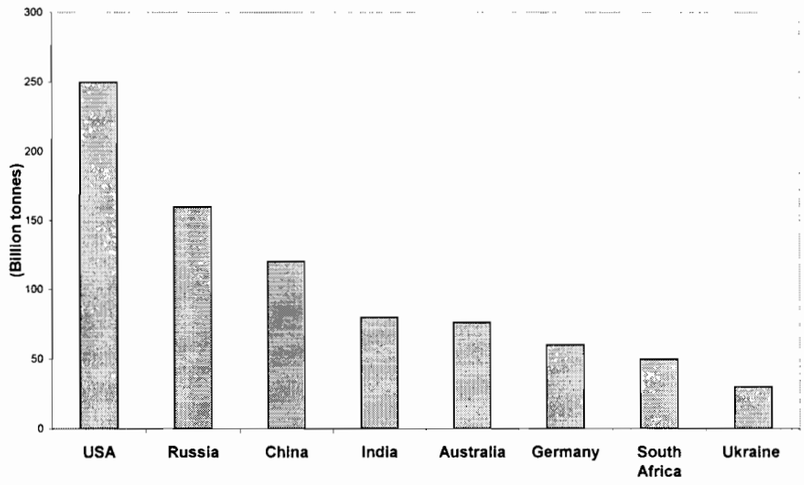

Figure 2.2: Countries with the largest reserves of coal in 2003 (Source, British Petroleum, 2004; Adapted from, World Coal Institute, 2005)

2.3 MICROBIAL POPULATIONS IN THE PRESENCE OF COAL

The presence of a microbial population on coal was first reported in 1962 by Rogof *et al.* However the ability of microorganisms to transform low rank coal to water-miscible liquid products at room temperature and atmospheric pressure was only reported later (Fakousssa, 1981; Cohen and Gabriele, 1982). Different types of aerobic bacteria and fungi have been shown to catalyse the transformation of coal. These are summarised in Table 2.2. Filamentous fungi and streptomycetous bacteria are most commonly associated with this solubilisation activity. The activity has been correlated with an extensive hyphal ramification throughout the coal particle in both surface and submerged culture (Faison, 1991). Many of these organisms were isolated from coal-based environments in nature i.e. PAH contaminated soil and open cast areas mining for lignitic coal. The coal solubilising activity of certain cultures from stock culture collections has also been demonstrated (Larbod*a et al,* 1999; Holker *et al,* 1995).

2.3.1 Coal degrading fungi

Comprehensive screening programs have been carried out to identify fungal strains that are capable of modifying the physicochemical structure of coal. The strains isolated have been classified into three main groups; namely Basidiomycetes, Ascomycetes and Deuteromycetes.

A significant fraction of the fungi able to transform low rank coal are Basidiomycetes. White-rot fungal strains are most common subset of these (Ralph and Catcheside, 1997). The white rot fungi offer particular promise as agents for depolymerisation of coal for the following reasons:

(a) They can depolymerise and mineralise lignin which, like the macromolecular phase of low rank coal, is an irregular high molecular mass aromatic polymer.
(b) A significant fraction of the organic component of low rank coal is derived from and retains structural similarities to lignin.
(c) White rot fungi are known to degrade a range of aromatic molecules other than lignin, apparently due to the broad substrate range of their lignin-degrading enzymes.

Gokacy *et al.* (2001) carried out a screening test on solid culture media to show coal solubilising ability of a selection of fungal strains on native and pretreated coal. They showed that *Trametes versicolor* and *Phanerochaete florida* were most effective in liquefying acid–pretreated lignites while *Phanerochatete chrysosporium* was the most effective in liquefying Elbistain lignites (Table 2.3). The coal was pre-treated with 8N HNO_3 for 48 hours and washed with distilled water. The lignites studied were from different coal reserves. Elemental composition of these lignites showed that Canakkale-can lignite had the highest carbon content.

Table 2.2: Selected micro-organisms with solubilising or depolymerising activity on lignite (Hofrichter and Fakoussa, 2001).

Organisms	Effect on Lignite	References
Bacteria		
Actinomycetes		
Streptomyces spp. *S.setonii*	solubilisation	Gupta *et al.* (1988)
Eubacteria	solubilisation	Strandberg and Lewis (1987)
Bacillus sp	solubilisation	Quigley *et al.* (1989a)
Bacillus lichiniformis	solubilisation	Polman *et al.* (1994)
Pseudomonas cepacia	solubilisation	Crawford and Gupta (1991)
Basidiomycetous fungi		
Wood-decaying white-rot fungi		
Clitocybula dusenii	depolymerisation	Ziegenhagen and Hofrichter (1998)
Nematomoloma frowardii	depolymerisation, solubilisation	Hofrichter and Fristche (1996) Ralph and Catcheside (1994), Torzilli and Isbister (1994)
Phanerochaete chrysosporium	depolymerisation, solubilisation	Cohen and Gabrielle (1982), Fakoussa and Frost (1999)
Trametes (Coriolus) versicolor	depolymerisation	Steffen *et al.* (2000)
Litter- decomposing fungi		
Agrocybe praceox	depolymerisation	Hofrichter and Fristsche (1996)
Stropharia rugosoannulata	depolymerisation	Willmann and Fakoussa (1997a,b)
Isolates RBS 1k, RBS 1b		
Wood-decaying brown-rot fungi		
Poria monticola	solubilisation	Cohen and Gabriele (1982)
Deuteromycetous and ascomycetous fungi		
Alternaria sp.	solubilisation	Hofrichter *et al.* (1997)
Fusarium oxysporium	solubilisation	Holker *et al.* (1995)
Paecilomyces spp.	solubilisation	Scott *et al.* (1986)
Penicillum citrium	solubilisation	Polman *et al.* (1994)
Trichoderma atroviride	solubilisation	Holker *et al.* (1997b, 1999a)

Table 2.3: Screening test for the most effective coal solubilising fungi (Gokacy *et al.* 2001).

Fungus	Liquefaction * (%)					
	Elbistain lignite		Beypazari lignite		Canakkale-Can lignite	
	Native	Pre-treated	Native	Pre-treated	Native	Pre-treated
P. chrysosporium	33.81	90.91	4.15	9.20	4.09	51.16
C. versicolor	12.93	100	-	100	7.59	100
P. sajor-caju	4.86	81.24	2.81	56.07	-	66.71
P. florida	18.90	100	7.89	100	10.94	100

*Liquefaction is defined as weight loss of lignite

Stewart *et al.* (1990) showed extensive surface colonisation on pretreated bituminous coal by *Penicillium* sp and *Cunninghamella* sp. In the native coal, there was little evidence of colonisation by these fungi.

Hofrichter and Fritsche (1996) developed a mini-scale screening system to detect depolymerisation of low rank coal by fungi. This system involves decolourisation (bleaching) of agar media containing coal humic acids. A total of 486 fungal strains (253 soil-derived Deuteromycetes strains, 233 wood and litter–decaying Basidiomycetes strains) were tested during the first screening step using humic acids as a carbon source. The mycelical growth on the humic acid-containing agar was lower for all fungi tested in comparison to growth on a comparable malt extract agar (0.05%). A limited number of basidiomycetes strains (*Auricularia* sp., *Stropharia rugosa amalat* E1 and E2) were able to form mycelia mats on the agar surface. Most of Deuteromycetes strains produced spores instead of hyphae (e.g. strains of genera *Trichoderma* sp., *Aspergillus* sp., *Penicillum* sp.). The ability to decolourise the dark–brown agar and form yellowish products was limited to the Basidiomycetes. Some 38 strains of this group decolourised the agar completely within 3 weeks, while 49 strains partially decolourised it. In contrast, the Deuteromycetes species tested were unable to decolourise coal humic acids derived from coal. The results illustrate that surface cultures can be used primarily to carry out screening tests for fungal metabolism of substrates (Holker *et al.* 1997b).

Attachment of the fungal cell wall to coal particles has been observed for all the strains of filamentous fungi involved in coal solubilisation (Hofrichter and Fakoussa, 2001; Larboda *et al.* 1999).

2.3.2 Bacteria

Certain bacteria are able to grow on coal as their sole source of carbon and energy. The most common strains cited to grow on coal are *Streptomyces*, *Bacillus* and *Pseudomonas*. The ability of bacteria to degrade bituminous coal was first demonstrated by Fakoussa in 1981. She observed poor growth rate of pleomorphic bacteria, probably belonging to the group of *Mycobacteria* or *Nocardia*, on hard coal. Further investigation indicated that these bacteria only grow on water-soluble coal substances which are released through surface pores during solubilisation (Fakoussa, 1990). She identified a coal solubilising *Pseudomonas fluorescens* which has been shown to produce a surfactant (Fakoussa, 1988). This organism achieved limited solubilisation of the high rank coal. Reports on the ability of mycelial bacteria belonging to the genus *Streptomyces* to solubilise lignite is well documented in the literature (Strandberg and Lewis, 1987, Quigley *et al.* 1989). These studies showed that bacteria could solubilise pre-treated coal. Recently, Larboda *et al.* (1999) observed that the bacterial strain *Bacillus amyloliquefaciens* was able to depolymerise humic acid. There are limited studies on bacterial solubilisation of low rank coal.

2.3.3 Potential of bacteria relative to fungi in coal biosolubilisation

Torzilli and Isbister (1994) compared coal solubilising agents produced by fungi and bacteria in terms of pH dependence, thermostability, molecular mass of product, mechanism of action and product diversity. The thermostability and low molecular weight exhibited by both bacterial and fungal solubilising agents indicated a non-enzymatic mechanism. The soluble products generated by each microbial coal-solubilising agent were similar.

2.4 MECHANISM OF COAL BIOCONVERSION

The ability of a microorganism to grow on lignite or other low rank coal must be distinguished from coal solubilisation (Faison, 1991). Growth on lignite may occur at the expense of low molecular weight, water soluble or volatile compounds incidental to the polymeric framework of the solid coal. These compounds may include fatty acids and alcohols which are known to be utilised by a wide variety of microbial species. The ability of fungi to solubilise coal has been reported in the literature (Cohen and Gabriele, 1982; Scott *et al.*, 1986; Larboda *et al.* 1999). However, the mechanism of coal bioconversion has not yet been resolved. Recently Fakoussa and Hofrichter (1999) proposed an ABCDE-system to describe all possible mechanisms which are involved in brown coal conversion as illustrated in the model system in Figure 2.3:

- Alkaline substances
- Biocatalysts (oxidative enzymes)
- Chelators
- Detergents (surfactants,)
- Esterases

Structural modification of lignite has been divided into two categories: solubilisation and depolymerisation (Hofricther *et al.* 1997; Ralph and Catcheside, 1997; Klein *et al.* 1999), as illustrated in Figure 2.4. It shows that biosolubilisation of brown coal (lignite) leads to the formation of humic acids (black liquids) while depolymerisation of lignite or coal-derived humic acids leads to the formation of fulvic acids. The humic acid fraction is not soluble in water under acidic conditions (pH < 2) but is soluble at higher pH values (7-10). Humic acids are the major extractable components of soil humic substances. They are dark brown to black in colour. The fulvic acid fraction of humic substances is soluble in water under all pH conditions. They remain in solution after removal of humic acid by acidification. Fulvic acids are light yellow to yellow-brown in color (Paul and Clark, 1996).

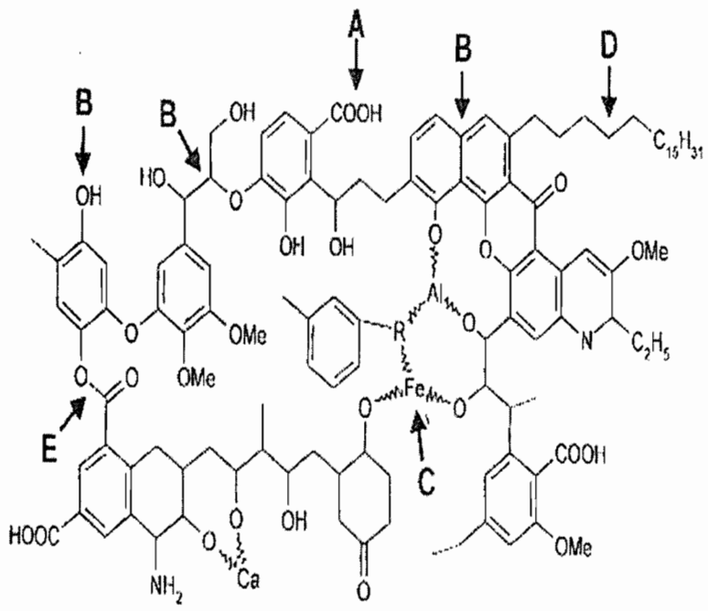

Figure 2.3: ABCDE–mechanism of biological conversion of brown coal (Hofrichter and Fakoussa, 2001). The arrows indicate structures that can be attacked by different microbial agents. A: alkaline substances; B: biocatalysts (oxidative enzymes); C: Chelators; D: detergents E: esterases.

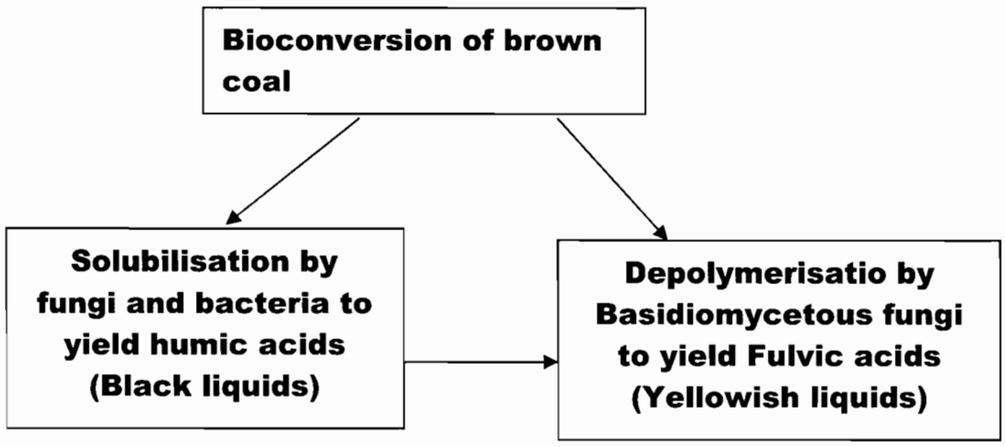

Figure 2.4: Structural modification of low rank coal by microorganisms (Hofrichter and Fakoussa, 2001).

In addition to structural modifications, microorganisms use the mobile phase of brown coal which is comprised of a complex mixture of low-molecular mass aromatics and wax-like aliphatics as a carbon source for growth (Ward, 1985; Ralph and Catcheside, 1993; Fakoussa and Hofrichter, 1999).

2.4.1 Biosolubilisation of low rank coal

The literature on the mechanism of solubilisation of low rank (lignite and sub-bituminous) coal, leading to the formation of a humic acid rich solution, is not consistent. Quigley *et a.l* (1989a, b) proposed that it is mainly a non-enzymatic dissolving process occurring at pH values of pH 7-10 due to the microbial formation of alkaline substances, chelating agents and surfactants. Holker *et al.* (1999b) showed that certain hydrolytic enzymes are involved in the solubilisation process. It was postulated that several classes of active compounds could be involved in coal biosolubilisation. These include:

- Alkaline substances (Quigley *et al.* 1988 , 1989b)
- Oxidative enzymes (Ralph and Catcheside, 1994; Hofrichter and Fristche, 1997b)
- Chelators (Quigley *et al.* 1989a; Cohen et al. 1990 ; Fakoussa 1994)
- Esterase enzymes (Holker *et al.* 1999)

2.4.1.1 Coal biosolubilisation by chelating agents

Treatment of coal with non-oxidising acids (HCl) has been shown to cause the removal of multivalent organic cations, presumably in the absence of ester hydrolysis (Quigley *et al* 1989b). Pretreatment of coal with acidic metal chelators such as citrate, ethylenediamineteraacetate and nitriloacetate resulted in alkali solubility and, usually, biosolublisation. Fungi are known to excrete a variety of dicarboxylic acids such as oxalate during their metabolism; certain coal solubilising fungi are known to produce metal-chelating compounds (Cohen *et al.* 1990).

The solubilisation of Leonardite (oxidised coal) has been linked to the removal of complexing metals by chelating agents. Quigley *et al.* (1989b) and Cohen *et al.* (1990) showed that the biosolubilisation of Leonardite by *Trametes versicolor* was as a result of excretion of ammonium oxalate ($C_2O_4(NH_4)_2$) in high amounts. When comparing different chelator molecules (oxalate, citrate, dihydroxybenzioc acids etc), it was found that oxalate

is indeed one of the most effective agents for solubilising pre-treated lignite, possibly due to its small molecular size (Fakoussa, 1994).

2.4.1.2 Alkaline catalysis and coal biosolubilisation

Alkaline biosolubilisation is attributed to the high content of carboxylic and phenolic functionalities (-COOH, -OH) in coal humic acids which can be deprotonated at higher pH, resulting in the formation of water soluble humates (typically dark-brown to black in colour). Microorganisms have two ways of generating such alkaline conditions:

(1) They may produce and secrete metabolites such as ammonia (NH_3) or biogenic amines ($R\text{-}CH_2\text{-}NH_2$), in response to high nitrogen levels in medium. The influence of high nitrogen level on the biosolubilisation of lignite regardless of whether complex nitrogen sources or inorganic salts were used, was demonstrated in different studies for both fungi and bacteria (Quigley *et al.* 1989a; Hofricther *et al.* 1997a; Torzilli and Isbister, 1994).

(2) Microorganisms may also increase the alkalinity of their surrounding medium through the utilisation of organic acids which results in the formation of free bases due to the remaining mono and dibasic metals (Na^+, K^+, Ca^{2+}). This phenomenon may be responsible for enhanced coal solubilisation by *Fusarium oxysporum* when sodium gluconate is used as carbon source instead of glucose (Holker *et al.* 1995).

2.4.1.3 The effect of detergents on coal biosolubilisation

The simplest method for achieving coal biosolubilisation is through the production of a surfactant. Addition of a surfactant to a polar material leads to the formation of aqueous suspension or emulsified solution without the breaking of covalent bonds. Tween 80, a non-ionic surfactant, has been shown to solubilise a low molecular weight fraction of coal (Polman *et al.* 1994). Coal solubilisation by *Pseudomonas* sp has been ascribed in part to the production of surfactant (Fakoussa, 1988).

Fakoussa (1988) investigated the role of bacterial surface active agents in coal biosolubilisation. She compared the efficiency of coal extraction of water and synthetic detergents. Surprisingly she found out that pure water extracted more organic material from coal than the detergents. None of the detergents were able to extract coal to such an extent that the colour of the supernatant was brown.

She suggested that this resulted from the detergents sticking to the coal and clogging the pores of the coal particles. The significance of surfactants in the solubilisation of coal is rather low when compared to alkaline and chelating agents, since their natural concentrations are mostly below the physicochemically effective levels (Fakoussa, 1994).

2.4.1.4 The role of hydrolytic enzymes in coal biosolubilisation

Biosolubilisation of lignite has been attributed to hydrolytic enzymes such as esterases which cleave ester bonds inside the coal molecule. *Trichoderma atroviride* was found to secrete a heat sensitive, partly inducible agent that facilitated the solubilisation of lignite and had hydrolytic properties (Holker *et al.* 1999a). In addition, *Trichoderma atroviride* produces effective non-enzymatic agents (alkaline substances, chelators) that affect the dissolution of coal humic substances.

2.4.2 Depolymerisation of low rank coal by oxidative enzymes

Depolymerisation of the macromolecular phase (coal humic acids) and lignite by microorganisms is a critical step limiting the development of the bioconversion process to yield low molecular weight products (Ralph and Catcheside, 1994). The depolymerisation of lignite or derived macromolecules (coal humic acids) is an enzymatic process at lower pH of 3 to 6 that results in the cleavage of bonds inside the coal molecule and leads to the formation of yellow fulvic acid-like substances with low molecular mass (Hofrichter and Fakoussa, 2001). Enzymes postulated to be responsible for the extracellular oxidation of lignin are:

- Peroxidases (manganese peroxidase, lignin peroxidase)
- Phenol oxidases(laccases)
- H_2O_2 generating oxidases

2.4.2.1 Lignin Peroxidase

Lignin peroxidase (LiP) is a glycoprotein containing iron protoporphyrin IX (heme) as prosthetic group and requires H_2O_2 for catalytic activity. The enzyme is expressed in multiple forms and has a catalytic cycle similar to horseradish peroxidase (Tien and Kirk, 1984, Dunford 1991). LiP has broad substrate specificity for aromatic compounds and oxidises both non-phenolic and phenolic rings.

Wondrack *et al.* (1989) reported that coal polymers prepared from nitric acid-treated North Dakota lignite and sub-bituminous German coal were in part depolymerised by partially purified *Phanerochaete chrysosporium* lignin peroxidase. The coal polymer soluble in water and organic solvents (N-N-dimethylformamide DMF) was depolymerised to smaller water–soluble fragments. Addition of vetratryl alcohol enhanced depolymerisation. Since the enzyme preparation also contained MnP and the *in vitro* depolymerisation assay was performed in the presence of $MnSO_4$ the conversion of the coal polymer may also be due to this enzyme.

Ralph and Catcheside (1994, 1997) have reported the partial depolymerisation of solubilised low rank coal (coal humic acids) by ligninolytic cultures of *Phanerochaete chrysporium*. The fungus converted about 85% of the coal after 16 days incubation, to a form which was not recoverable by alkali washing and acid precipitation. Extensive bleaching of coal substances coincided with the presence of extracellular LiP. The decrease in absorbance of native and methylated alkali–solubilised lignite by LiP isolated from *Phanerochaete chrysporium* was also reported by Ralph and Catcheside (1999). The enzymatic decolorisation reactions showed an absolute requirement for veratyl alcohol and decolorisation did not occur in the presence of metavanadate, which inhibits LiP. The general catalytic cycles for the lignin peroxidase reaction are shown in Figure 2.5. Compound II is a non-phenolic aromatic compound veratryl alcohol which is oxidised by LiP and led to a reduction of peroxide to water.

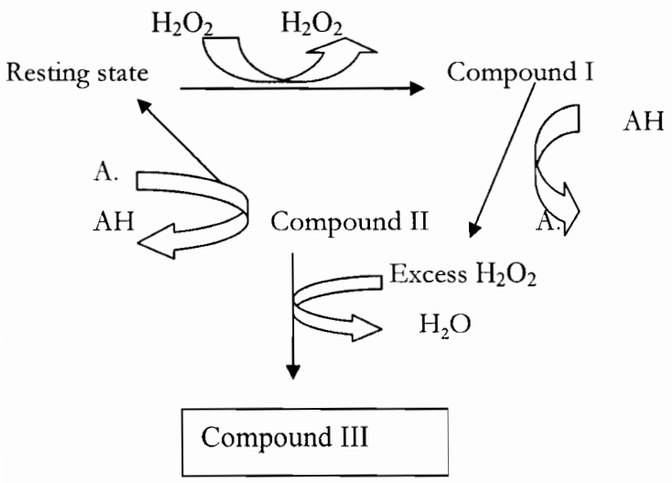

Figure 2.5: Catalytic cycles for lignin peroxidase (Ralph and Catcheside, 1999)

2.4.2.2 Manganese Peroxidase

Manganese peroxidase (MnP) has been successfully used in lignite depolymerisation. Willmann and Fakoussa (1997b) demonstrated the induction of MnP during the bleaching of water-soluble macromolecules (Rhenish lignite, litho type A) by the basidiomycete strain RBS1K. In an *in vivo* experiment, Mn (II)–induced cultures of the basidiomycete fungi *Nematoloma frowrdii* and *Clitocybula dusenii* depolymerised coal humic acids rapidly by forming low molecular weight fulvic acids (Hofrichter and Fritsche, 1996). A maximum of 2 g l^{-1} humic acids were converted within a week in a batch process (Hofrichter *et al.* 1998). After coal was added to the cultures, the activity of MnP increased considerably, indicating an inductive effect of the coal humic substances and the involvement of MnP in the depolymerisation process. *In vitro* depolymerisation using MnP from *Nematoloma frowardii* showed that the enzyme was capable of depolymerising coal humic substances in cell free system (Hofrichter and Fritsche, 1997b). The depolymerisation of humic acid was accompanied by a high loss in absorbance at 450 nm (bleaching) while the formation of low molecular weight fulvic acid-like substances, absorbing at 360 nm, was observed.

Larboda *et al.* (1999) reported that coal solubilisation was achieved by two fungal strains: *Trichoderma sp.* (M2) and *Penicillium sp.* (M4). Esterase, Mn-peroxidase and mostly phenol oxidase activities were detected in the culture supernatants. None of these enzymes were detected when fungi were grown in the absence of coal. This suggests that Mn- peroxidase and esterase participated in the mechanism of coal biosolubilisation by M2 and M4 strains and that the enzymes were induced by coal.

2.4.2.3 Laccase

Laccases are blue copper oxidases that catalyse the one-electron oxidation of phenolics and other electron rich substrates (Burton, 2003). Most ligninolytic fungi produce laccases. Some reports have shown that laccases are involved in lignite conversion by *Trametes versicolor* (Cohen *et al.* 1987; Fakoussa and Frost, 1999, Temp *et al.* 1999). This enzyme has been proposed as the agent responsible for the fungal ability to solubilise coal (formation of black liquid from solid coal; Cohen *et al.* 1987). Laccase, partly purified from *Trametes versicolor,* appeared to be active towards Leonardite ("weathered" highly oxidised form of lignite).

Fakoussa and Frost (1999) showed that the decolourisation of coal derived humic acids by *Trametes versicolor* expressing laccasse is associated with depolymerisation of humic acids and the production of lower molecular weight fulvic acid–like compounds. They measured the correlation between laccasse secretion and the decolourisation of coal derived humic acids. They found out that an increase in laccasse activity lead to an increase in the degree of decolourisation. In another experiment carried out by Temp *et al.* (1999), laccase was the only ligninolytic enzyme secreted by *Pycnoporus cinnabarinus* during the coal humic acid degradation. A summary of the enzymes reported to be involved in coal bioconversion is shown in the Table 2.4.

Table 2.4: Enzymes involved in coal bioconversion.

Fungal strains	**Enzymes involved**	**Mechanism**	**Reference**
Nematoloma frowardii, Clitobula dusenii	Manganese peroxidase	*In-vitro* attack on humic acids matrix and coal particles	Ziegenhagen and Hofrichter (1998); Hofrichter *et al.* (1998)
Phanerochaete chrysosporium	Lignin peroxidase	*In-vitro* decolorisation and depolymerisation of native methylated brown coal	Ralph and Catcheside (1999)
Trametes versicolor	Laccase	*In-vivo* decolorisation and depolymerisation of humic acids and lignite	Fakoussa and Frost (1999)

2.4.3 Mechanism of phenolics degradation

Scott *et al.* (1986) reported that results of infrared spectroscopy (IR) and nuclear magnetic resonance (NMR) studies on biosolubilised coal product suggest that the product is aromatic in nature, possibly containing aromatic hydroxyl groups (phenolic). The yield of solubilised coal product is currently reported to be low (Holker and Hofer, 2002; Laborda *et al.* 1999). Some publications report the absence of these coal derived-monomers (Ralph and Catcheside, 1997). There is clearly a need to establish whether solubilised products are taken up by fungal cells or further degraded by enzymes.

Larboda *et al.* (1999) identified some chemical features of humic acids derived from fungal biosolubilisation of lignite and compared these with chemically derived humic acids, seen in Table 2.5. Humic acids extracted chemically from residual lignite were similar to those of the original lignite. However, several differences were observed in humic acids extracted microbially from lignite. These include the increase in total acidity and the proportion of phenolic compounds. Furthermore, 80 % of the total biosolubilised products from lignite were humic acids while the remainder was fulvic acids. This observation suggests that phenolics are not degraded further by the fungi. A rather low yield of fulvic acids is the reason for low phenolic yield. This is in agreement with the observation of Paul and Clark (1996) that the COOH (carboxyl) and phenolic OH content of fulvic acids is much higher that of humic acid.

Table 2.5: Some chemical characteristics chemically extracted, microbially extracted humic acids (mEq g^{-1} humic acids) (Source: Larboda *et al.* 1999)

	Chemically extracted[a]	**Microbially extracted [b]**	**Unsolubilised Solid residue**
Total acidity	8.5	12.5	10.0
C=O	3.4	2.0	3.3
COOH	2.7	2.2	4.0
Phenol	5.8	10.3	5.9

[a] Lignite was pretreated with 2M HNO_3 (original coal)

[b] Biosolubilised lignite by action of the S10H strain (*Aspergillus sp*)

Holker and Hofer (2002) also observed the composition of the supernatant from lignite biosolubilisation in a 25-litre bioreactor. This consisted of 70 % humic acids and 30 % fulvic acid-like compounds.

LiP extracted from *Phanerochaete chrysosporium*, a coal solubilising fungus has been reported to degrade mono-cyclic and poly-cyclic aromatic compounds (Odier *et al.* 1988). In cell-free systems containing LiP from *Phanerochaete chrysosporium,* methylated solubilised coal was converted into a range of low molecular-mass products. While unmethylated (native) coal was partially decolourised, it was not significantly depolymerised.

This observation further suggests that depolymerisation and degradation of native coal is limited and leads to low yields of fulvic acids and phenolics (Ralph and Catcheside 1999).

2.5 KINETICS OF COAL BIOSOLUBILISATION

2.5.1 Rate and extent of biosolubilisation

Most of the results presented on coal solubilisation are qualitative or at best, semi-quantitative. The kinetics of coal biosolubilisation has not been reported. In the evaluation of coal biosolubilisation, an important quantity for the assessment of process feasibility is the yield i.e. the determination of the mass of product obtained per unit mass of coal solubilised. Holker *et al.* (1995) measured the increase in absorbance of the liquid medium as a measure of coal solubilisation. In their study, the coal was pretreated with 4% H_2O_2 before coal solubilisation and the degree of solubilisation was measured photometrically at 450 nm and at 650 nm. The highest degree of coal solubilisation measured at 650 nm was 1.35 absorbance units and 2.5 absorbance units measured at 450 nm. Recently in another experiment, Holker and Hofer (2002) measured the degree of coal solubilisation photometrically at 450 nm qualitatively and quantitatively by dry weight analysis after evaporation of the supernatant at 95^0C. They reported that 140 g of 1.5 kg was solubilised in a 25-litre Airmix II solid state bioreactor, over a period of 40 days. The process was carried out with untreated lignite at 10 % (w/v) coal loading and particle size fraction of 1-10 mm, with no pretreatment of the coal particles. The organism, *Trichoderma atroviride* CBS 349, was grown for 5 days in a minimal inorganic medium containing glutamate in order to induce its coal solubilising capacity at shake flask conditions. Two litres of *Trichoderma atroviride* CBS cultured for 5 days was inoculated into the bioreactor which contained 11.5 litres distilled water. No growth medium was added to the culture in the bioreactor. The fungus started to solubilise the coal after a lag phase of 6 days. Gravimetrically, 9.3 % of the lignite was solubilised and the absorbance value at 450 nm was about 5.

Gokacy *et al.* (2001) also reported the extent of coal solubilisation in terms of total dissolved solids. They carried out the solubilisation in 25 litre of stock growth medium containing 10 g l^{-1} acetic acid and 50 g l^{-1} lignite of 1-2 mm fraction. The total dissolved solids obtained after 20 days of coal biosolubilisation was 15 g l^{-1} and they reported a 30% coal solubilisation. They did not take account of the components of the growth medium. When the components of the growth medium are included, the degree of coal solubilisation is 24%.

2.5.2 Biomass measurement on solid substrate.

The process kinetics have not been determined rigorously, largely because measurement of fungal growth during coal solubilisation is hindered by the presence of the solid coal substrate. Conventional ways of estimating cell concentration such as plate counts or dry weight determination by filtration or centrifugation are not feasible. Biomass estimation in this presence of solid substrates has been demonstrated by respirometry, infrared spectroscopy and image analysis (Koutinuas *et al.* 2003a; Desgranges *et al.* 1991; Larboda *et al.* 1999).

2.5.2.1 Respirometry

Biomass production may be estimated through respirometry, based on the stoichiometric relationship between biomass synthesis, oxygen consumption and carbon dioxide evolution using material balances. In this way it is possible to estimate the rate of biomass production by measuring the carbon dioxide evolution rate (CER) or oxygen consumption rate (OCR). Koutinuas *et al.* (2003ab) demonstrated this for the growth of filamentous fungi on solid grain substrate. Such an approach assumes constant maintenance energy as well as a constant partitioning of substrate between biomass synthesis and extracellular product formation (i.e. no shift in metabolic pathway), hence the yield coefficient based on O_2 or CO_2 remains constant. Further, it assumes no consumption or evolution of O_2 in competing reactions. A mass balance over the biological system provides a simple way in which to relate the theoretical ratio of the substrates used to products formed in the reaction. Andrews (1991) reported a standard form of the mass balance equation for coal biosolubilisation using fungi (Equation 2.1):

Coal + O_2 + N-source + further nutrients $\rightarrow$

biomass + phenolics + other organic compounds + CO_2 + H_2O + other products

$CH_aO_bNS_d + Y_o O_2 + Y_n NH_3 + Y_a CH_eO_fN_gS_h$ + further nutrients →

$Y_b CH_iO_j N_k S_l + Y_p CH_mO_n N_p S_q + Y_c CO_2 + Y_h H_20 + Y_s H_2S0_4$ + other products

Equation 2. 1

The stoichiometric coefficients $\mathbf{Y_i}$ provide theoretical yield values, expressed as moles of compound produced or consumed per carbon equivalent.

2.5.2.2 Infrared spectroscopy

Estimation of biomass by infrared spectroscopy is based on the characteristic compounds present in microbial cell walls and membranes. These display distinct spectroscopic features (Desgranges *et al.* 1991). Mohebby (2005) used the technique to study the biodegradation of wood by *Trametes versicolor.*

2.5.2.3 Image analysis techniques

Image analysis has been used extensively in the characterisation of fungal cell growth in the presence and absence of solid substrate (Cox and Thomas, 1992). It has been used to measure growth of fungi on solid particles in a slurry bioreactor and a packed bed bioreactor (Vinegra-Gonzalez *et al.* 1993, 1994; Scott *et al.* 1994; Larboda *et al.* 1999). It is based on the fact that mycelial organisms only display growth at the hyphal tips; hence the specific growth rate is proportional to the maximum elongation rate of hyphae. Photomicrographs of fungi growing on coal show an extensive hyphal ramification throughout the solid particles in both surface and submerged cultures (Scott *et al.* 1986). Larboda *et al.* (1999) also observed growth of bacteria and fungi on humic acid using scanning electron micrographs (SEM). They observed that only bacteria were attached to the humic acid; however both organisms showed extensive growth.

2.6: REACTOR CONFIGURATION

The bioreactor configuration for a coal bioprocess includes a four-phase interacting system containing two discrete forms of the solid phase. There is a particulate phase consisting of coal particles; a biomass phase containing suspended biocatalyst, a liquid phase that may include nutrients as well as solubilised products; and a gas phase containing either reactants such as oxygen or by-products such as CO_2 (Scott, 1990). Three possible bioreactor configurations which allow continuous process conditions are:

- Gas-phase continuous culture in a fixed–bed reactor
- An aqueous suspension culture in a fluidised-bed reactor
- An aqueous suspension culture in a stirred aerated slurry reactor

2.6.1 The fixed bed bioreactor

A fixed bed reactor is based on using a solid–phase bioreaction surface culture. A bed of stationary particles of coal is exposed to microorganisms and humidified air. The nutrient solution and inolocum are trickled down through the bed of coal with or without recirculation. The liquid product flows to the bottom of the reactor where it is collected whilst fresh coal is continuously or periodically added to the top of the bed (Figure 2.6).

A fixed bed bioreactor is characterised by long retention times, excessive external biomass build up and large particles. The transport of liquid nutrient through the bed is hindered by the presence of external biomass buildup. Sales *et al.* (2005) developed a mathematical model for the liquid phase in a fixed bed reactor. This is illustrated in Equation 2.2

$$D_{ax,L}\frac{\partial^2 C_L}{\partial Z} = u_L\frac{\partial C_L}{\partial Z} + h_L\frac{\partial C_L}{\partial t} + \frac{3(1-e)}{R}D_{ef,L}\frac{\partial C_{L\_in}}{\partial r}\Big|_R fe \qquad \textbf{Equation 2.2}$$

where C_L, $C_{l.in}$ and $D_{ax,\,L}$ are the external and internal liquid phase concentrations and the axial dispersion coefficient, respectively; u_L is the liquid phase superficial velocity, h_L the liquid hold up, $D_{ef,L}$ the internal effective diffusivity and f_e the wetting efficiency.

2.6.2 The fluidised bed bioreactor

The fluidised-bed reactor can be used to provide conditions of suspension culture. Small particles are suspended by the up-flowing aqueous stream that includes nutrient and an appropriate microorganism. Air is supplied to the bottom of the reactor to maintain adequate aeration. As the solubilisation proceeds, the solid residues would be swept out of the reactor and collected in settling chamber and fresh coal feed is added either continuously or periodically.

Fluidisation is a process that involves the transport or suspension of solid particles by liquid or gas. When a fluid is passed upward through a bed of solid particles at low velocity, the fluid passes through the void spaces. This form of contact is called a fixed bed. Higher velocity leads to particle suspension by the fluidising medium which may be either gas or liquid. When the total frictional force on the particle is equal to the effective bed weight, the bed is at the minimum fluidisation or incipient fluidisation (Kunii and Levenspiel, 1977). This is further illustrated in Equations 2.3 to 2.5.

Drag force by upward moving fluid= Weight of particles **Equation 2.3**

$-\Delta P = (1-\varepsilon)\ (\rho_s - \rho)\ l\ g$ **Equation 2.4**

Where the bed has unit cross sectional area, length l and voidage ε. Kunii and Levenspiel (1977) developed a correlation for minimum fluidisation velocity of irregular particles from Equation 2.4, shown in Equation 2.5.

$$U_{mf} = \frac{d^2 p}{150\mu}(\rho_s - \rho)g\frac{\varepsilon^3{}_{mf}\Phi^2 s}{1-\varepsilon_{mf}} \qquad \textbf{Equation 2.5}$$

where U_{mf} = minimum fluidisation velocity, cm s^{-1}

d_p = average particle diameter, cm

ρ_s = particle density of fluidising solids, g cm^{-3}

ρ = density of fluidising medium, g cm^{-3}

μ = viscosity of fluidising medium, g cm^{-1} s^{-1}

g = acceleration of gravity cm s^{-2}

ε_{mf} = minimum fluidised bed voidage

Φ_s =shape factor

An increase in velocity above the minimum fluidisation velocity results in smooth, progressive expansion of the bed as shown in Figure 2.7.

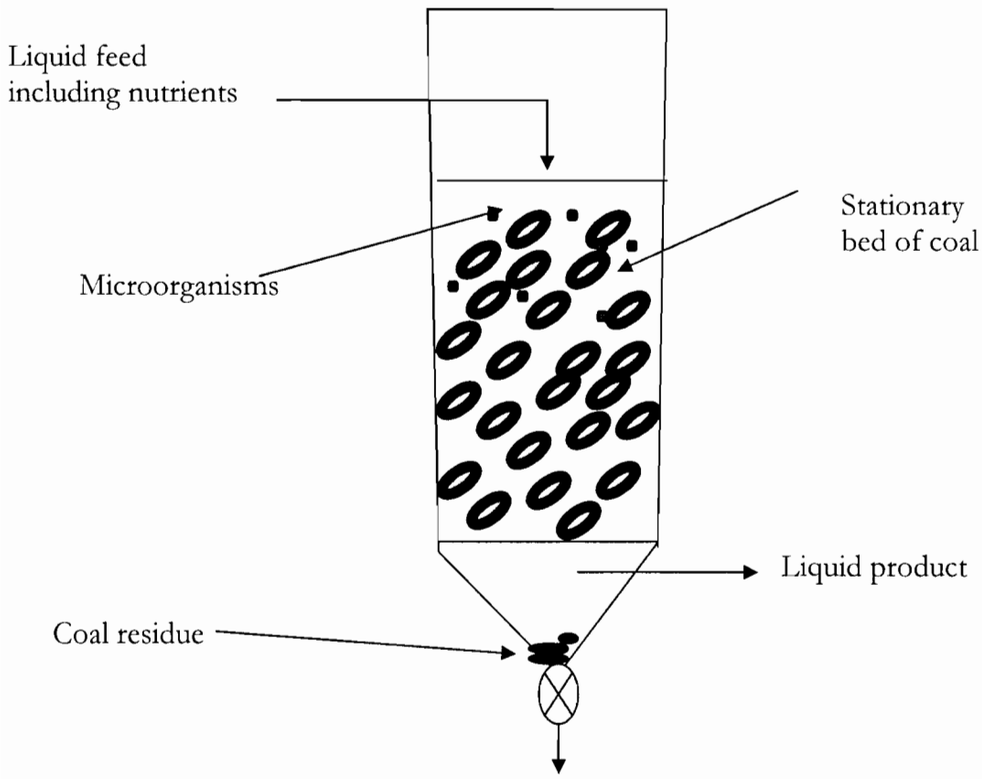

Figure 2.6: Schematic diagram of a fixed bed reactor. Adapted from Scott (1990)

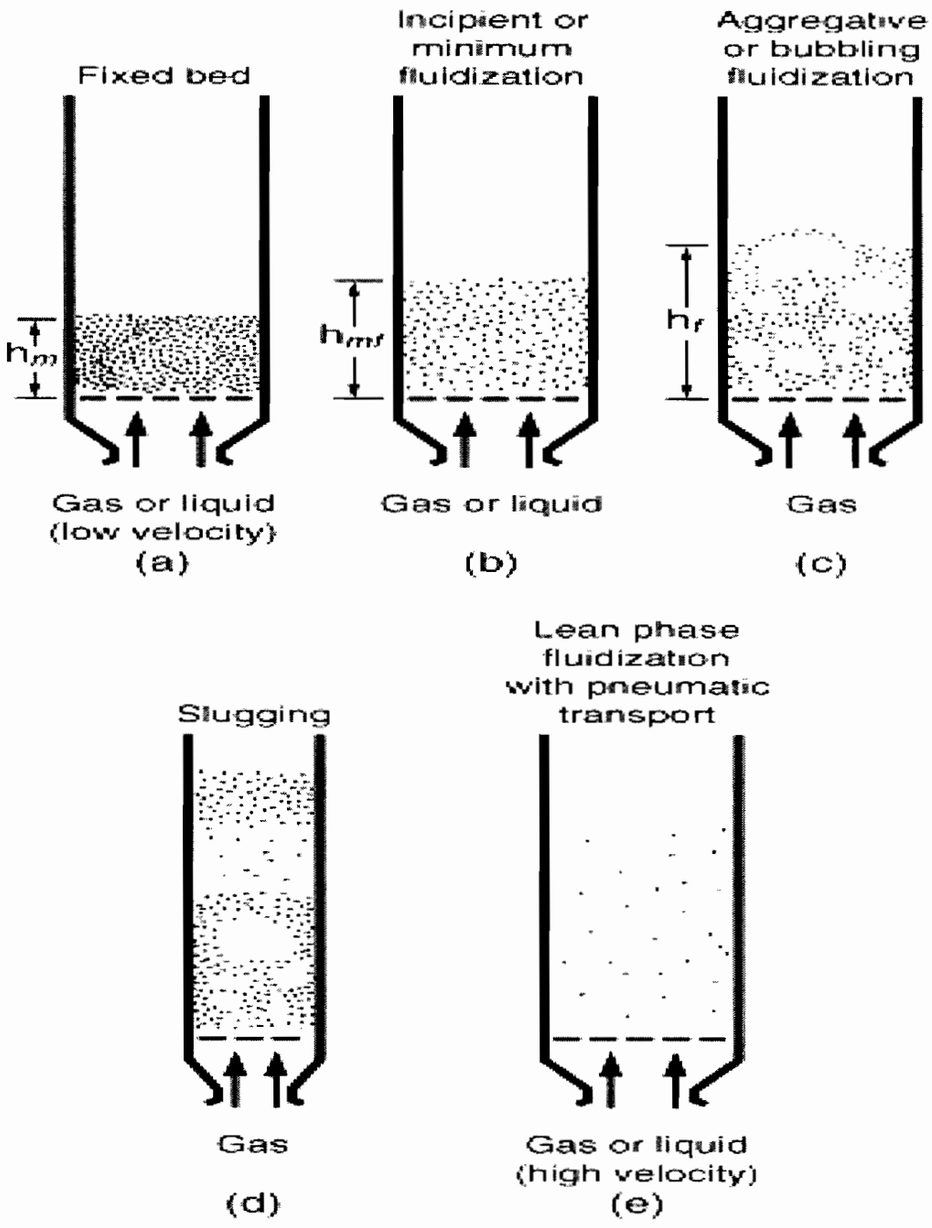

Figure 2.7 Typical flow regimes observed in fluidisation. Adapted from Kunii and Levenspiel (1977)

2.6.3 Stirred tank slurry bioreactor

The stirred tank slurry reactor in which the liquid forms a continuous phase while gas and solids exist as dispersed phases provides the same contact between suspending fluid, particles and microorganisms as the fluidised–bed reactor; however, energy is added via an impeller. Stirred tank reactors are the most commonly used reactors in the biological process. A schematic diagram of a continuous stirred tank bioreactor is presented in Figure 2.8. Mixing is supplied by means of an impeller or motion imparted to the liquid phase by rising bubbles. In aerobic systems, supply of oxygen to the organism generally occurs via air sparging. Mass balance equations for the cell and substrate in a well-mixed continuous reactor are shown in Equation 2.6 and 2.7 respectively.

$$\frac{dX}{dt} = \frac{F}{V}(X_o - X) + \mu X \qquad \textbf{Equation 2.6}$$

$$\frac{dS}{dt} = \frac{F}{V}(S_o - S) - \frac{1}{Y_{X/S}}\mu X \qquad \textbf{Equation 2.7}$$

where

X_o = cell concentration in input

X = cell concentration in reactor

μ = specific growth rate of cells

S_o = inlet concentration of substrate

S = outlet concentration of substrate

Stirred tank slurry reactors have a wide range of applications which include mineral bioleaching (de Kock *et al.* 2004; Rawlings *et al.* 2003) and bioremediation of soil (Ryan *et al.* 1991). One of the limitations of the stirred tank reactor is the maximum solid loading of 20% (Rawlings *et al.* 2003; Garcia-Ochoa *et al.* 1999). Increase in solid loading above the maximum loading has been reported to lead to significant reduction in mass transfer (Bailey and Hansford 1993) and also imposes hydrodynamic stress on the microbial cultures (Nemati *et al.* 2000; Nemati and Harrison, 2000; Harrison *et al.* 2003).

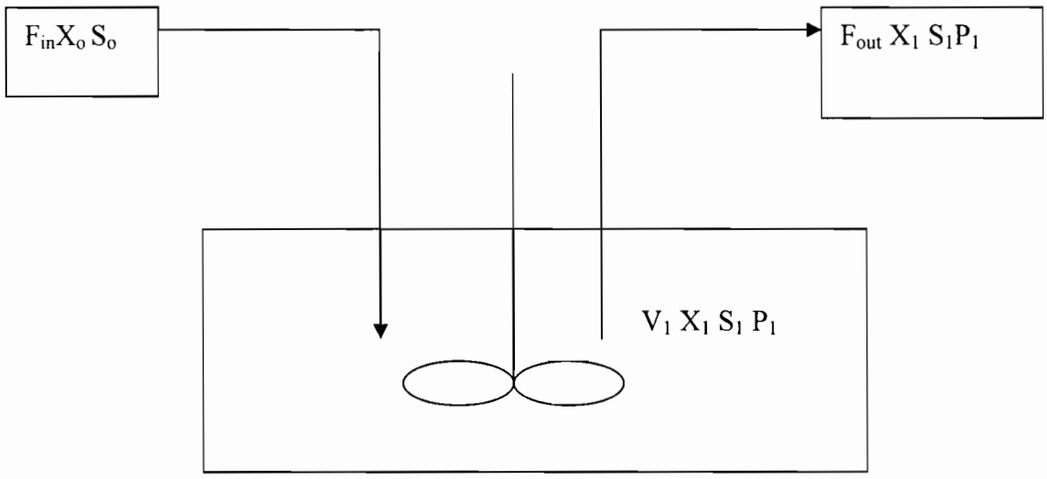

Figure 2.8: A schematic diagram of a continuous stirred tank bioreactor

2.6.4 Reactor studies

Literature on coal biosolubilisation in reactor systems is limited. Coal biosolubilisation has been carried out in three reactor configurations: the fluidised bed, the aerated tank slurry bioreactor and the packed bioreactor. The efficiencies of coal biosolubilisation in these reactors are compared in Table 2.6 while the properties of the reaction are compared qualitatively in Table 2.7. These reactors were all operated at laboratory scale.

Table 2.6: Efficiency of reactors used in coal biosolubilisation

Reference	**Reactor Type**	**Efficiency based on coal weight loss**	**Efficiency based on Absorbance at 450 nm**
Scott *et al.* (1994)	Tapered fluidised bed		40%
Gokacy *et al.* (2001)	Aerated stirred tank reactor		30%
Wilson (1987)	Packed bed reactor		8-10%
Holker and Hofer (2002)	Airmix II solid state bioreactor	9.7%	

The stirred aerated slurry reactor provides effective O_2 mass transfer and liquid transfer, as well as effective mixing, but has a disadvantage of microbial damage as result of agitation (Table 2.7). The fixed–bed or packed bed reactor causes minimal microbial damage due to particle attrition owing to the static bed, but restricted internal mass transport is further aggravated by channeling or maldistribution. The fluidised bed is effective in enhancing mass transfer. The effect of shear and turbulence are smaller than the stirred tank reactor (Garcia Ochoa *et al.* 1999). Fluidisation overcomes operational problems such as bed clogging and high pressure drop in packed bed reactors.

Table 2.7: Comparison of reactor configuration in coal bioconversion (Compiled from Sokol, 2003; Scott, 1990; Kaufman *et al.* 1995).

Characteristics	Slurry reactor	Fixed bed reactor	Fluidised bed reactor
Mass transfer	Good	Poor	Good
Microbial damage due shear forces	Yes	No	Yes
Clogging	No	Yes	No
Adequate Mixing	Yes	No	Yes
Retention time	Low	High	Low

Asif *et al.* (1993) developed a mathematical model for the distribution of coal during biosolubilisation in a fluidised bed (Equation 2.8). The model is based on the particle dispersion and convection. Equation 2.8 is governing mass balance equation for particles of species i present in the fluidised bed bioreactor.

$$\frac{\partial Ci}{\partial t} = \frac{\partial}{\partial z}\left[Di\left(\frac{\partial Ci}{\partial z} - \frac{Ci}{\rho}\frac{\partial \rho}{\partial z} \right) - UiCi \right] \qquad \textbf{Equation 2.8}$$

where C_i is the fractional volumetric concentration of particle species i

ρ is the density of the solid particles of species i, kg m^{-3}

D_i is the dispersion coefficient of particles i, $m^2 s^{-1}$

z is the distance along the mixing region in the bed, m

U_i is the velocity of particle i, m s^{-1}

This model can be used to predict transient and steady state behaviours of coal particles in a fluidised bed bioreactor. This does not account for the effect of microbes or dissolved catalysts on coal particle or density.

2.7: EFFECTS OF PROCESS CONDITIONS ON COAL BIOSOLUBISATION

2.7.1 Effect of operating variables

The utilisation of biosolubilised coal for further biotransformation processes require s continuous and adequate supply of these biosolubilised products. Several factors are important in the optimisation of gas–liquid-solid bioprocesses of which coal solubilisation is an example. Six main factors have been identified from the literatures that are critical in such processes (Bailey and Hansford, 1993; Garcia Ochoa *et al.,* 1999; Fakoussa and Frost, 1999; Gokacy *et al.,*2001).

- Coal particle size
- Nutrient requirements
- Coal and humic acid concentration
- Oxygen availability
- pH
- Coal loading

2.7.1.1 Solid loading

Coal loading is the ratio of solid particles to liquid medium and is also called the pulp density. The presence of a high concentration of particles has significant effect on bio-oxidation of sulphide concentrates by limiting oxygen concentration, inhibition of cells and mechanical destruction of organisms (Bailey and Hansford 1993). Scholtz-Brown (1998) and Harrison *et al.* (2003) showed that agitation of stationary phase *Saccharomyces cerevisiae* in the presence of a chemically inert quartzite solid phase in a slurry reactor at 5 % (v/v) and 750 rpm, caused significant disruption of the cell wall. Furthermore, Lamaignere (2003) showed that at a solid loading of 2 % (v/v), *Saccharomyces cerevisiae* growing in a stirred tank slurry reactor had a lag phase of 6.5 hours as compared to a lag phase of 3 hours in the absence of solids. At 5 % (v/v), no cell growth was observed.

Nemati *et al.* (2000) investigated the effect of solid loading on the rate of bioleaching of pyrite by *Sulfobus metallicus* in a stirred tank slurry reactor. They showed that the optimum solids concentration for bioleaching under these conditions was 9 % (v/v). At solid loadings of 12-15 % (v/v) there was a decrease in cell concentration. This was further corroborated by Sissing and Harrison (2003) who showed that in the presence of 24 % (v/v) solid loading of inert silica, there was no metabolic activity of *Sulfobus metallicus* in the slurry reactor containing 3% pyrite. Bailey and Hansford (1993) showed that solids loading tolerated is controlled by oxygen transfer rate (OTR) relative to the oxygen utilisation rate. The required oxygen is a function of both solids present (solids loading) and the grade of mineral (pyrite content/ amount available to react). They reported a maximal solid loading of 20% for a high grade ore and 60% for a low grade ore.

There are few studies on the effects of solid loading on coal biosolubilisation. Gokacy *et al.* (2001) reported that a coal loading at 10% (w/v) had a higher coal solubilisation than at 5 %(w/v). Their study was carried out, using untreated coal of particle size fraction of 1-2mm, at 30^{0}C, under aerobic conditions in shake flask conditions.

2.7.1.2 Particle size

Coal particle size is also an important factor to consider in coal bioconversion. The milling of coal to provide the necessary size fraction is an energy intensive operation. In addition, particle size affects fluid flow and the pressure drop in the reactor system. Specific surface area for reactivity of particles is an inverse function of particle size for surface reactions (Levenspiel, 1972) as shown in Equation 2.9.

$$A = \frac{6}{dD_p} \qquad \textbf{Equation 2.9}$$

where A = specific surface area ($cm^2 g^{-1}$)

d = density of lignite ($g\ cm^3$)

D_p = the average particle diameter (cm)

Since coal solubilisation is a surface phenomenon, small particle sizes are expected to give high reaction rates (Gokacy *et al.* 2001). Based on the calculation of surface area and the assumption of reaction area controlling the process rate, it is expected that rate of biosolubilisation will be inversely proportional to particle diameter.

Drossou (1986) showed that the mesophilic bio-oxidation rate of gold bearing sulfide ores is directly proportional to the surface area of concentrates (Equation 2.10).

$$\text{Bio-oxidation rate} = \frac{A}{T} \qquad \textbf{Equation 2.10}$$

where A= surface area of concentrates (kg m^{-2})

T= Time (days).

This is in agreement with the results of Nemati *et al.* (2000) for the thermophilic bioleaching. Nemati *et al.* (2000) reported that a particle size fraction of 25-45 micron with a mean diameter of 42.5 μm of a size fraction yielded the highest bioleaching rate in the bioleaching of pyrite by acidophilic thermopile, *Sulfolobus metallicus* across the range 6 to 150 μm. On decreasing the particle size to a mean diameter of 6.4 μm there was cell damage and a loss of the oxidising ability. They further explained that decreasing the particle size below the optimum particle size fraction of 25-45 μm could increase the extent of the particle-particle collision and impose severe attrition on the cells. Hence Nemati *et al.* (2001) recognised both the surface area effect on leaching and the particle number effect on damage. Pearce (1993) investigated the effect of the particle size of quartize on the disruption of *Saccharomyces cerevisiae.* The particle size ranged from 114-1245 μm. She observed that the extent of disruption increased significantly with increasing particle size from 114 to 304 μ m (60%) and then reached a maximum of c omplete disruption maintained across particle sizes of 450 to 1245 μm. It was recognized that cell damage increased with increasing momentum of collision until a certain critical momentum was reached. Hence, it is clear that particle size influences cultivation and leaching of a solid medium through several factors. These include surface area for reaction, number of particle-cell interactions and intensity of particle-cell interactions. The relative contribution of these may be expected to vary based on the micro-organism and the nature and size of the particulate.

Biosolubilisation of coal will produce a broad distribution of particle sizes. As the coal particles solubilise, they will gradually become smaller. The effect of particle size on coal biosolubilisation has been investigated both in cell–free (isolated enzyme) and whole cell systems under shake flask conditions (Gokacy *et al.,* 2001; Cohen *et al.,* 1987).

Cohen *et al.* (1987) compared three different size fractions of leonardite (oxidised coal) using a cell free-enzyme: 149-250 μm, 106-149 μm and < 106 μm. They found that the particle fraction with diameter less than 105 μm showed the highest extent of solubilisation (Table 2.8). Above this size fraction, there was no significant effect in particle size difference. Conversely, Gokacy *et al.* (2001) reported that the lignite particle size fraction of 1-2 mm showed higher dissolution than the particle size fraction of 150-185 μm, using a whole cell culture. They postulated that inhibition occurred in the presence of the small particle size (as illustrated by Nemati *et al.* (2001) in the thermophilic mineral bioleaching system). Hence the influence of particle size on coal solubilisation has not yet been resolved.

Table 2.8: Effect of particle size on solubilisation of pre-oxidised coal (Source: Cohen *et al.* 1987)

Particle size fractions(μm)	Absorbance at 3 hours (450 nm)
+149-250	0.5
+105-149	0.5
-105	1.5

2.7.1.3 Nutrient requirements

Faison (1991) reported that fungi are able to grow on coal particles by utilising the low molecular weight mobile fraction as a source of carbon; however detail of the nature of these organic sources is not available in the literature. Different carbon sources have been used in an attempt to induce growth of fungi on coal based substrates (Gokacy *et al.* 2001, Hofrichter and Fritsche, 1997). These studies indicated the need for additional carbon source such as glucose for effective biosolubilisation. Gokacy *et al.* (2001) compared growth at 2 g l^{-1}, 10 g $l^{-1}$and 20 g l^{-1} glucose concentrations. The 10 g l^{-1} glucose concentration produced the highest extent of coal solubilisation. They further compared coal biosolubilisation, following growth of *Phanerochaete chrysosporium* on glucose or acetate, both at the same concentration of 10 g l^{-1}. Prior growth on acetate induced higher coal biosolubilisation. Maximum biomass concentration attained on glucose was 100 mg l^{-1} as against 30 mg l^{-1} on acetate. However the maximum coal biosolubilisation, measured spectrophotometrically as colour release at 450 nm, following growth on acetate was 4-fold higher than observed for glucose.

Holker *et al.* (1995) showed that the ability of the fungus *Fusarium oxysporium* to solubilise lignite depended on the presence of a specific carbon source. When grown on glucose, the fungus was unable to solubilise coal. When grown on the organic acid gluconate, it solubilised lignite.

2.7.1.4 Coal humic acid concentration

Solubilisation of low rank coal which leads to the formation of humic acids and depolymerisation of coal humic acids are essential processes in coal bioconversion. Fakoussa and Hofrichter (1999) optimised the concentration of humic acid for coal depolymerisation. They found that a humic acid concentration of 0.1 to 2 g l^{-1} resulted in a high extent of depolymerisation within 2 weeks of incubation. Above these concentrations, the reaction was inhibited.

2.7.1.5 Oxygen availability

Oxygen transfer is often a rate-limiting step in aerobic bioprocesses due to the low solubility of oxygen in the medium (Doran, 1995). The oxygen demand is a function of the culture growth phase, carbon nutrients, pH and the nature of the desired microbial process, i.e., substrate utilisation, biomass production, or product yield (Bailey and Ollis, 1986). The oxygen demand is presented in Equation 2.11.

$$\frac{dC_L}{dt} = OTR - OUR \qquad \textbf{Equation 2.11}$$

Oxygen utilisation rate can be determined from reaction stoichiometry. This is shown in Equation 2.1.

The mass transfer capability of a bioreactor system is represented by the product of the overall volumetric mass transfer coefficient (K_La) and the oxygen concentration driving force. The K_La can be determined experimentally or estimated from correlations for a specific reactor design. For stirred tank bioreactors, K_La can be correlated with u_s, the superficial gas flow rate (m s^{-1}) and the power input per unit volume P_g/V (W m^{-3}) according to the form shown in Equation 2.12 (Prosser, 1995):

$$K_L a = k\, u_s^{\alpha} \left(\frac{P_g}{V} \right)^{\beta}$$ **Equation 2.12**

The parameters k, α *and* β are defined for a specific system; with typical values listed in Table 2.9. Other correlations replace u_s by the volume gas flow rate Q and P_g/V by the agitation rate N.

Table 2.9 Parameters values for K_La correlation in stirred tank bioreactor

Medium	k	α	β	Agitator	Reference
Coalescing	0.025	0.5	0.4	Six-bladed Rushton Turbines	Moo-Young and Blanch (1981)
	0.00495	0.4	0.593	Six-bladed Rushton Turbines	Linek *et al.*(1987)
	0.01	0.4	0.475	Various agitators	Moo-Young and Blanch (1981)
	0.026	0.5	0.4	Not specified	Van't Riet (1979)
Noncoalescing	0.018	0.3	0.7	Six-bladed Rushton Turbines	Moo-Young and Blanch (1981)
	0.02	0.4	0.475	Various agitators	Moo-Young and Blanch (1981)
	0.002	0.2	0.7	Not specified	Van't Riet (1979)

Other variables, like solid concentration and apparent viscosity, may also affect the volumetric mass transfer coefficient in stirred tank reactors. Oguz *et al.* (1987) developed an empirical relationship for K_La as a function of relative viscosity using data collected from a range of mineral slurries. The correlation is given in Equation 2.13.

$$k_L a = 6.6 \times 10^{-4} (\mu_{rel})^{-0.39} (Q)^{0.5} (P/V)^{0.75}$$ **Equation 2.13**

where μ_{rel} is the relative slurry viscosity

Q is the gas sparge rate (L min^{-1})

(P/V) is the power input per unit volume (Kw m^{-3})

Above a critical solid concentration there is a substantial increase in viscosity which corresponds to a decrease in the K_La. Derksen *et al.* (1999) used the correlation of Oguz *et al.* (1987) without the relative viscosity parameter to predict K_La for silica and pyrite slurries at different gas flow rates. They obtained better results for the silica slurry than the pyrite slurry. This may be due to the effect of the solid slurry properties and is agreement with the hypothesis by Rao (1977) that the critical solid concentration is dependent on the particle size and material. Above this concentration, there was a significant decrease in K_La.

In bubble columns which are similar to fluidised bed bioreactors, the general K_La correlation is shown in Equation 2.14 as a function of superficial gas velocity. The key parameters are the superficial velocity and the liquid properties (Blanch and Clark, 1997). Typical values of α and β are in Table 2.10.

$$K_L a = \alpha\, u_s^{\beta} \qquad \textbf{Equation 2.14}$$

Table 2.10: Parameters values for K_La correlation in bubble columns (Blanch and Clarke, 1997).

Liquid phase	Sparger Type	DT(cm)	HT (cm)	v_s (cm/sec)	α	β
Sulphite solution (0.3N)	Single Orifice	7.7-60	90-350	3.0-22.0	0.42	0.93[2]
Sulphite solution (0.3N)	Single Orifice	15.2	400	3.0-22.0	0.24	0.9[33]
Water	Multi-Orifice	20	723	0.2- 9.0	0.73	0.96[34]
0.7N Na_2S0_4	Multi-orifice	20	723	0.2-9.0	0.75	0.80

Liquid mass transfer in packed bed bioreactor depends on the surface area of the solid particles, the efficiency of wetting of the solid particles by the flowing liquid phase, the gas-liquid flow pattern. The mass transfer in packed bed bioreactor can be described by Equation 2.2.

$$D_{ax,L}\frac{\partial^2 C_L}{\partial Z} = u_L\frac{\partial C_L}{\partial Z} + h_L\frac{\partial C_L}{\partial t} + \frac{3(1-e)}{R}D_{ef,L}\frac{\partial C_{L\ in}}{\partial r}\Big\|_R fe$$

where C_L, C_{Lin} and $D_{ax,\,L}$ are the external and internal liquid phase concentrations and the axial dispersion coefficient, respectively; u_L is the liquid phase superficial velocity, h_L the liquid hold up, $D_{ef,L}$ the internal effective diffusivity and f_e the wetting efficiency.

2.7.1.6 pH value

The influence of pH on rate of biosolubilisation of oxidised coal has been reported (Quigley *et al.* 1988; Cohen *et al.* 1987). Their studies showed that oxidised coal is better solubilised at a pH range of 5.2-5.8. However, the rate of biosolubilisation of native coal is not a function of pH. Holker *et al.* (1995) and Larboda *et al.* (1997) reported that there was no correlation between increase in pH and coal solubilisation. This suggested that the alkaline buffer used for pre-treatment of coal might account for the increase in colour absorbance. Absorbance of the supernatant at 450 nm was used as a qualitative tool for coal biosolubilisation in these studies.

2.8: POTENTIAL USES OF THE COAL BIOSOLUBILISATION PROCESS

Coal biosolubilisation offers new options for utilisation of low rank coal. These include coal purification, facilitation of transportation of liquid fuel from coal and production of diverse range of specific low-molecular weight products (Ralph and Catcheside, 1999). The use of solubilised coal to enhance coal or water slurries is advantageous in transportation of liquid fuel. It also has potential as a form of coal purification before combustion and may find an appropriate market in clean solid–fuel technologies (Klein *et al.* 1999).

Biosolubilised coal has ion exchange, chelating and non-specific absorptive properties that may be useful in agricultural applications as a soil conditioner or for water treatment (Faison, 1993).

Aromatic compounds derived from coal biosolubilisation provide a reservoir of substrates that can potentially be accessed for enzymatically catalysed bioconversion processes to produce valuable products such as antioxidants (Ralph and Catcheside, 1997). Examples of antioxidants are butylated hydroxyanisole (BHA), butylated hydroxytoluene (BHT) and reseveratrol. BHA and BHT are used as preservatives in foods and cosmetics. It has been demonstrated that polyhydroxyalkanoate (PHA), synthesising bacteria can grow in the presence of biosolubilised coal and accumulate intracellular PHA, using the coal humates as carbon source (Fuchtenbusch and Steinbuchel, 1999). Industry has increasing interest in PHA, not only for packing materials but also for medical and pharmaceutical applications and as a source for the synthesis of enantiomeric pure chemicals (Klein *et al.* 1999).

2.9: CONCLUSIONS

The ability of microorganisms to grow on coal, especially low rank coal (lignite and sub-bituminous coal) and to modify its physico-chemical properties is well established in the literature (Cohen and Gabriele 1982; Fakoussa 1981). High rank coal is much more resistant towards fungal attack than low rank coal because of its high hydrophobicity, high proportion of condensed aromatic rings and low oxygen content (Fakoussa, 1994).

Structural modification of coal by microorganisms involves two processes, namely solubilisation and depolymerisation (Hofrichter and Fakoussa, 2001). Coal biosolubilisation leads to the formation of black liquid through a mainly non enzymatic process that occurs at high pH values (Hofrichter and Fakoussa, 2001). The mechanisms involved in coal biosolubilisation are the production of alkaline substances, chelating agents, surfactants and hydrolytic enzymes. Depolymerisation involves the cleavage of bonds inside the coal molecule, leading to the formation of fulvic acid-like compounds. This results from activities of oxidative enzymes (peroxidases such as manganese peroxidase and lignin peroxidase, phenol oxidases, laccases) (Ralph and Catcheside 1994; Hofrichter and Fristche 1997b).

The process of lignite solubilisation occurs more in Deuteromycetes (e.g. *Trichoderma atroviride, Fusarium* spp) and certain bacteria, while the depolymerisation of coal has evidently been limited to Basidimomycetes (wood-decaying and litter–decomposing fungi, e.g. *Phanerocheate chrysosporium* (Klein *et al.* 1999). Solubilisation and depolymerisation of coal are facilitated when coal particles are pre-oxidised chemically or physically before bioconversion (Scott *et al.* 1986; Ward *et al.* 1993; Achi, 1993).

Scott *et al.* (1986) reported that results of infrared spectroscopy (IR) and nuclear magnetic resonance (NMR) studies on the biosolubilised coal product suggest that the product is aromatic in nature, possibly containing aromatic hydroxyl phenolic groups. The yield of solubilised coal product is reported to be low (Holker and Hofer, 2002; Laborda et *al.* 1999) while in some publications these coal derived-monomers are absent (Ralph and Catcheside, 1997). There is need to establish whether solubilised products are taken up by fungal cells. Other possible products from coal solubilisation that have been reported in the literature include propionic acids, butanediol and ethanol (Andrews, 1991).

Small volumes of solubilised coal products are currently available as raw materials for further bioprocess reactions. The reason for this is that solubilisation of low rank coal is currently limited to laboratory-scale study using P etri dishes or Erlenmeyer flasks of moderate volume (Ward 1993; Gokacy *et al.* 2001). There are some reports of coal biosolubilisation in bioreactors of mini-to-pilot scale (Scott *et al.* 1986; Holker and Hofer, 2002). Large scale designs for coal biosolubilisation bioreactors are constrained by several problems encountered in the control of parameters such as pH, temperature, aeration, mass and oxygen transfer and agitation. An appropriate reactor configuration that takes into account biocatalyst concentration, mass transfer between interacting phases and, ultimately, economic feasibility must be developed.

In conclusion from review of the literature, low yields of product from coal biosolubilisation and small volumes of solubilised products are currently attained. These are critical in economic development of the coal biosolubilisation process. This leads to the main objectives of this study which include optimisation of key operating variables for coal biosolubilisation and development of a methodology by which fungal growth can be quantified in the slurry reactor system. Comparisons of the stirred tank slurry bioreactor,

the fluidised bed bioreactor and the fixed bed bioreactor configurations for the fungal biosolubilisation of coal are also investigated to further inform reactor selection.

CHAPTER 3
EXPERIMENTAL PROCEDURE

This chapter describes the experimental procedure used to investigate and optimise key operating variables of the solubilisation and depolymerisation of low rank coal. Section 3.1 describes the materials and methods for fungal growth. Section 3.2 describes the equipment in terms of reactor systems used and standard their experimental conditions. Section 3.3 describes the analytical techniques used. In Section 3.4, the experiments used to determine their operating conditions for optimal coal biosolubilisation are described, including both factorial and single variable approaches. Section 3.5 describes the mineralisation experiments used to evaluate role of enzymes and volume of carbon dioxide produced. Section 3.6 describes the experimental approach to determine the best reactor configuration for coal biosolubilisation. Section 3.7 provides the approach to analysis of process kinetics.

3.1 EXPERIMENTAL MATERIALS

3.1.1 Microorganisms

The fungal strain, *Trichoderma atroviride* (ES 11) was obtained from the laboratory of Prof. D Cowan at the University of the Western Cape, South Africa. This fungal strain was isolated from soil samples. It was maintained on 3% malt extract agar plates at 4^0C for up to 6 months. These plates were used for inoculum preparation.

3.1.2 Coal

Sub-bituminous coal from SASOL (SA) was used. Coal samples were dry sieved into 1500-2000 μm, 600-850 μm and 150-300 μm size fractions using laboratory sieves. The dry coal samples were autoclaved at 120^0C for 20 min. An approximate chemical analysis of the SASOL coal sample was performed using micro analysis by the Department of Chemistry, UCT.

The elemental composition in laboratory of C, H, N, and S closely approximated the chemical formula reported in the literature for sub-bituminous coal by Andrews (1991). This is shown in Table 3.1. Hence this literature formula $CH_{0.8}O_{0.22}N_{0.02}S_{0.01}$ was used to represent the coal in these studies.

Table 3.1 Elemental analysis of coal (wt %)

	Sample	C	H	N	S	H/C	N/C	S/C
Mass %	**Andrews**	**74.1**	**4.9**	**1.7**	**2.0**	**0.066**	**0.023**	**0.027**
	This study	**59.9**	**3.7**	**1.5**	**1.3**	**0.062**	**0.025**	**0.022**
Molar %	**Andrews**	**54.8**	**43.0**	**1.06**	**0.55**	**0.79**	**0.02**	**0.01**
	This study	**50.96**	**37**	**1.09**	**0.41**	**0.73**	**0.02**	**0.01**

3.1.3 Inoculum preparation and propagation

The pre-inoculum was prepared by cutting five plugs of fungal culture from the stock plates with a 5 ml sterile Pasteur pipette tip and inoculating these into 100 ml sterile growth media. The growth medium contained 0.1% (w/v) coal of 150-300 μm size fractions. Ten glass beads (6mm diameter) were added and the culture was incubated for 4 days at 28^{0}C in an orbital incubator shaker at an agitation rate of 120 rpm. The inoculum was prepared by transferring a 10 ml aliquot of the pre-inoculum culture into 100 ml fresh growth medium. The inoculum was cultured for 2 days at 28^{0}C with agitation at 120 rpm.

3.1.4 Growth medium and culture conditions

The inoculated reactor used 900 ml of growth medium and 100 ml of 48 h inoculum. In shake flask experiments, 90 ml growth medium and 10 ml inoculum were used. The growth media used for agar plates, inoculum preparation and experimental studies contained (per litre): 1 g $NH_4(SO_4)$, 3 g malt extract, 0.52 g $MgSO_4.7H_2O$, 7.6 g KH_2PO_4,

0.005 g $FeSO_4.7H_20$ and 0.003 g $ZnSO_4.7H_2O$. The standard growth medium was supplemented with 10 g glucose per litre, unless otherwise stated. The growth medium was selected through optimisation studies in the laboratory of Prof Don Cowan in the University of the Western Cape (Personal communication).

3.2 EQUIPMENT

3.2.1 The stirred tank reactor

Experiments were carried out in a 2 L jacketed Z61104CT04 Applikon autoclavable bioreactor made of borosilicate glass. The bioreactor had a height to diameter ratio (H/D) of 1.32 and working volume of 1 litre. The bioreactor was maintained at constant temperature of 28^0C by circulating water from a Grant Y6 constant temperature bath through the bioreactor jacket (Figure 3.1). The geometry of the reactor is shown in Table 3.2.

The mixing and gas dispersion was achieved by a pitched (45^0) six-blade turbine impeller rotating at 560 rpm, located 2 cm from the base of the bioreactor. The impeller was driven by a flexible coupling, linked to an Applikon P100 motor and Applikon 1012 stand–alone speed controller. Inlet gas was supplied by Peak Scientific OAG200DA oil-less air compressor. The flow rate was set at 350 ml min^{-1} by a Brooks model 5850S mass flow controller. The CO_2 concentration of the bioreactor off-gas was determined using a Hartmann & Braun Uras 4 NDIR (non-dispersive infrared) industrial photometer and the O_2 concentration determined using a Hartmann & Braun Magnos 6 G oxygen analyser.

Table 3.2 Geometry of the stirred tank reactor

Symbols denote the following: T: tank diameter; Height: height of liquid in vessel; B_i: baffle width; C: impeller clearance above the vessel base; D: impeller diameter; L: length of impeller blade; W: width of impeller blade

Dimension (mm)		**Dimension ration**	
Vessel		**Vessel**	
T	100	H/T	1
H	100	B_i/T	0.15
B_i	15	C/T	0.2
C	20		
Pitched-blade Impeller		Pitched-blade Impeller	
D	50	D/T	0.5
L	12.5	L/D	0.25
W	8	W/D	0.16
Blade angle	45^0		

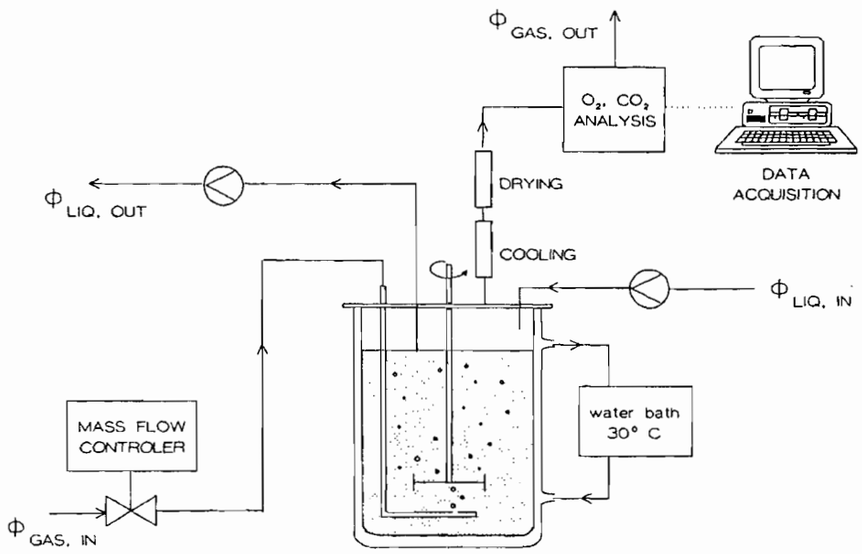

Figure 3.1: Applikon bioreactor set-up used, including controlled air supply through the mass flow controller and on-line off-gas analysis. (Breed *et al.* 1999)

3.2.2: The fluidised bed bioreactor

The fluidised bed reactor was 50 cm in length with an inner diameter of 10 cm and an outer diameter of 12 cm. The bioreactor design incorporated an internal gas-liquid-solid separation area to permit the settling of solids (microorganism and coal). Prior to its entering the fluidised bed, dry air was humidified by bubbling into sterile water. This humid air was used to fluidise the bed of coal at flow rates of 0.46 cm s^{-1} and 0.64 cm s^{-1}. The working volume of the fluidised bed reactor was approximately 2 litres, with a solid loading of 5% (w/v) and 10 % (w/v) used as specified for each experiment. The reactor set-up is shown in Figure 3.2. A schematic diagram of the fluidised bed bioreactor and the fixed bed bioreactor is presented in Figure 3.4.

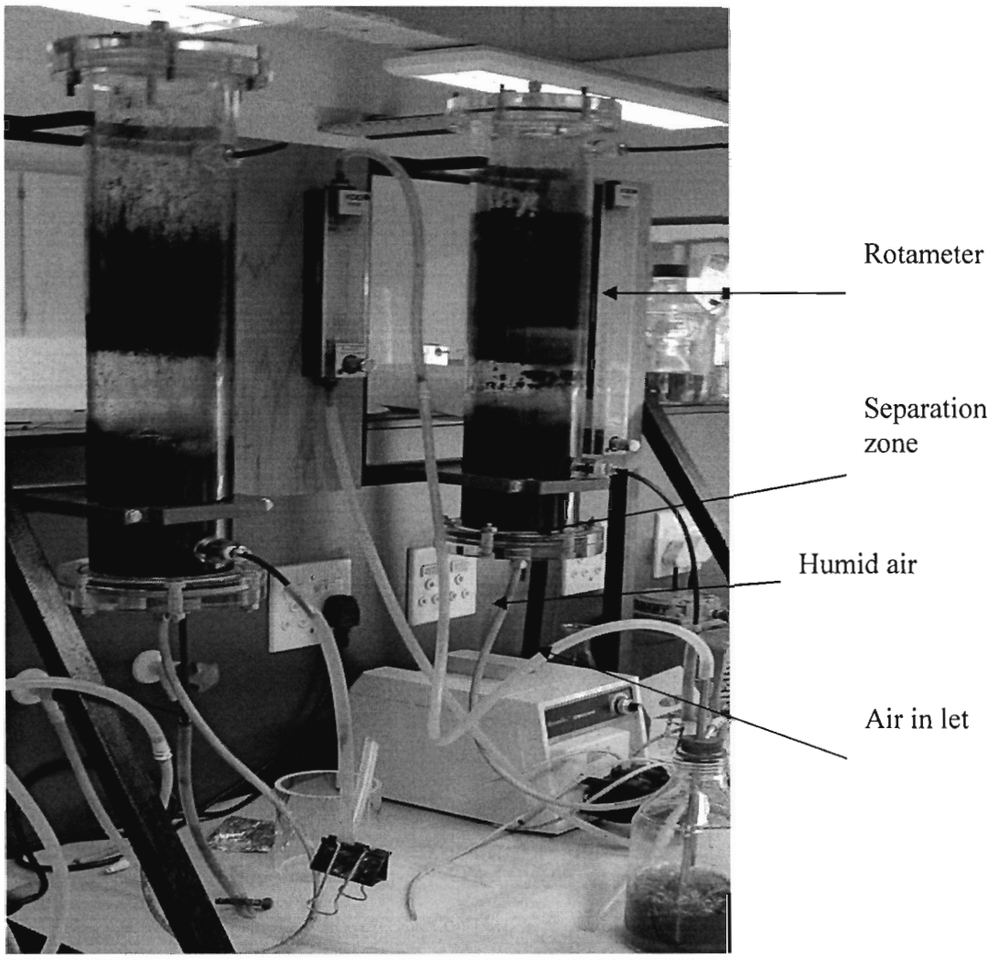

Figure 3.2: Experimental set-up of the fluidised bed bioreactor

3.2.3: The fixed bed bioreactor

The fixed bed bioreactor was 50 cm in length with an inner diameter of 10 cm and a 12 cm outer diameter. The lower plate used for coal packing has a sieve size of 6 mm diameter. The bed was packed with 50 g glass beads (5 mm) to increase the bed height and 200 g sub-bituminous coal (4 mm). Initially, 15ml of inoculum (5-days old) was applied to the top of the bed. Thereafter the liquid growth medium was pumped at 33 ml min^{-1}, 23 ml min^{-1} and 12 ml min^{-1} between time 0 to 24 hours, 24 to 72 hours and 96 to 336 hours respectively. The feed rate was decreased due to reduced bed porosity caused

by fungal presence. This caused an increase in the residence time of the liquid feed. The reactor set-up is shown in Figure 3.3. The schematic representation of the fixed bed and the fluidised bed bioreactors is shown in Figure 3.4.

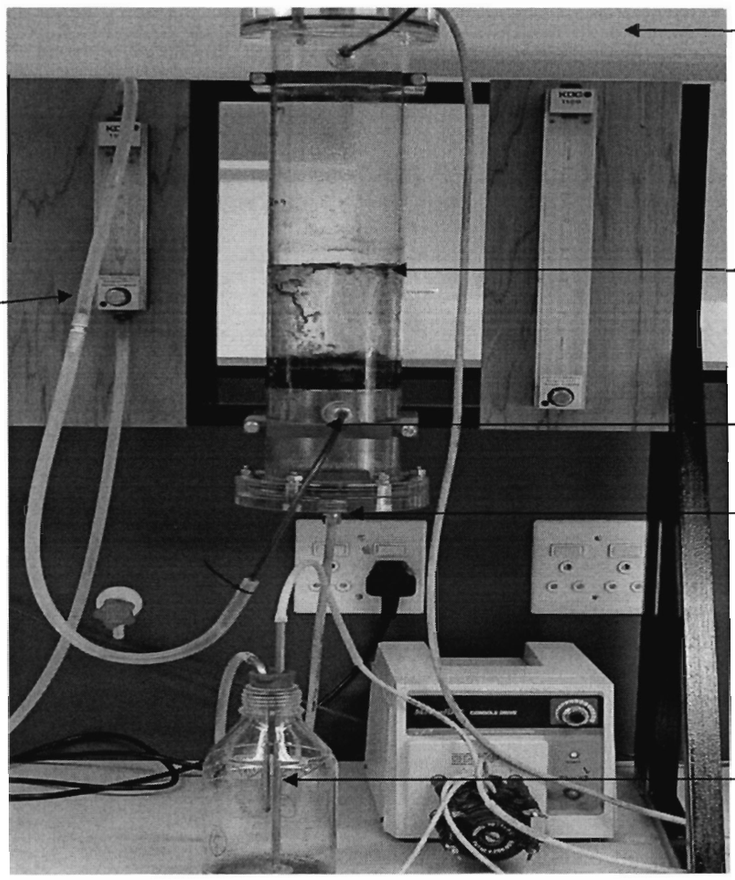

Figure 3.3: Experimetal set-up of the fixed bed bioreactor

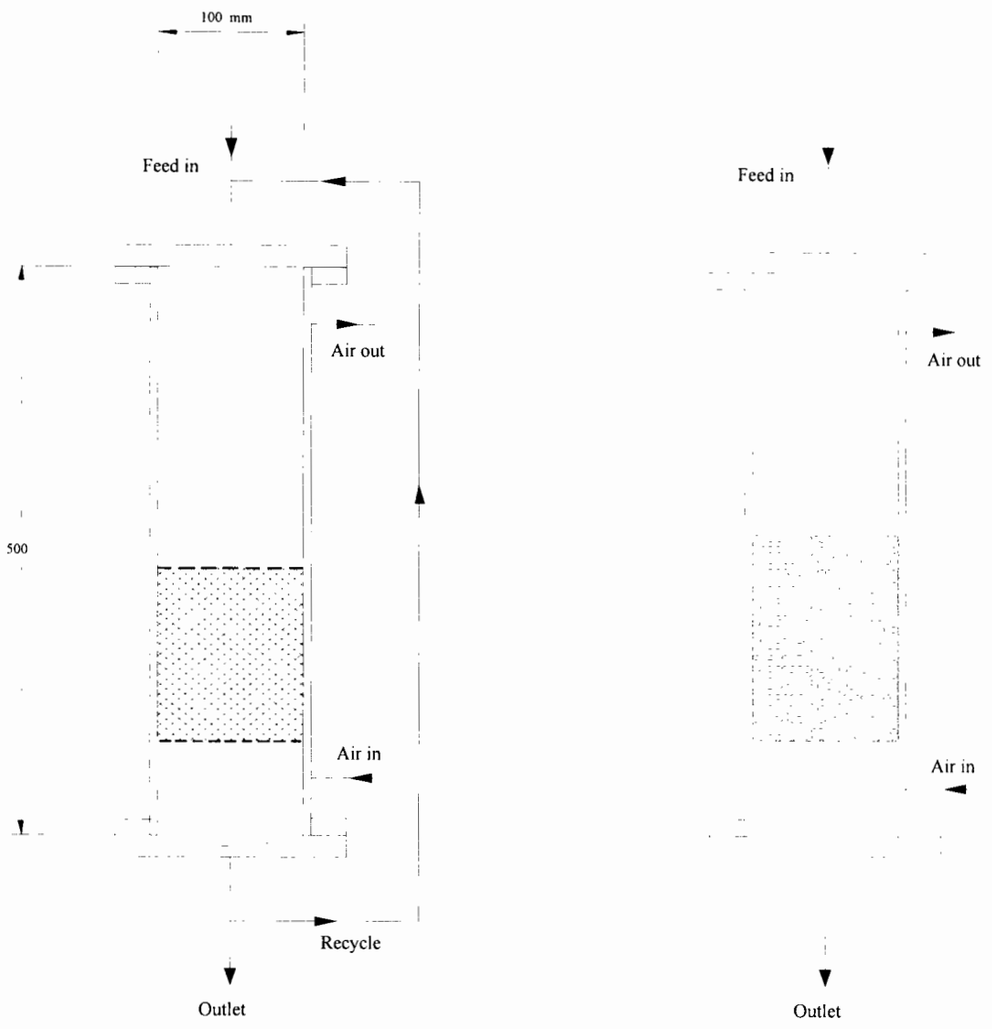

Figure 3.4: Schematic representation of the fixed bed and the fluidised bed bioreactors

3.3 ANALYTICAL TECHNIQUES.

Coal biosolubilisation was monitored qualitatively by measuring the increase in absorbance at 450 nm and quantatively by measuring coal weight loss and total dissolved solids present. Other parameters measured are total organic carbon (TOC), pH, glucose concentration, biomass concentration, concentration of phenolics, oxygen utilisation rate (OUR) and carbon dioxide production rate (CPR). Analytical protocols are given in detail in Appendix A.

3.3.1 Absorbance

Coal biosolubilisation was measured qualitatively by different researchers by measuring the colour absorbance at 450 nm (Cohen *et al.* 1987; Larboda *et al.* 1997; Fakoussa and Frost, 1999; Gokacy *et al.* 2001; Holker and Hofer, 2002). The rationale behind this is that the liquid product includes humic acid and fulvic acids which impart a dark-brown colour; hence it displays a maximum absorbance at 450 nm. The coefficient of variance of absorbance measurements is 0.37%.

3.3.2 Total dissolved solids

A quantitative measurement of coal biosolubilisation by dry weight was carried out (Holker and Hofer, 2002) after evaporation of the supernatant at 95^{0}C for 24 hours. For the purpose of this study, supernatant was evaporated at 80^{0}C for 24 hours as detailed in Appendix A2. The coefficient of variance was 5.3%.

3.3.3 Coal weight loss

Coal weight loss was measured gravimetrically after 14 days of coal solubilisation. This was done by decanting the supernatant from the flask or reactor. The spent biomass was washed off with water. Coal samples were dried in the oven at 80°C for 48 hours. Dried coal samples were weighed on 4 place balance. This was then used to determine the extent of degradation as indicated in Appendix A3. The coefficient of variation was 6.03%.

3.3.4 Dry biomass concentration

The biomass concentration of *Trichoderma atroviride* ES 11 before the addition of coal as sole carbon source and energy source was determined by cell dry weight analysis. A 5 ml of cell suspension was filtered by vacuum filtration using a 0.45 μm membrane filter. The membrane filter and filter cake was dried in an oven at 80^{0}C for 2 days. The dry weight concentration was determined from the quotient of the dry cell mass (final minus initial weight of the filter paper) and the volume of the suspension. The coefficient of variance was 1.44%.

3.3.5 pH

The pH was measured every 48 hours with the aid of Mettler Toledo pH meter. This was carried out by placing the probe into the sample.

3.3.6 Glucose measurement

The growth of the fungus on glucose before addition of coal as carbon source increases the coal solubilising activity of the fungi (Larboda *et al.* 1997, Holker *et al.* 1995). The glucose concentration was measured by determining the reducing sugar concentration. In this method, known as the dinitrosalicylic acid (DNS) colorimetric method for glucose determination (Miller, 1959), the presence of free carbonyl groups (C=O) is tested. The carbonyl groups are oxidised as the 3, 5-dintrosalicylic acid (DNS) is reduced to 3-amino, 5-nitrosalicyclic acid. This occurs in alkaline conditions and is quantified spectrophotometrically by absorbance at 510 nm. The detailed analytical method is given in Appendix A6. The coefficient of variance was 3.16%.

3.3.7 Phenolics concentration

Total phenolic content was analysed using Folin–Ciocalteau reagent (Box, 1983). The Folin–Ciocalteau phenol reagent contains phosphomolydic and phosphotungstic acid, which are reduced to heteropoly blue in alkaline solution. The absorbance of the sample is measured at 725 nm. The phenol concentration is estimated from a calibration curve

in terms of gallic acid equivalent (GAE) concentrations. The analytical procedure is detailed in Appendix A7. The coefficient of variance for this measurement is 0.51%.

3.3.8 Total organic carbon measurement

Total organic carbon (TOC) analysis was performed in order to enable the carbon balance to be closed. The total organic carbon was quantified using an Anatoc Series II TOC analyser. This analysis is based on the oxidation of all the organic carbon in the supernatant to carbon dioxide. The Anatoc Series II TOC analyser uses a unique photocatalytic oxidation process. In the presence of UV light and oxygen, titanium dioxide catalyses the oxidation of organic compounds in an aqueous medium. This reaction yields carbon dioxide and water. The CO_2 is then quantified as the concentration of carbon, while the reaction is carried out at room temperature. The assay procedure is detailed in Appendix A8. The coefficient of variance in this measurement is 2.86%.

3.3.9 Oxygen and carbon dioxide measurement

Measurement of the carbon dioxide and oxygen concentration in the gas phase were used to estimate fungal biomass in coal biosolubilisation. Inlet gas was supplied by Peak Scientific OAG200DA oil-less air compressor. The flow rate was set at 350 ml min^{-1} using a Brooks model 5850S mass flow controller. Air was introduced via an air-inlet pipe located under the impeller. The holes in the air–inlet sparger were located on its lower side to minimise blockages. The off-gas was dried using a reflux condenser through which an ethylene/glycol mixture (75%/25%) from a Grant LTD6G low temperature bath was circulated. The low temperature bath maintained the coolant at 6 °C. Before entering the gas analyser, the off-gas was also passed through a cloth filter and a Hartmann & Braun CGEK sample gas conditioner fitted with a CGKA 1 automatic condensate outlet. The CO_2 concentration of the bioreactor off-gas was determined using a Hartmann & Braun Uras 4 NDIR (non-dispersive infrared) industrial photometer and the O_2 concentration determined using Hartmann & Braun Magnos 6 G oxygen analyser. The concentration range for carbon dioxide was within 0-500 ppm.

The carbon dioxide and oxygen concentrations in the slurry bioreactor off-gas from the stirred tank bioreactor and the inlet air were logged by computer.

3.4 IDENTIFICATION OF KEY OPERATING VARIABLES AND THEIR OPTIMISATION

The use of a factorial experimental design allows a study of multi-parameter processes in which the dominant variables and interactions can be established. In addition, it aids the search for optimum conditions (Box *et al.* 1978). In this study, two-level factorial experiments were employed to investigate the parameters of coal loading and particle size fraction. A simple linear model, shown below, was used:

$$Y= ß_o+ß_1x_1+ ß_2x_2 + ß_{12}x_1x_2 \qquad \text{Equation 3.1}$$

where Y is the measured response, x_1 is the variable i and $ß_1$ is the parameter obtained by fitting the model to the experimental results.

Analysis of a factorial experiment falls into two parts: calculation of main effects and the interaction effects, and the assessment of their significance using an ANOVA.

In order to optimise coal biosolubilisation, experiments were conducted in 500 ml Erlenmeyer flasks containing different coal and particle size distributions. The ranges studied are detailed in Table 3.3. Experiments were initiated by adding a 10 ml aliquot of the pre-inoculum culture into the respective test flasks as detailed in Table 3.4. Where coal was used as carbon source, the fungal culture was established by growth on glucose for 5 days. On its depletion, coal was added to the medium and culturing continued. These flask cultures were incubated in a rotary incubator for 14 days at 28^{0}C with agitation at 120 rpm. Samples of 5 ml were taken from the shake flask in a sterile environment at regular time intervals. These were filtered by vacuum filtration. The supernatants were analysed in terms of pH, absorbance, phenolics concentration and total organic carbon concentration. Following the washing off of biomass, residual coal was measured gravimetrically.

Table 3.3: Variables and levels of factorial design.

Variable	Coal loading(% m/v)	Particle size(μm)
Factor	X_1	X_2
High	10	1500-2000
Low	5	600-850

Table 3.4: Flask contents for the factorial experiment

Flasks	Coal loading (% m/v)l Loading	Particle size(μm)
1	5	600-850
2	10	600-850
3	5	1500-2000
4	10	1500-2000
5 Negative control (No Inoculum)	5	1500-2000
6 Positive control (No Coal)	-	-

Following selection of the smaller size fraction, the effect of solid loading was further investigated by running a series of experiments over a range of solid volume fractions of 0%, 2%, 5% and 10% at the 600-850 μm particle size fractions. Further, the effect of particle size fraction was investigated across the extended range from 150-300 μm to 600-850 μm under shake flask conditions using an agitation rate of 120 rpm and solids loading of 5 %(w/v). The same sampling and analysis protocol was carried out.

3.5 FURTHER METABOLISM OF SOLUBILISED COAL.

Scott *et al.* (1986) used infrared spectroscopy (IR) and nuclear magnetic resonance (NMR) to characterise biosolubilised coal product. They reported that bioslubilised coal product is aromatic in nature, possibly containing aromatic hydroxyl groups (phenolic). The low yields of solubilised coal product are currently reported (Holker and Hofer, 2002; Laborda *et al.* 1999). In some publications, these coal derived-monomers are absent (Ralph and Catcheside, 1997). Based on these reports and data presented in this thesis, there is a need to establish whether solubilised products released from the coal are taken up by fungal cells. It has also been suggested that biosolubilised coal can be degraded completely to CO_2 and other low–value products within a non optimised microbial system (Faison, 1991). In order to investigate the role of fungal biomass and extracellular enzymes in both coal biosolubilisation and subsequent degradation of phenolic intermediates, two different experiments were set up to investigate the mineralisation of the products.

3.5.1 Cell free experiments

In order to establish whether solubilised products are metabolised by fungal cells or further degraded by extracellular enzymes, coal biosolubilisation was carried out initially in the presence of fungal biomass. The fungus was incubated on an orbital shaker at 120 rpm at 28^0C. On the 8^{th} day of culture, the cells were removed by vacuum filtration in a sterile environment. Fresh coal was added to the culture supernatant and further incubated. Production or degradation of the phenolic compound was monitored to assess whether these processes were carried out by extracellular enzymes. The supernatants were analysed in terms of phenolic content, using the Folin reagent and spectroscopic analysis at 725 nm (Box, 1983).

3.5.2 Carbon dioxide measurement

On–line measurements of CO_2 evolution in the stirred tank slurry reactor system (discussed in Section 3.2.1) were carried out to determine if phenolic compounds and other products are mineralised further to carbon dioxide. Production of phenolics, total organic carbon and coal weight loss assays were carried out. These were used to determine the carbon balance. Carbon dioxide production rate is calculated from Equation 3.2. Derivation of Equation 3.2 is provided in Appendix B.

$$CPR = \frac{F_{in}}{V}\left[\left(Y_{CO_2}\right)_{in} - \frac{\left(Y_{N_2}\right)_{in}\left(Y_{CO_2}\right)_{out}}{1-\left(Y_{O_2}\right)_{out}-\left(Y_{CO_2}\right)_{out}}\right] \quad \text{----------3.2}$$

where CPR = carbon dioxide production rate (mmoles l^{-1} h^{-1})

F_{in} = inlet aeration rate ($l\ h^{-1}$)

$(Y\ CO_2)_{in}$ = inlet mole fraction of carbon dioxide

$(YN_2)_{in}$ = inlet mole fraction of nitrogen

$(Y\ CO_2)_{out}$ = outlet mole fraction of carbon dioxide

$(Y\ O_2)_{out}$ = outlet mole fraction of oxygen

3.6 REACTOR CONFIGURATION

Coal biosolubilisation was investigated in the stirred tank slurry bioreactor, fluidised bed bioreactor and fixed bed bioreactor. The advantages and shortcomings of each reactor configuration were assessed.

3.6.1 Stirred tank reactor experiment

Experiments were carried out in the slurry reactor system described in Section 3.2.1. Batch reaction was carried out at 5% (w/v) coal loading, with a particle size fraction of 600-850 μm. The air flow rate was set at of 350 ml min^{-1}. Samples were withdrawn using a syringe under aseptic conditions. A 10 ml aliquot was sampled every 48 hours. Samples were subjected to vacuum filtration and the supernatant was analysed for phenolic concentration, absorbance at 450 nm, total organic carbon and total dissolved solids. Residual coal was estimated gravimetrically. A carbon balance was determined over the system. Oxygen utilisation rate (OUR) in the stirred tank reactor was measured by conducting an "Oxygen Balance" across the inlet and outlet gas streams. OUR was determined from the analysis of the flow rate and oxygen concentration of these streams coming into and exiting the STR, according to Section 3.3.9..

3.6.2 Fluidised bed biorector experiment

Experiments were carried out in the fluidised bed bioreactor described in Section 3.2.2. Batch fluidisation was carried at 5 % and 10 % coal loading with a particle size fraction of 125 -300 μm and 5% coal loading with a particle size fraction of 600-850 μm. The hydrodynamic behaviour of the fluidised bed was evaluated by experimentally determining the minimum fluidisation velocity, gas hold up and dissolved oxygen concentration. Sampling was carried every 48 hours and supernatant was analysed for the production of phenolics, change in absorbance at 450 nm and total organic carbon. Gravimetric coal analysis was carried out after coal biosolubilisation. The gas hold-up was determined using the method described by Chisti in 1989 (Appendix C1). Owing to

concern that O_2 transfer limitation may occur, oxygen mass transfer was measured by the "dynamic" method using a polarographic oxygen electrode (Ingold–Mettler Toledo) (Appendix C2). The "Dynamic gassing-in-gassing-out" method is also known as the "Unsteady state" method. The "Dynamic" method was chosen over the "Oxygen Balance" owing to limited access to online off-gas analysis equipment. It was selected over the "Sulphite" method because the "Sulphite" method measures the rate of a chemical oxidation and assumes that this is limited only by the rate of oxygen transfer. This also introduces some error into the method as the reaction rate can also be affected by other factors, such as the catalyst used. Furthermore, the 50 cm height of the fluidised bed was less than the 1m maximum height stipulated for a vessel when using the dynamic method (Doran, 1995) and the average residence time of gas in the system, when deoxygenating, was quite low.

3.6.3 Packed bed bioreactor experiment

Experiments were carried out in the packed bed bioreactor reactor described in Section 3.2.3. The reactor was operated over a two week period. Liquid samples were collected for analysis of phenolic concentration, colour absorbance and total organic carbon. Gravimetric coal analysis was carried out after coal biosolubilisation. The residence time distribution experiment was conducted using a 200 g l^{-1} NaCl solution as a tracer. The residence time distribution experiment was carried out in the absence of fungi. The tracer was added in at the top of packed bed reactor using a Watson Narlow peristaltic pump (503S) with a flow rate of 33 ml min^{-1}, using the step input technique. The conductivity was recorded over time using the YSI 30-10SCT portable conductivity meter. No oxygen analysis was conducted in the fixed bed bioreactor as it was only used in preliminary studies.

3.7 BIOMASS ESTIMATION

The use of the indirect method for the estimation of the growth and metabolism of fungal biomass was investigated by measuring CO_2 evolution and O_2 consumption using an off–gas analyser. Coal biosolubilisation was carried out in a stirred tank slurry bioreactor with a working volume of 1.0 litre. Complete suspension of the coal fraction with a particle size distribution in the range 650-800 μm diameter was achieved at an agitation rate of 560 rpm. When coal was used as carbon source, the fungal culture was established by growth on glucose for 5 days. On its depletion, coal was added to the medium at 5 % (w/v) and culturing continued. Growth yield coefficients for the fungi of interest based on CO_2 evolution and oxygen consumption as well as maintenance coefficients were calculated from growth of the fungus under the same conditions using a non-coal carbon source such as glucose. These data were then used to determine biomass concentration X as function of time for coal solubilisation. This is illustrated in Chapter 5.

3.8 CHAPTER SUMMARY

The study aims to define the methodology and experimental approach used to investigate key operating variables of the biosolubilisation. The influence of the operating variables solids loading and particle size on coal biosolubilisation was investigated by factorial experiment. Coal loading and the particle size fraction distribution were studied to determine optimum conditions for coal biosolubilisation. These experiments were carried out under shake flask conditions using an agitation rate of 120 rpm. Six analytical parameters were used to assess coal biosolubilisation. These include absorbance at 450 nm, total dissolved solids (TDSS), coal weight loss, pH, phenolic concentration and total organic carbon concentration (TOC).

Two different experiments were used to investigate the mineralisation of phenolic compounds. In cell free experiments, incubation of fresh coal in the culture supernatant was used to investigate the activity of extracellular enzymes. Production or degradation

of the phenolic compounds was monitored. In cell based experiments, on-line measurement of CO_2 evolution in a stirred tank slurry reactor system was used together with monitoring of the production of phenolics, total organic carbon and loss of coal weight. These were used to determine the carbon balance. A mass balance approach, based on off-gas analysis, for the quantification of fungal biomass was developed. This was then used for the evaluation of product yield.

Coal biosolubilisation was investigated in a stirred tank slurry bioreactor, a fluidised bed bioreactor and a fixed bed bioreactor. The advantages and shortcomings of each reactor configuration were assessed. Slurry tank reactor experiments were carried out in the Applikon bioreactor. Batch fluidisation was carried out in a column reactor. The hydrodynamic behaviour of the fluidised bed was evaluated by experimentally determining the minimum fluidisation velocity, gas hold up and dissolved oxygen concentration. Coal biosolubilisation was carried out in a packed column with 200 g coal samples of 4 mm particle size and 50 g glass beads of 5 mm diameter. The residence time distribution of phenolic products was determined using a 200 g l^{-1} NaCl solution as tracer. In the three reactor configurations investigated, sampling was carried out every 48 hours and the supernatant was analysed for production of phenolic compounds, absorbance, pH and total organic carbon.

CHAPTER 4: KEY OPERATING VARIABLES IN THE COAL BIOSOLUBILISATION PROCESS

4.1 KEY OPERATING VARIABLES AND THEIR OPTIMISATION

In order to investigate the key operating variables in coal biosolubilisation in a suspended culture system, factorial design experiments were carried out. The theory as well as the experimental protocol is given in Section 3.4. Coal particle size and loading were varied across the ranges 600-850 μm and 1500-2000 μm and 5 to 10 % (w/v) respectively. The responses measured were colour absorbance, total dissolved solids, coal weight loss, pH, concentration of phenolics and total organic concentration. The data collected are presented in Figures 4.1 to 4.8 and tabulated in Appendix D. The coal weight loss data was subjected to analysis of variance (ANOVA).

4.1.1 Colour measurement

Coal biosolubilisation has been determined qualitatively by different researchers by measuring the colouration of the supernatant by absorbance at 450 nm (Cohen *et al.* 1987; Larboda *et al.* 1997; Fakoussa and Frost, 1999; Gokacy *et al.* 2001; Holker and Hofer, 2002). The rationale behind this is that liquid product from coal biosolubilisation includes humic and fulvic acids which impart a dark-brown in colour and display a maximum absorbance at 450 nm. Figure 4.1 shows colour measurement as a function of time under different experimental conditions. There was no increase in absorbance in the control tests containing growth medium only. The results also showed that there was an increase in absorbance for both fungal culture with coal and the control containing fungal culture only. The increase in absorbance was higher in the fungal culture with coal than in the fungal culture only. This suggests that there may be a correlation between release of colour and coal solubilisation. The highest increase in absorbance occurred at 5 % (w/v) coal loading and 600 to 850 μm particle size fraction. This suggests that a decrease in particle size led to a higher degree of biosolubilisation.

An increase in coal loading of the same particle size fraction is expected to lead to an increase in absorbance owing to increased substrate availability. However, from our results, 5% (w/v) coal loading resulted in higher coal biosolubilisation in terms of colour increase than the 10% (w/v) case. This suggests that optimum coal loading may occur between 5 and 10% (w/v). Increase above this optimum may be postulated to lead to inhibition of micro-organisms (ES11) that are involved in coal biosolubilisation owing to

cell damage as reported by Nemati and Harrison (2000) and Harrison *et al.* (2003) for bacterial and yeast systems. This was confirmed by monitoring the microbial culture under both conditions microscopically (Figure 4.2) where fragmentation of the fungal mycelium was observed at 10% (w/v) loading.

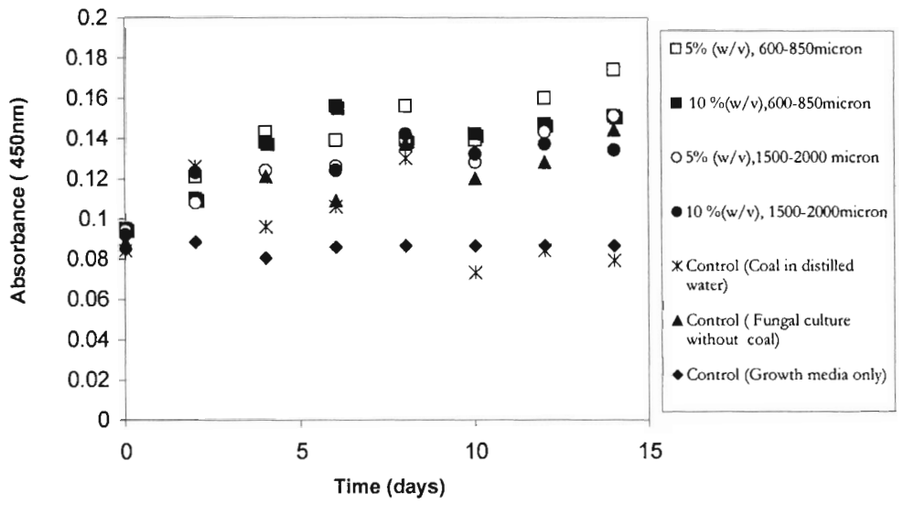

Figure 4.1: Biosolubilisation of coal by *Trichoderma atroviride* (ES 11) in shake flasks, measured in terms of colouration of the supernatant. The coal was added to a five-day *Trichoderma atroviride* culture on day 0 of the experiment.

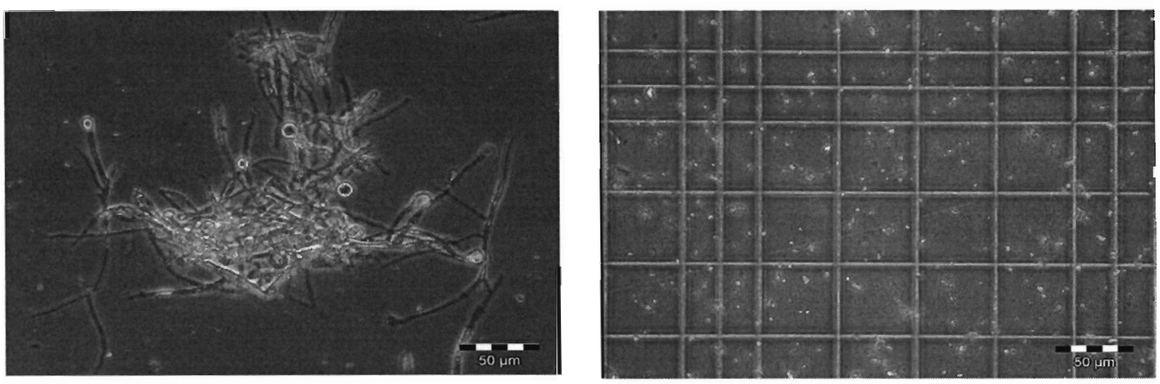

A **B**

Figure 4.2: Micrographs of coal solubilisation at day 6 of *Trichoderma atroviride* growing with coal as carbon source at (A) 5%(w/v) and (B) 10%(w/v) . Experiments were conducted in shake flasks. Magnification 40x.

4.1.2 Total dissolved solids (TDS)

Holker and Hofer (2002) and Gokacy *et al.* (2001) measured coal biosolubilisation quantitatively in terms of total dissolved solids. Figure 4.3 shows the TDSS concentration as a function of time. Less coal was dissolved in the control experiment containing coal and distilled water. There was no dissolved coal in the control test containing coal and distilled water after day 8 of incubation.

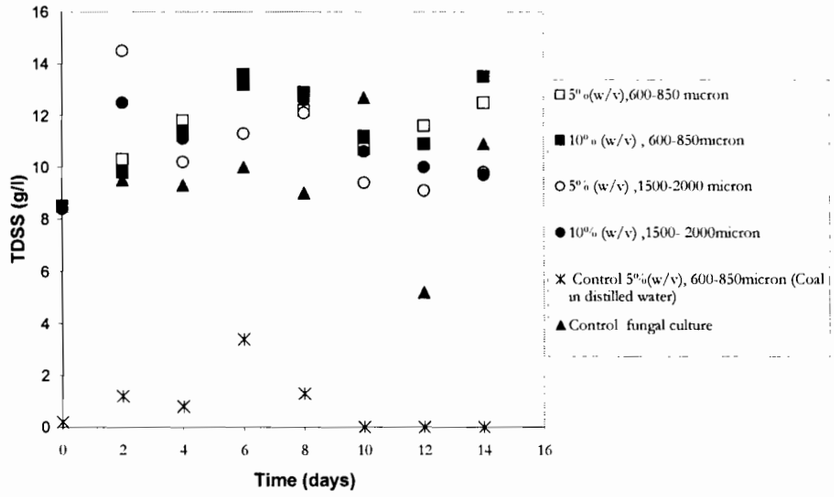

Figure 4.3: Total dissolved solids as measure of coal solubilisation by *Trichoderma atroviride*. Experiments were conducted in shake flasks. The coal was added to a five-day culture on day 0.

The difference in the amount of TDSS resulting in cultures with and without coal (Figure 4.3) was negligible. Holker and Hofer (2002) reported a direct relationship between coal biosolubilisation measured photometrically at 450 nm and biosolubilisation measured quantitatively by TDSS. Conversely, this study did not show a linear correlation between coal biosolubilisation measured by absorbance at 450 nm and by TDSS, as shown in Figure 4.4. Data are presented for coal biosolubilisation at 5% coal loading and at 600-850 μm. This may due to the interference of the growth nutrient medium used in this study which was absent in their study. In summary, since growth nutrient medium is necessary for coal biosolubilisation, TDSS cannot be used as quantitative tool to measure coal biosolubilisation.

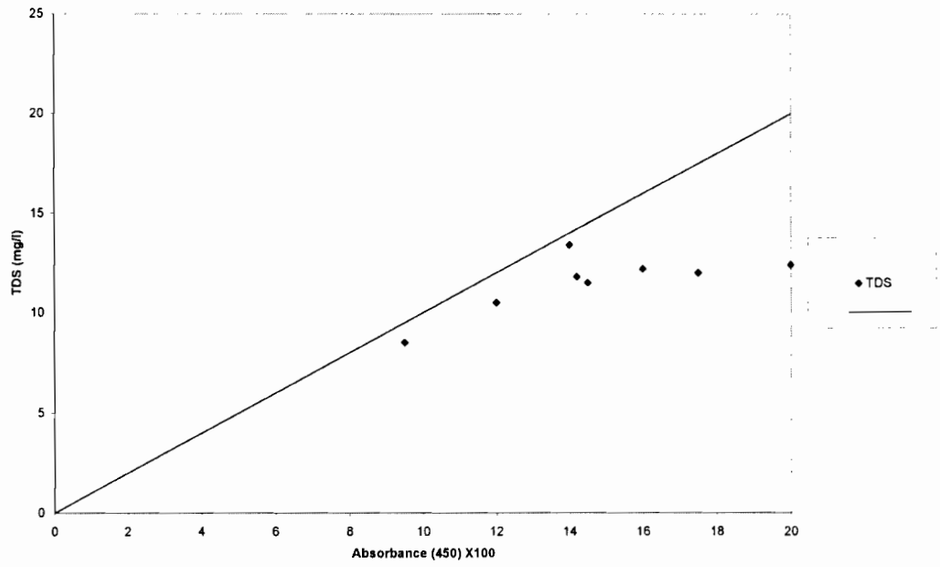

Figure 4.4: Coal biosolubilisation by *Trichoderma atroviride* measured in terms of colouration of the supernatant(A_{450nm}) and of total dissolved solids. Data compared for the experiment conducted at 5 %(w/v) and at 600-850μm in shake flasks. The coal was added to a five-day *Trichoderma atroviride* culture on day 0 of the experiment.

4.1.3 Coal weight loss

Reduction in coal weight has been used as a quantitative tool to determine coal solubilisation (Larboda *et al.* 1997). Figure 4.5 shows percentage of coal conversion after 14 days of incubation with *Trichoderma atroviride* ES11. The smaller particle size resulted in higher coal weight loss. This supports the hypothesis that coal biosolubilisation is a surface phenomenon. There was very little coal weight loss in the control experiments containing coal and distilled water. This suggests that degradation of coal was fungal-mediated rather than a leach reaction. In this study the process condition that showed the highest degree of coal biosolubilisation in terms of percentage dry weight loss was 5 % (w/v) and 600-850 μm, which resulted in 9% biosolubilisation. Larboda *et al.* (1997) reported 60 % biosolubilisation of lignite in terms of coal weight loss. The high degree of biosolubilisation was attributed to pre-oxidation of lignite by nitric acid prior to

biosolubilisation. This is also supported by the findings of Quigley *et al.* (1988) who showed that 35% coal was degraded during oxidation of low–rank coal with nitric acid.

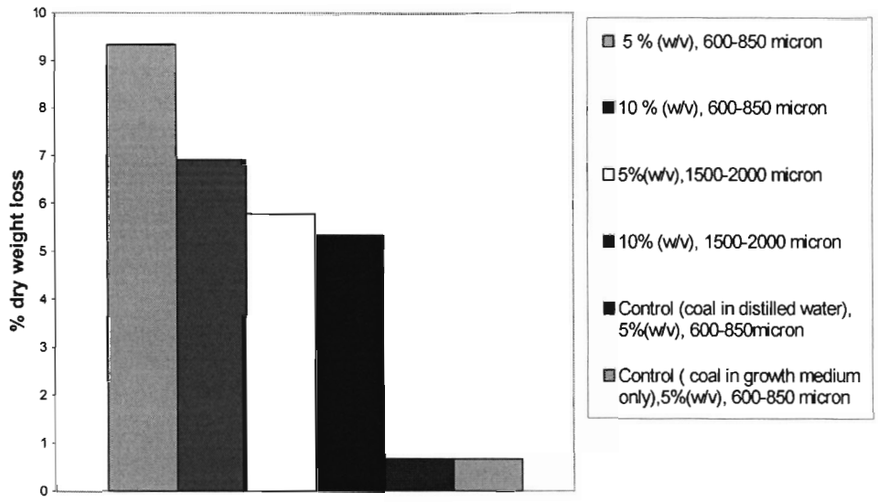

Figure 4.5 Coal biosolubilisation as a measure of decrease in percentage dry weight in relation to the initial coal weight. Factorial experiments were conducted in shake flasks. The coal was added to a five-day *Trichoderma atroviride* culture on day 0.

Since coal weight loss provided a reliable quantitative tool to determine coal biosolubilisation, it was used as the object of the factorial analysis and subjected to an analysis of variance (ANOVA). The coal weight loss data and factorial combination are presented in Table 4.1.

The estimate of the effect of each variable and their interaction was computed by Yates algorithm, shown in Table 4.2. The ANOVA table, generated from the sum of squares for each operating variables and the interaction between the variables, is shown in Table 4.3.

Table 4.1: Coal weight loss in the factorial analysis. Run 1 and 2 were independent replicates

Factor		Coal loading	Initial wt	% Coal weight loss (Run 1)	% Coal weight loss (Run 2)	Sum of coal weight loss (runs 1 & 2)
Size a	Loading b					
-1	-1	5%, 600-850μm	7.5	9.3	18.76	28.09
+1	-1	10%,600-850μm	15	7.0	12.77	19.67
-1	+1	5%, 1500-2000μm	7.5	5.78	5.16	12.28
+1	+1	10%,1500-2000μm	15	5.3	5.26	11.12

Table 4.2: Effect estimate and sum of squares estimated using Yates method of statistical analysis

Combination	Response (% coal weight loss)	(1)*	(2) #	Effect estimate	Sum of Squares (SS)
(1)	28.09	47.76	71.23	Total	188
a	19.67	23.46	-9.53	-2.38	22.72
b	12.28	-8.43	-24.30	-6.08	148
ab	11.12	-1.10	7.32	1.83	10.43

(1)* - The first entry in column (1)* represents the sum of the response of the first two entries in response column (i.e (1)+a). The second entry is the sum of the second two entries in the response column (i.e b and ab). The third entry is the difference between the first two entry responses. (i.e a-(1)).The fourth entry is the difference between the second pair of responses (ab-b).

(2)# -The same procedure.

Table 4.3 ANOVA table for 2^2 factorial table with two replications

Sources of variation	Sum of squares	Degree of freedom	Mean square	F
Coal loading	22.72	1	22.72	13.85
Particle size fraction	147.69	1	148	90.04
Interaction	10.43	1	10.43	6.39
Error	6.45	4	1.64	
Total	187.54	7		

The F-test was used to test the sum of squares, following their conversion to units of variance by division by corresponding degrees of freedom, to give the mean square. The F-test assesses whether the mean square (MS) due to solids loading, particle size or interactions is significantly greater than that due to error. The critical F values from the F table are: $F_{90;1,4}$ of 4.54, $F_{95;1,4}$ of 7.71 and $F_{99;1,4}$ of 21.2. Thus the particle fraction size fraction effect was significant at the 99% confidence interval, while coal loading and the interaction between size and loading were significant at 95% and 90% respectively.

An empirical relationship was developed from the factorial analysis to provide a prediction of coal biosolubilisation in terms of percentage weight loss (Y) in terms of particle size fraction (b), coal loading (a):

$$Y = \frac{1}{2}\langle\ 17.79 + (-2.38)A + (-6.08)B + (1.83)AB\ \rangle \qquad \textbf{Equation 4.1}$$

where 17.79 is the average response across 2 data sets and A and B can be +1 or -1. Equation 4.1 can be decoded to the actual values of particle size and coal loading. This is shown below:

$$Y = 8.895 - 1.19\left[\frac{a - 0.5(10+5)}{0.5(10-5)}\right] - 3.04\left[\frac{b - 0.5(1.75+0.725)}{0.5(1.75-0.725)}\right] + 0.915\left[\frac{a - 0.5(10+5)}{0.5(10-5)}\right]\left[\frac{b - 0.5(1.75+0.725)}{0.5(1.75-0.725}\right]$$

Equation 4.2

Further simplification gives

$$Y = 26.43 - 1.38a - 11.28b + 0.713ab \qquad \textbf{Equation 4.3}$$

where Y is coal weight loss (%), a is % loading and b is nominal diameter (mm). Equation 4 suggests that the particle size fraction, coal loading and the interaction between particle size and coal loading affects the degradation of coal.

4.1.4 Phenolic concentration

While there is no direct report of phenolic product release from coal biosolubilisation in the literature, the product of coal biosolubilisation is reported to be a mixture of polar organic compounds with high a degree of aromaticity (Scott *et al.* 1986). Further, based on coal structure, release of phenolics and polyphenolics on solubilisation can be expected. Figure 4.6 shows the time profile for the accumulation of phenolic products in solution on coal biosolubilisation. There was no significant release of phenolics on incubation of coal with the fungus. The phenolic concentrations in the control test containing the growth medium and no coal were comparable to those measured in the tests with coal. Hence the major source of phenolics is the growth medium. Release of phenolics on biosolubilisation on coal by *Trichoderma atroviride* ES11 is negligible.

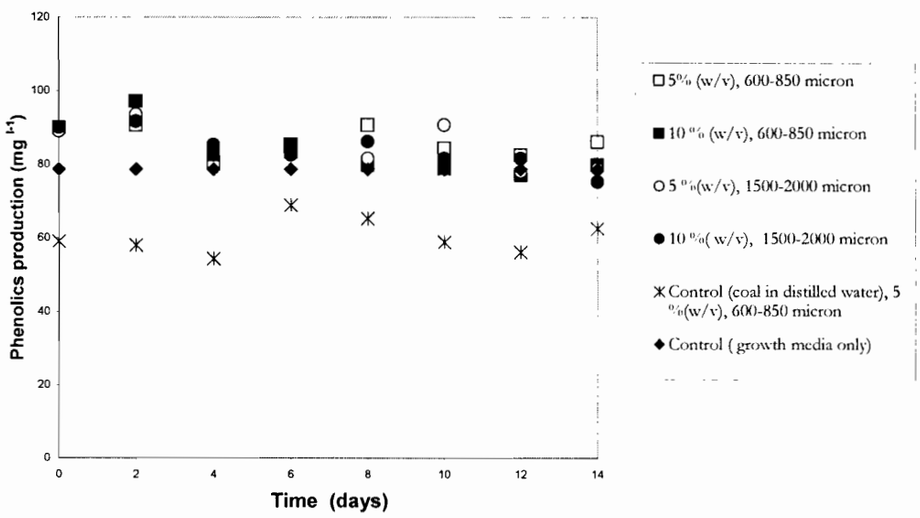

Figure 4.6: Phenolic production from *Trichoderma atroviride* ES 11 fungal strain biosolubilisation of coal. Experiments were conducted in shake flasks. The coal was added to a five-day *Trichoderma atroviride* culture on day 0.

4.1.5 Total organic carbon (TOC)

The time profile of the total organic carbon (TOC) in solution during fungal coal biosolubilisation is illustrated in Figure 4.7. The TOC provides a measurement of carbon content of the liquid phase. On growth of fungi on glucose media prior to coal addition over 5 days, the TOC decreased from 1800 mg l^{-1} to 250 mg l^{-1} (data not shown). After the addition of coal, the TOC increased by 80 to 750 mg l^{-1} over a 2 day period depending on the operating conditions. The low increase in TOC in the presence of 10% coal loading with large particles may be postulated to result from fungal damage in the slurry bioreactor as illustrated in Figure 4.2. A sharp decrease in TOC was observed after the second day of coal biosolubilisation. This may be attributed to the metabolism of the soluble products released from coal. Limited TOC release or utilisation was observed in the control experiments with coal in distilled water (in range 30-100 mg l^{-1}), coal in growth medium (in range 1550-1700 mg l^{-1}) and growth medium only(in range 1715-1850 mg l^{-1}). The absence of an increase in TOC in the solution of coal in distilled water is consistent with the low coal weight loss (0.5%) shown earlier. High TOC values in the control test which contained coal in growth medium and growth medium only suggest that the growth medium is the major source of carbon. Further, the control experiments containing coal suggest that both the initial release of TOC 0 to 2 days after the addition and subsequent depletion is the result of microbial action rather than physical leaching.

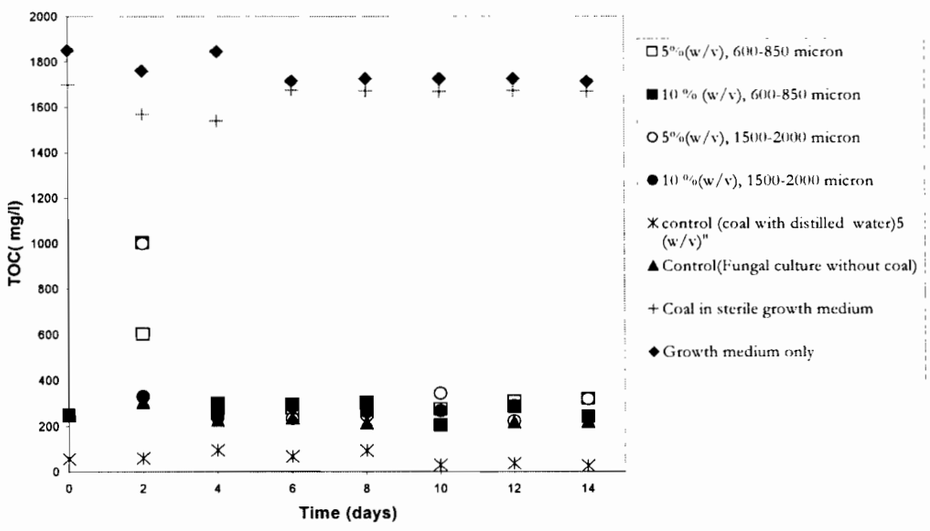

Figure 4.7: Total organic carbon concentration of fungal biosolubilisation of coal by *Trichoderma atroviride*. Experiments were conducted in shake flasks and coal added to a five-day *Trichoderma atroviride* culture on day 0.

4.1.6 pH measurement

Quigley *et al.* (1988) reported on the correlation between pH and biosolubilisation of oxidised, low rank coal. They observed an increase in pH from 6.5 to 7.5 and corresponding increase in absorbance at 450 nm from 0.0 to 0.5 during coal solubilisation of treated coal by *Streptomyces setonii*. Holker *et al.* (1999) also suggested that the growth of fungi on carboxylic groups from the coal macromolecule leads to an increase in culture pH. Conversely, Larboda *et al.* (1994, 1997) reported that biosolubilisation of untreated coal does not influence pH. They observed that variation in pH of the supernatant did not correspond to the observed increase in absorbance. The time profile of pH on treatment of coal with *Trichoderma atroviride* is illustrated in Figure 4.8. These results showed that there was an increase in pH on fungal culture with coal as well as in the control test where fungi are grown in the absence of coal, and the control test where coal is incubated in distilled water. On comparison of data for the controls in both absence of coal and the fungi, it is apparent that both biological and non-biological acid-consuming reactions occur. The consumption of protons under each experimental condition is presented in Table 4.4. The results also showed that the change observed in the presence of both coal and fungi was independent of coal loading, and was not directly related to the extent of coal solubilisation. This is illustrated in Figure 4.9. Hence the data presented here support the findings of Larboda *et al.* (1994, 1997) in that variation in pH does not correlate with coal solubilisation on loading.

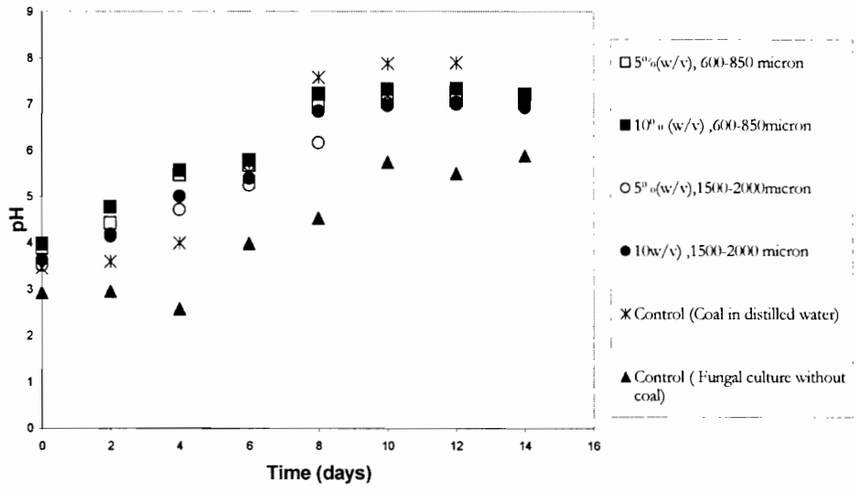

Figure 4.8: pH measurements of fungal biosolubilisation of coal by *Trichoderma atroviride*. Experiments were conducted in shake flasks. The coal was added to a five-day *Trichoderma atroviride* culture on day 0.

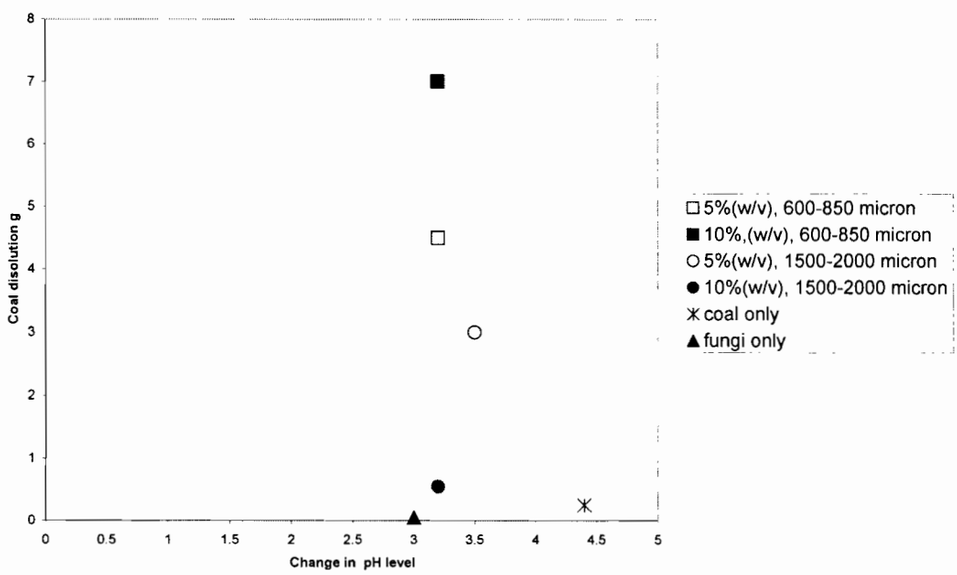

Figure 4.9 Effect of coal dissolution on pH level.

Table 4.4: Analysis of the change in pH in the factorial experiment.

Condition	Initial pH	Final pH	ΔH+ (M)	Coal weight loss (%)
5%(w/v), 600-850μm	3.8	7.0	-0.0215	9.3
10%(w/v) 600-850μm,	4.0	7.2	-0.0176	7.0
5%(w/v) 1500-2000μm,	3.5	7.0	-0.0293	6.0
10%(w/v) 1500-2000μm,	3.6	6.8	-0.0262	5.5
Coal only	3.4	7.8	-0.0330	0.5
Fungi only	2.8	5.8	-0.0578	

4.1.7 Summary of factorial experiments

Critical and succinct assessment of the relative merits of the techniques used to evaluate the extent of coal solubilisation is given in Table 4.5. The photometric method (increase in absorbance) has been widely used to determine the extent of coal biosolubilisation because it is a simple method; however, it is qualitative. The coal weight loss method is not widely to determine coal solubilisation because it is tedious; however results from this study showed that it gave a reliable quantitative measurement of coal solubilisation. The TDS method is not widely used to determine the extent of coal solubilisation because it is also tedious. In this study, TDS measurements did not give a reliable quantitative measurement for coal solubilisation.

There was no release of phenolic compounds during coal solubilisation. This suggests that it can not be used to determine the extent of coal solubilisation. In addition, results from pH measurement suggested that there were other dominant acid-consuming reactions interfering with coal solubilisation, hence pH measurement is not recommended as a method to determine the extent of coal solubilisation. TOC measurement provided a qualitative method for monitoring coal solubilisation and can be used in the carbon balance, in conjunction with CO_2 evolution.

The factorial design experiments were set up to determine the optimum conditions for coal solubilisation and to investigate the effect of coal loading and particle size fraction and its interaction with, or effect on, coal biosolubilisation under the condition studied,

the highest coal biosolubilisation was obtained at 5 % (w/v) coal loading and particle size fraction of 650-850 μm. The interaction between coal loading and particle size was not significant, whereas the key variables, coal loading and particle size are significant at 99 % confidence level.

Table 4.5: Analytical methods used in coal biosolubilisation

Parameters	**Qualitative/ Quantitative**	**Interferences**	**Used in literature**	**Recommendation**
Absorbance	Qualitative	No	Widely used	Yes
Weight loss	Quantitative	No	Not widely used	Yes
Phenolics		No release	Not used	No
TOC	Qualitative	Intermediate Metabolised	Not widely used	Yes
pH	Qualitative	Other dominant acid consuming reaction	Not widely used	No

4.2 EFFECT OF COAL LOADING ON COAL BIOSOLUBILISATION

The effect of coal loading was investigated at 1% (w/v) and 5% (w/v) coal loading using the particle size fraction of 200-250 μm.

4.2.1 Coal weight loss

Coal biosolubilisation can be quantified in terms of the measurement of the decrease in dry mass, illustrated in Figure 4.10. There was an 18 % coal weight loss at 1% (w/v) coal loading compared with a 14 % coal weight loss at 5 % (w/v) coal loading. This indicates that there is a higher conversion at a lower coal loading.

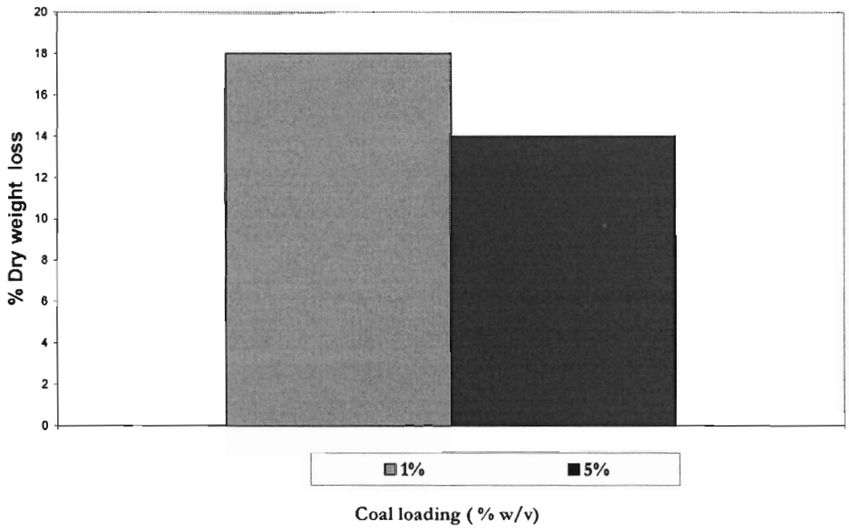

Figure 4.10: Coal biosolubilisation measured as percentage decrease in dry weight related to the initial coal weight.

4.2.2 pH measurement

The pH profile as a function of time on the fungal biosolubilisation of coal at loadings of 1% (w/v) and 5% (w/v) is illustrated in Figure 4.11. There was a higher increase in the change in the $[H^+]$ at 5% than at 1% (w/v) loading. This does not correlate to the coal weight loss data presented in Section 4.2.1. These results support the conclusion in Section 4.1.6 that the pH change is not directly related to coal loading.

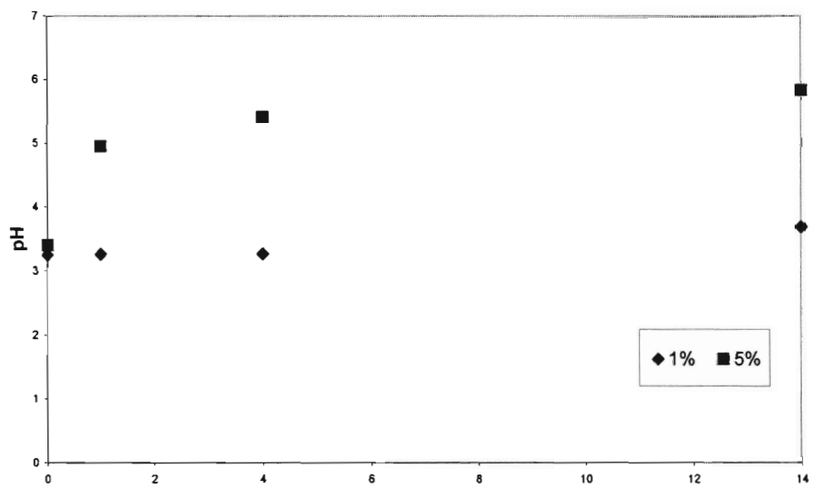

Figure 4.11: Effect of coal loading on pH during coal solubilisation with *Trichoderma atroviride* ES11

4.3: EFFECT OF PARTICLE SIZE ON COAL BIOSOLUBILISATION

In order to extend the operating window of particulate size considered, experiments were carried out at 600-850 μm and 150-300 μm at 5 %(w/v) coal loading.

4.3.1 Coal biosolubilisation

The effect of particle size on coal solubilisation is presented in Figure 4.12. Results from both qualitative (release of coloured compounds measured as absorbance at 450 nm) and quantitative (decrease in dry mass of coal) analyses of coal biosolubilisation show that the 150-300 μm particle size fractions had better coal solubilisation. The extent of coal degradation was increased by 4-fold when using a size fraction of 150-300 μm in comparison with the 600-850 μm fraction.

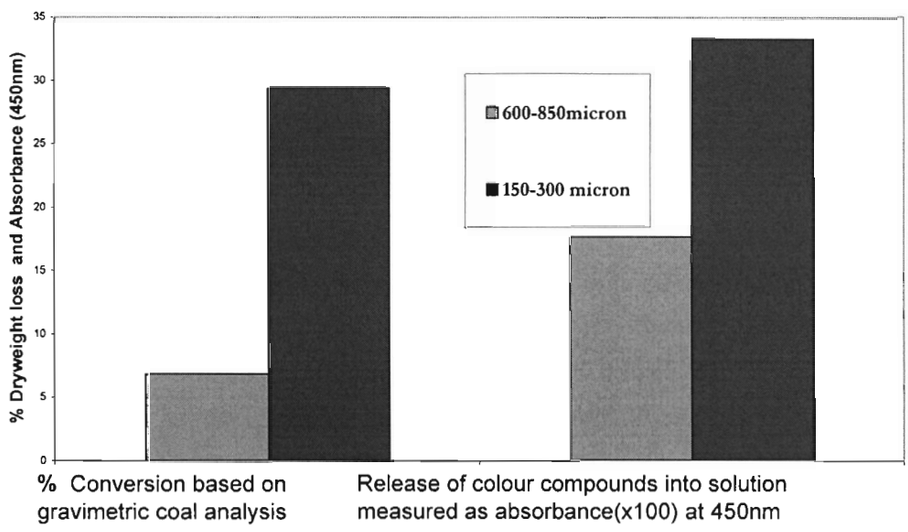

Figure 4.12: Effect of particle size fraction on coal solubilisation during coal biosolubilisation with *Trichoderma atroviride* ES11

Coal biosolubilisation is a surface phenomenon, demonstrated by obtaining better biosolubilisation when a smaller size fraction is used (Gokacy *et al.* 2001). Results from Table 4.6 support this hypothesis. The extent of decrease in dry coal weight across 150-300 μm with a specific surface area of 2.17 $cm^2 g^{-1}$ was 28 % coal weight loss compared with a 7.8% coal weight loss at 600-850 μm (0.54 $cm^2 g^{-1}$) and a 5.6% coal weight loss at 1500-2000 μm (0.21 $cm^2 g^{-1}$).

Table 4.6: Effect of particle size fraction on coal biosolubilisation

Particle size fraction	**Initial coal**	**Mass solubilised**	**Specific surface area** ($cm^2 g^{-1}$)	**% Coal weight loss**
150-300 μm	7.5	2.5	2.17 $cm^2 g^{-1}$	28
600-850 μm	7.5	0.6	0.54 $cm^2 g^{-1}$	7.8
1500-2000 μm	7.5	0.375	0.21 $cm^2 g^{-1}$	5.6

4.3.2: Phenolics production

The time profile of phenolic production on solubilisation of coal particle size fractions of 150 to 300 and 600 to 850 μm is illustrated in Figure 4.13. There clearly was no release of phenolic compounds into the supernatant. The results further support the data presented in Section 4.1.4 and 4.2.3 and the conclusion that growth medium accounts for the significant amount of phenolic in the supernatant.

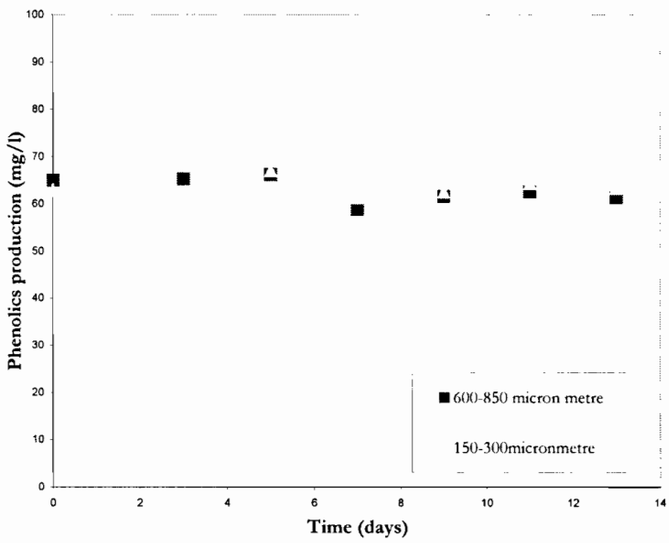

Figure 4.13: Effect of particle size on phenolics production during coal biosolubilisation

4.3.3 pH measurement

Figure 4.14 shows the pH profile on fungal treatment of different coal particle size fractions as a function of time. The results showed that the pH increased in both case from pH 5.2 to pH 5.6 to 5.8 over the 13 day period. Consistent with previous findings reported in Figure 4.8, pH was not a reliable indicator of coal biosolubilisation.

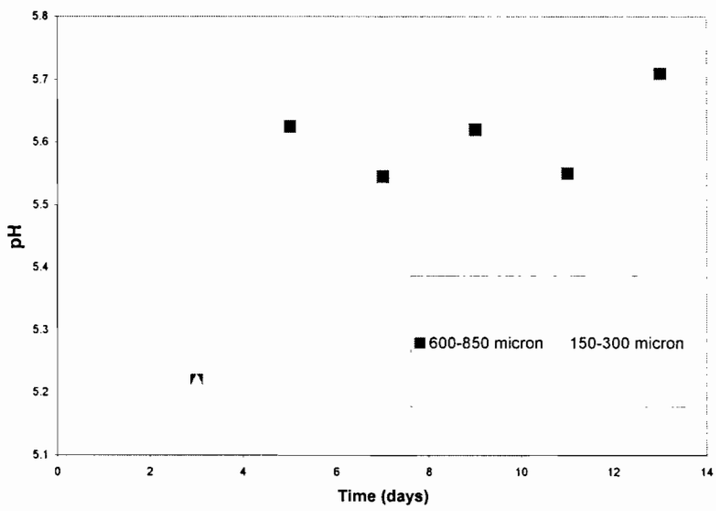

Figure 4.14: Effect of particle size fraction on pH during coal solubilisation with *Trichoderma atroviride* ES11

4 .4 CHAPTER SUMMARY AND CONCLUSIONS

This study shows that the particle size fraction and coal loading affect the coal biosolubilisation process. The factorial experiment was set up to investigate optimum slurry conditions for coal solubilisation in submerged cultures and also to investigate the effect of coal loading and particle size fractions and their interactions on coal biosolubilisation. Coal biosolubilisation is a surface phenomenon, demonstrated by obtaining better biosolubilisation when a smaller size fraction is used (Gokacy *et al.* 2001). The extent of coal solubilisation in terms of coal weight loss of the 150-300 μm coal size fraction with a surface specific area of 2.17 $cm^2 g^{-1}$ was 28 % compared with a 7.8 % coal weight loss at 600-850 μm (0.54 $cm^2 g^{-1}$) and a 5.6% coal weight loss at 1500-2000 μm (0.21 $cm^2 g^{-1}$). The highest coal solubilisation in the factorial experiment was obtained at 5 % (w/v) coal loading of particle size fraction 650-850 μm.

The empirical factorial equation describing these data indicated that particle size fraction was the most significant variable in coal biosolubilisation. Coal loading was also significant but the interactions between coal loading and particle size were not significant.

Further coal biosolubilisation experiments were carried out at 1% (w/v) and 5% (w/v) coal loading and the same particle size fraction. The result showed a higher coal biosolubilisation based on gravimetric coal analysis at 1% (w/v) coal loading. The pH change observed was independent of coal loading, and was not directly related to the extent of coal solubilisation. Furthermore, extending the operating window investigated by carrying out coal biosolubilisation experiments with particle size classes of 600-850μm and 150-300 μm at 5% (w/v) coal loading, qualitative and quantitative analyses of coal solubilisation showed that higher coal biosolubilisation was obtained at particle size fraction of 150-300 μm. Coal biosolubilisation increased by 4-fold in terms of percentage of coal weight loss. Analysis of mass of coal solubilised per unit surface area indicated that the process is controlled by available surface area.

The concentration of phenolics in solution was not a function of coal loading and particle size fraction. A similar concentration at different coal loading and particle size fraction was observed. Furthermore, these concentrations represented a very low fraction of the potential phenolic production on conversion of coal to phenolics. Also, the results

showed that growth medium accounts for significant amount of phenolic in the supernatant.

In conclusion, the effects of coal loading and particle size fractions on coal biosolubilisation both qualitatively and quantitatively have been demonstrated. These have not been reported in the literature previously.

CHAPTER 5: EVALUATION OF PRODUCT YIELD

5.1 INTRODUCTION

In the evaluation of coal biosolubilisation, an important parameter for the assessment of process feasibility is the yield *i.e.* the determination of the mass of product obtained per unit mass of coal solubilised. To date, results for coal biosolubilisation reported in the literature are qualitative or, at best, semi-quantitative indicating trends with operating variables (Gokacy *et al.* 2001; Cohen *et al.* 1987). The process kinetics have not been determined rigorously, largely because measurement of fungal growth during coal biosolubilisation is hindered by the presence of the solid coal substrate. Knowledge of the profile of biomass growth is required for the rigorous determination of the kinetic parameters necessary for process design and optimisation.

Scott *et al.* (1986) reported that results of infrared spectroscopy (IR) and nuclear magnetic resonance (NMR) studies of the biosolubilised coal product suggest that the product is aromatic in nature, possibly containing aromatic hydroxyl (phenolic) groups. The biosolubilised product is an aqueous solution containing complex solutes that are primarily polar, moderate to high molecular weight organic compounds with a high degree of aromaticity (Scott *et al.* 1986). Andrews (1991) also reported that organic chemicals like propionic acid, butanediol, ethanol and methane may be produced by coal biosolubilisation. Typically a mixture of products is formed. The yield of the solubilised coal products is currently reported to be low (Holker and Hofer, 2002; Labroda *et al.* 1999). Furthermore, Ralph and Catcheside (1997) report the absence of these coal derived-monomers hence, there is a need to establish whether high molecular weight organic products released on biosolubilisation of coal are taken up and metabolised further by fungal cells.

Based on this understanding, the role of fungi and extracellular enzymes in coal biosolubilisation needs to be investigated. Also, the nature of the soluble products formed from coal biosolubilisation and the role of fungal enzymes in the degradation of high molecular weight phenolic compounds requires understanding. In addition, a methodology for biomass estimation needs to be developed.

In this chapter, a methodology is presented to allow the biomass formed to be estimated in the presence of solid substrate. The estimated biomass concentration was then used to evaluate process kinetics and product yield.

5.2 ANALYSIS OF *TRICHODERMA ATROVIRIDE* (ES 11) GROWTH ON GLUCOSE

The fungus was grown on defined media with glucose for five days before the addition of coal, as detailed in Section 3.5.1, to provide adequate biomass for coal biosolubilisation. Figure 5.1 represents the time profile of the biomass and glucose concentrations during fungal growth on glucose. Stationary phase was reached at day 3. The residual glucose concentration at day five of incubation was negligible (0.12 g l^{-1}), hence glucose utilisation exceeded 98%. The highest biomass concentration measured was 5.6 g l^{-1}. The overall biomass yield ($Y_{x/s}$) calculated from the experimental results was 0.56 g biomass g $glucose^{-1}$. The stoichiometric equation for fungal growth on glucose in the absence of the formation of extracellular organic products is given in Equation 5.1. The general form of Equation 5.1 was presented in Equation 2.1. In order to calculate the stoichiometric coefficients, it was assumed that biomass was the only product. The stoichiometric coefficients were then evaluated from the five element balances and one degree of reductance balance.

$$\mathbf{CH_2O + 0.24\ O_2 + 0.14\ NH_3 \rightarrow 0.56\ H_2O + 0.28\ CO_2 + 0.73\ CH_{1.8}O_{0.5}N_{0.2}}$$

Equation 5.1

The theoretical biomass growth yield from the stoichiometric equation, $Y^{max}_{x/s}$ is 0.59 g biomass g $glucose^{-1}$. Hence a good correlation was observed between the theoretical and measured biomass yields, indicating limited metabolism of glucose for cell maintenance.

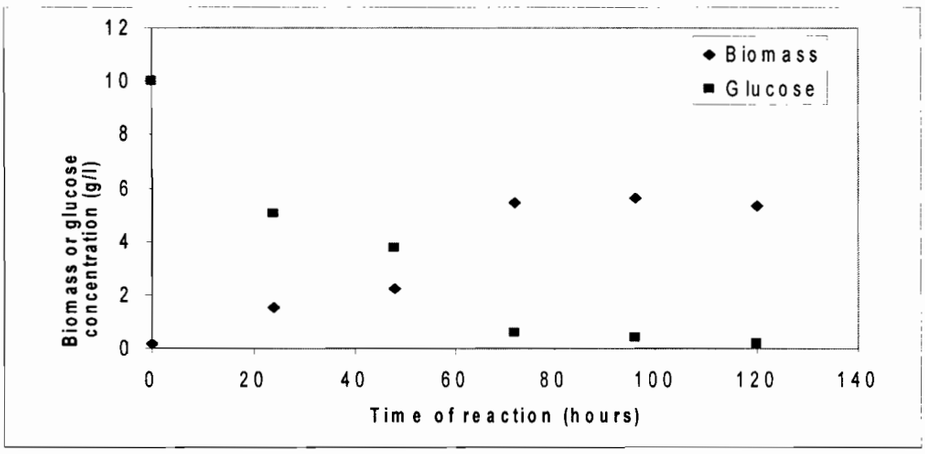

Figure 5.1: Growth curve of *Trichoderma atroviride* (ES 11) using glucose as substrate in a stirred tank slurry bioreactor.

Figure 5.2 represents the cumulative profiles of O_2 utilisation and CO_2 production during fungal growth on glucose. Kinetic parameters were calculated using these experimental data for both the primary growth (0 to 72 h) and overall process (0 to 120 h) components of the growth profile, allowing the determination of parameters associated with growth and cell maintenance. The theoretical yield coefficient from stoichiometry (Equation 5.1) and yield coefficients calculated from experimental data are compared in Tables 5.1 and 5.2. A sample calculation for the experimental values is provided in Appendix I. The yield coefficients calculated from experimental data for primary growth were 0.81 g biomass g O_2^{-1} and 0.57 g biomass g CO_2^{-1} for O_2 utilisation and CO_2 production respectively. The overall biomass yield coefficients calculated across the complete 5 day period of experimental data were 0.51 g biomass g O_2^{-1} and 0.36 g biomass g CO_2^{-1}. The theoretical yields calculated from stoichiometry were 2.36 g biomass g O_2^{-1} and 1.49 g biomass g CO_2^{-1}. This indicates that the growth reaction is less energy efficient than predicted stoichiometrically in the absence of extracellular products or significant maintenance energy. The data based on off gas analysis are not in agreement with yield on glucose which supports the stoichiometric analysis. Further it is not expected that the oxygen consumption and CO_2 production rates should remain little changed in the stationary phase, as seen in Figure 5.2. Hence, while the data generated are used to demonstrate the methodology of biomass prediction, it is necessary to refine these data for accurate application. Further, potential contribution of non-biological reactions to oxygen consumption requires investigation.

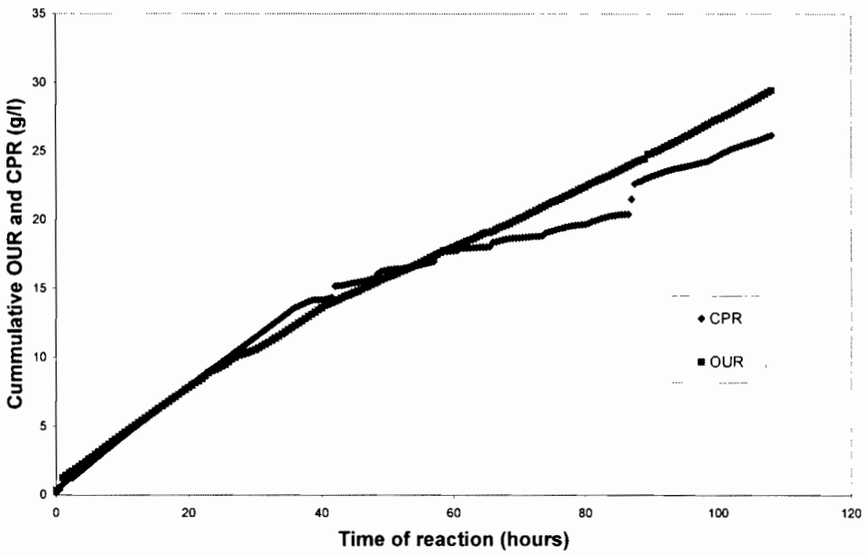

Figure 5.2: Cumulative oxygen utilisation and CO_2 production on fungal growth on glucose in the stirred tank slurry bioreactor.

Table 5.1: Maximum yield coefficients calculated based on stoichiometric substrate consumption for biomass formation using glucose as limiting substrate in the absence of extracellular product formation.

Yield coefficient	Fungal growth based on glucose	
	Molar basis	Mass basis
$Y_{X/glucose}$	0.73	0.59 g g^{-1}
$Y_{X/O2}$	3.08	2.36 g g^{-1}
$Y_{X/NH3}$	5.18	7.49 g g^{-1}
$Y_{X/CO2}$	2.66	1.49 g g^{-1}

Table 5.2: Experimental yield coefficients determined for fungal growth on glucose, given on a mass basis.

Yield coefficient	Based on Oxygen Consumption (average instantaneous)	Based on CO_2 (average instantaneous production
Overall yield coefficient (0-110h)	0.51 g biomass g O_2^{-1}	0.37 g biomass g CO_2^{-1}
Growth yield coefficient (0-72h)	0.81 g biomass g O_2^{-1}	0.59 g biomass g CO_2^{-1}

5.3 METHODOLOGY FOR BIOMASS DETERMINATION IN THE PRESENCE OF COAL

Measurement of fungal growth during coal biosolubilisation is hindered by the presence of the solid coal substrate. Knowledge of the biomass growth profile is required for the rigorous determination of the kinetic parameters necessary for process design and optimisation. A mass balance over the biological system provides a simple way in which to relate the theoretical ratio of the substrates used to products formed in the reaction. The stoichiometry relies on the product spectrum. This is demonstrated in Equations 5.2 and 5.3. In order to calculate the stoichiometry, certain assumptions were required. For Equation 5.2, it was assumed that the major product formed was biomass with no extracellular product formation. For Equation 5.3, formation of biomass and propionic acid were assumed. The general form of Equations 5.2 and 5.3 was presented in Equation 2.1. In all cases, NH_3 was assumed as the nitrogen source and the standard literature-based analysis of coal was used (Andrews, 1991). Based on these, the stoichiometric coefficients were evaluated from the five element balances, a charge balance and one degree of reductance balance.

Coal ⟶ biomass only

$$CH_{0.8}O_{0.22}N_{0.02}S_{0.01} + 0.49\ O_2 + 0.098\ NH_3 \rightarrow$$
$$0.02\ H^+ + 0.006H_2O + 0.41\ CO_2 + 0.59\ CH_{1.8}O_{0.5}N_{0.2} + 0.01\ SO_4^{2-}$$ **Equation 5.2**

Coal ⟶ biomass and propionic acid

$$CH_{0.8}O_{0.22}N_{0.02}S_{0.01} + 0.55\ O_2 + 0.056\ NH_3 \rightarrow$$
$$0.02\ H^+ + 0.012\ H_2O + 0.50\ CO_2 + 0.38\ CH_{1.8}O_{0.5}N_{0.2} + 0.01\ SO_4^{2-} + 0.12CH_2O_{0.66}$$
Equation 5.3

Here, the use of an indirect method for the estimation of the growth and metabolism of fungal biomass, by measuring CO_2 evolution and O_2 consumption using an off–gas analyser, is investigated in the study of coal biosolubilisation by *Trichoderma atroviride*. Coal biosolubilisation was carried out in a stirred tank slurry bioreactor with a working volume of 1.0 litre. Complete suspension of the coal fraction (600-850 μm) used as the standard particle size in this study was achieved at an agitation rate of 560 rpm. Growth yield coefficients based on CO_2 evolution rate and oxygen consumption rate, as well as maintenance coefficients were calculated experimentally for growth of the fungus when using either coal or glucose as a carbon source. These data were used to determine the stoichiometric coefficients for biomass growth. Through this approach, a method was developed through which the biomass concentration in the bioreactor could be predicted in the presence of a particulate substrate. Calculation of the yield following growth on coal or glucose and comparison of these with the stoichiometric analysis, allowed for determination of the performance of coal biosolubilisation. Furthermore, these studies allowed analysis of the nature of coal biosolubilisation with respect to primary metabolism.

5.3.1 The mathematical model

Fungal growth can be modelled using Luedeking-Piret kinetics (Luedeking and Piret 1959). The CO_2 production rate (CPR) and O_2 utilisation rate (OUR) provide a measure of the respiratory activity of the fungal culture. Hence,

$$OUR\ (t) = (\mu A + B)\ X$$ **Equation 5.4**

where

OUR (t) is the oxygen utilisation rate (O_2 g l^{-1} h^{-1})

μ is the specific growth rate (h^{-1}), given as $\left(dx/dt\right)/X$

A is the inverse of the growth yield coefficient $1/Y_{O2}$ (g O_2. g biomass^{-1})

B is yield coefficient for cell maintenance (g O_2. g biomass $^{-1}$.h^{-1}).

X is biomass concentration (g).

The first term of the right hand side of Equation 5.4 describes oxygen consumption attributed to growth while the second term describes oxygen consumption attributed to cell maintenance (or formation of a secondary metabolite in a product-forming system). Equation 5.4 is re-arranged to give Equation 5. 5.

$$\frac{dX}{dt}+\frac{B}{A}X=\frac{1}{A}OUR(t) \qquad \textbf{Equation 5.5}$$

The general solution of Equation 5.5 is given in Equation 5.6, which can be solved numerically using the trapezoidal rule, yielding Equation 5.7 as its solution.

$$X(t_i)=\frac{1}{A}e\left(-\frac{B}{A}t\right)\left(\int_{t0}^{tn}e\left(\frac{B}{A}t\right)OUR(t)dt+AC\right) \qquad \textbf{Equation 5.6}$$

$$X(t_i)=\frac{1}{A}e\left(-\frac{B}{A}t\right)*\left\langle \sum_{i=0}^{n}\frac{h}{2}(z(t_i)+z(t_i+1))+AX_o \right\rangle \qquad \textbf{Equation 5.7}$$

where **C** is the integration constant, **h** represents the average time interval, $\mathbf{X_0}$ is the initial biomass concentration and **z** is given by:

$$z(t_i)=\exp\left(\frac{B}{A}t_i\right)OUR(t_i) \qquad \textbf{Equation 5.8}$$

Hence, with knowledge of the growth yield based on either O_2 consumption or CO_2 production (1/A) and the O_2 consumption or CO_2 production associated with maintenance (B), the biomass concentration, X, can be calculated as a function of time t, based on the consumption of O_2 or production of CO_2.

5.3.2 The Glucose frame-work

Using the modelling approach presented in Equations 5.5-5.9, biomass concentrations were estimated as a function of time from both stoichiometric yield parameters and experimental parameters using both OUR and CPR values presented in Table 5.3. The derived biomass concentrations are compared with the experimental biomass concentrations in Figure 5.3. The stoichiometric yield accounts for biomass formation only. Where the stoichiometric yields were used, the predicted values approximated measured values well at low biomass concentration but underestimated them at higher concentrations. Where experimental yields were used, the predicted biomass concentration was higher than the measured biomass.

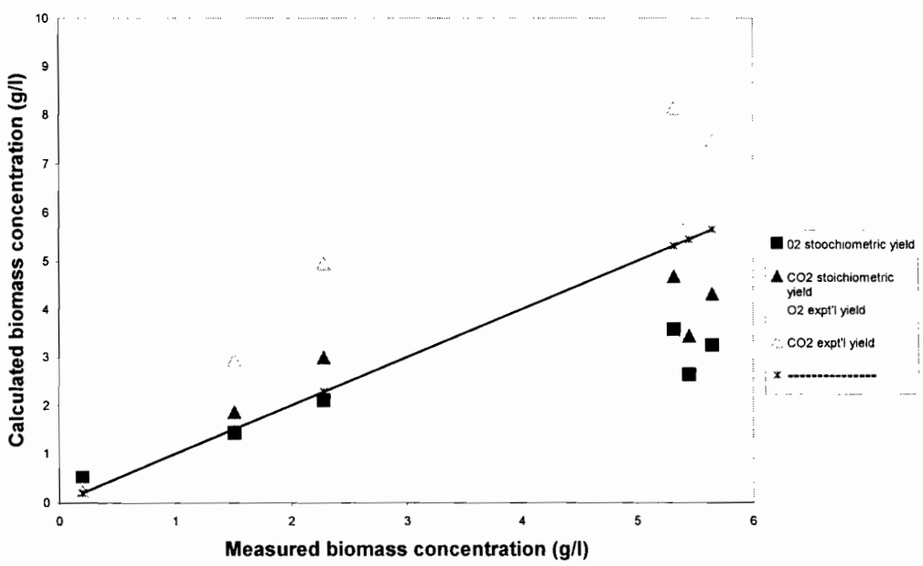

Figure 5.3 Biomass concentration determined stoichiometrically and experimentally during growth on glucose.

5.3.3 Growth of *Trichoderma atroviride* ES11 using coal as a carbon source

Estimation of fungal biomass in solid state fermentation using on–line measurements of CO_2 evolution or O_2 consumption have been reported in the literature (Koutinas *et al.* 2003ab, Brand *et al.* 1999). However, there has been no report of fungal biomass estimation in the biosolubilisation of coal. Biomass concentration in this bioprocess can be estimated using the kinetic model incorporating OUR and CPR values by performing a carbon mass balance.

The biomass concentration was estimated as a function of time using experimental yield coefficients of fungal growth on glucose from Table 5.3, in combination with OUR and CPR values and Equation 5.7. Figure 5.4 represents the change in biomass concentration during fungal growth on coal over time. The estimated biomass concentration formed by growth on coal in terms of CO_2 production rate and O_2 consumption rate were 2.3 g l^{-1} and 2.1 g l^{-1} respectively. The estimated biomass concentration in each instance was similar.

Table 5.3: Maximum yield coefficients calculated based on stoichiometric substrate consumption for biomass formation using coal and glucose as limiting substrate.

Yield coefficient	Fungal growth based on glucose		Fungal growth based on sub-bituminous coal	
	Molar basis	Mass basis	Molar basis	Mass basis
$Y_{X/C\text{-}mole}$	0.73	0.60	0.59	1.10
$Y_{X/O2}$	3.08	2.36	1.25	0.97
$Y_{X/NH3}$	5.18	7.49	6.02	8.71
$Y_{X/CO2}$	2.66	1.49	1.44	0.80

5.4 ANALYSIS OF PRODUCT SPECTRUM FROM COAL BIOSOLUBILISATION

5.4.1 Multiple products of coal biosolubilisation

Biosolubilisation of brown coal (lignite) leads to the formation of humic acids (black liquids) (Hofrichter and Fakoussa, 2001). Depolymerisation of lignite or coal-derived humic acids leads to the formation of fulvic acids. Andrews (1991) reported that coal biosolubilisation does not produce a single product but a mixture of two or more. The total organic carbon (TOC) analysis of the solution from coal biosolubilisation in a slurry bioreactor at 5% (w/v) coal loading supports that there are multiple products from coal biosolubilisation. The TOC concentration after two weeks was 528 mg l^{-1} while the compound phenolics concentration was 85 mg l^{-1}.

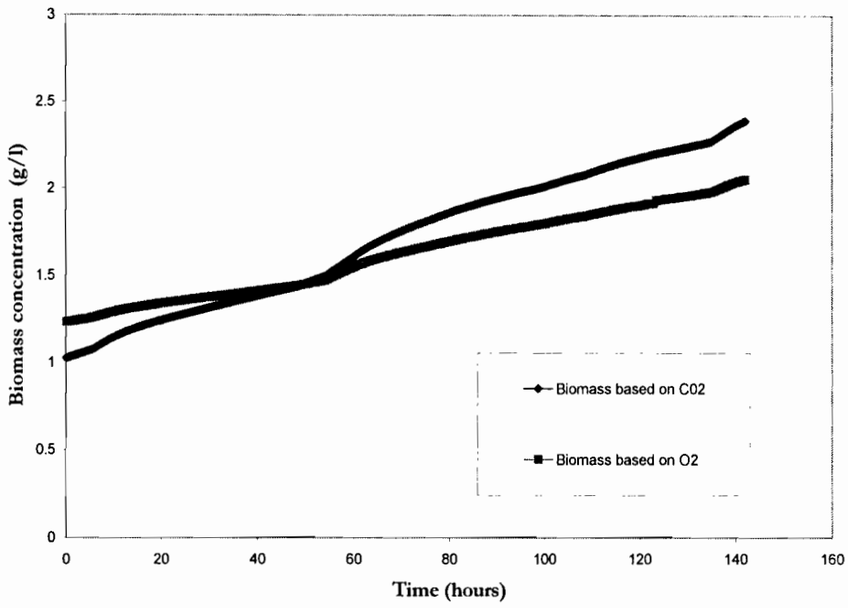

Figure 5.4: Estimated biomass concentrations from OUR and CPR measured using off-gas analyser.

5.4.2 Potential for product degradation

Ralph and Catcheside (1999) suggested that fungal cells may degrade soluble organic products from coal biosolubilisation. This is only feasible if depolymerisation occurs following solubilisation. Solubilisation leads to the formation of humic acids while depolymerisation leads to the formation of fulvic acids. Paul and Clark (1996) reported that phenolic OH content of fulvic acid is much higher than that of humic acids. It was observed by Klein *et al.* (1999) that minor amounts of phenolic groups are found after alkaline oxidation of coal.

In order to establish whether the degradation of phenolics to carbon dioxide occurs in the coal biosolubilisation process, quantitative measurement of carbon dioxide, phenolics, total organic carbon and HPLC analysis of soluble products were carried out. The CO_2 evolution rate was measured in the stirred tank slurry reactor system to which an initial coal loading of 5 % (w/v) was added (as described in Sections 3.2.1 and 3.5.2).

Figure 5.5 shows oxygen utilisation rates (OUR) and carbon dioxide production rates (CPR) as function of time. The highest CPR was 0.05 mmole l^{-1} hr^{-1}, which was 10-fold less than the CPR predicted if there was mineralisation of phenolics to CO_2.

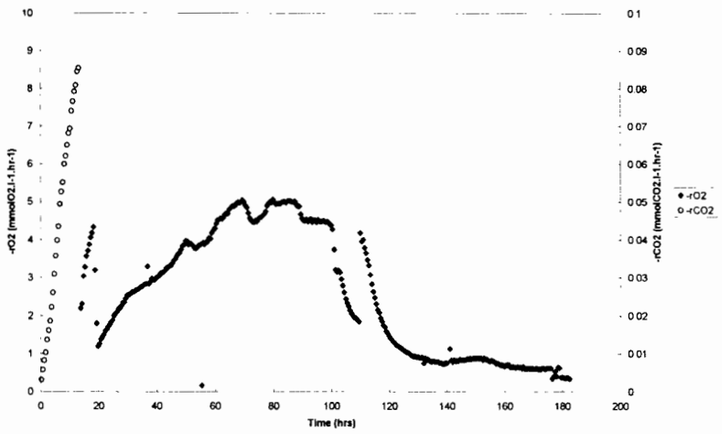

Figure 5.5: Oxygen utilisation rate and carbon dioxide production rate in the slurry batch reactor in which 5 % (w/v). Coal is treated in the presence of fungal biomass (*Trichoderma atroviride* ES 11).

The concentration of phenolics was measured in the stirred tank slurry reactor system to which an initial coal loading of 5 % (w/v) was added. Figure 5.6 presents the total phenolic concentration as a function of time. The concentration of phenolics remained little changed between 70 and 80 mg l^{-1} between the addition of coal and day 6. Thereafter, a small increase to approximately 90 mg l^{-1} from day 8 to 14 was observed. The maximum phenolic concentration of 106 mg l^{-1} at day 10 followed by decrease back to 90 mg l^{-1} suggests potential for utilisation of phenolics by the fungi. The accumulation of some 18 mg l^{-1} phenolics over 14 days period indicates that phenolics are not a major product.

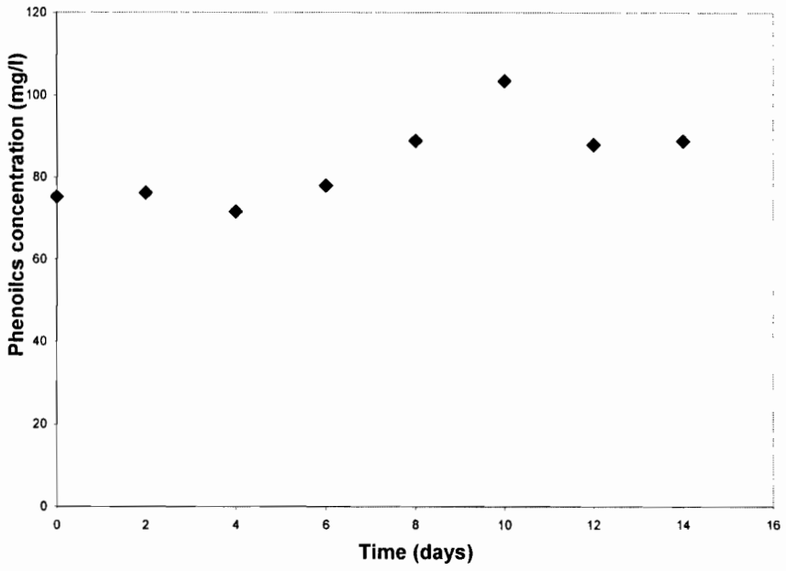

Figure 5.6: The release of phenolic compounds from coal in slurry batch reactor in which 5 % (w/v) . Coal (particle size of 600-850μm) is treated in the presence of fungal biomass

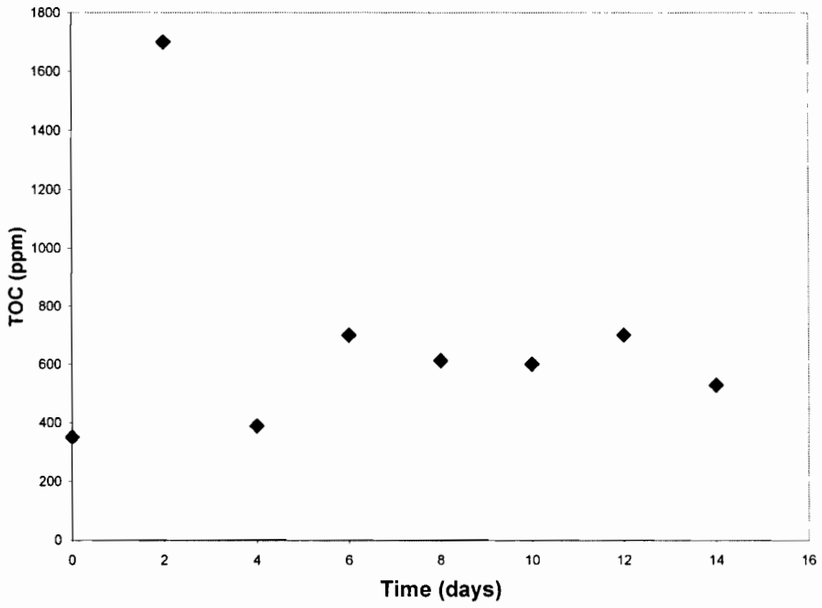

Figure 5.7: Total organic carbon concentration in slurry batch bioreactor in which 5 % (w/v). Coal (particle size of 600-850μm) is treated in the presence of fungal biomass.

The total organic carbon concentration is illustrated as a function of time in Figure 5.7. There was an increase in the TOC from 350 mg l^{-1} following the addition of coal to 1700 mg l^{-1} on day 2. Thereafter the TOC decreased by day 4 to the starting value on day 0. This suggests that there was release of volatiles from coal followed by degradation of soluble carbon. Similar findings were reported on analysis of TOC in shake flask studies of coal solubilisation (Figure 4.7). Following day 4, there was a further increase in TOC concentration from about 350 mg l^{-1} to 600-700 mg l^{-1}, where it plateaued from day 6 to 14. This suggests that the rate of release of soluble carbon products is equal to the rate of their oxidation to CO_2 during this period.

HPLC analysis to determine organic acids

The solution resulting from biosolubilisation of coal on day 6 of incubation was analysed for organic acids and ethanol using high performance liquid chromatograph (HPLC). The data are shown in Figure 5.8. The organic acids identified were acetic acid and propionic acid at a retention time of 8.0 and 9.5 minutes respectively. Table 5.4 shows concentration of acetic acid and propionic acid measured. The presence of additional unidentified organic compounds is also observed. Relating the amount of phenolics (equivalent of a TOC of 61.3 mg l^{-1}) and the organic acids identified to the TOC concentration of 700 mg l^{-1} as (indicated in Table 5.4) indicates that there are other products present.

Table 5.4: Organic acid production at day 6 of coal solubilisation

Product	Concentration (mg l^{-1})	Equivalent TOC (mg l^{-1})
Acetic acid	35	17.5
Propionic acid	176	85.6

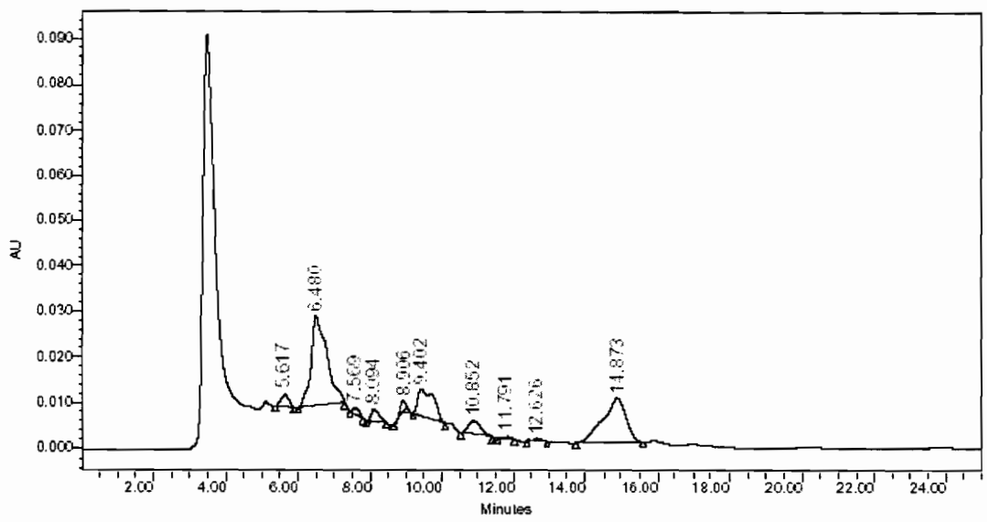

Figure 5.8: HPLC analysis of solution resulting on biosolubilisation of coal in the slurry batch bioreactor in which 5 % (w/v). Coal is treated in the presence of fungal

5.4.3 Mass balance

A mass balance on coal solubilised can be used to indicate if there was further degradation of soluble products. The stoichiometric equation for fungal growth on coal and the formation of propionic acid is presented in Equation 5.3. The amount of coal solubilised after 14 days of incubation of 1 litre of a 5% (w/v) coal suspension with *Trichoderma atroviride* was 12 g. This is shown in Table 5.5. The overall mass balance of the biosolubilisation of 12 g of coal predicted by the stoichiometric coefficients from Equation 5.3 and is shown in Table 5.6. The overall mass balance for experimental values could not be evaluated because water, ammonia and sulphate were not measured experimentally. The carbon mass balance was evaluated for solubilised coal. The carbon from the coal could be converted to biomass (solid phase), liquid organic products (liquid phase) and CO_2 (gaseous phase). The results are shown in Table 5.7. The mass of carbon in the coal particle was estimated from the mass of the coal determined from coal weight loss data. The mass of carbon in the gaseous phase was estimated from the mass of the CO2 measured; while the mass of carbon in the liquid phase was measured experimentally (TOC). Furthermore, the biomass concentration was calculated from the difference between the mass of carbon in the coal and the mass of carbon in the liquid products and CO_2. On comparing the stoichiometric estimation of mass of carbon in

Table 5.6, with the experimental values in Table 5.7, the measured values of carbon in the liquid products and CO_2 were lower than the theoretical mass in Table 5.6. However, the mass of carbon in the biomass in Table 5.7(experimental) was higher than the mass of carbon in Table 5.6. These indicate the yield of CO_2 was higher than the theoretical value from concomitant production of biomass and extracellular organic products.

Coal ⟶ biomass and propionic acid

$$CH_{0.8}O_{0.22}N_{0.02}S_{0.01} + 0.55\ O_2 + 0.056\ NH_3 \rightarrow$$
$$0.02\ H^+ + 0.012\ H_2O + 0.50\ CO_2 + 0.38\ CH_{1.8}O_{0.5}N_{0.2} + 0.01\ SO_4^{2-} + 0.12CH_2O_{0.66}$$

Equation 5.3

Table 5.5: Amount of coal metabolised by *Trichoderma atroviride* ES 11 fungus after 14 days of incubation in a slurry bioreactor

Initial coal present	Unsolubilised coal	Coal solubilised
50 g	38 g	12 g

Table 5.6: The overall mass balance predicted for the solubilisation of 12 g coal in the stirred tank slurry bioreactor, using Equation 5.3.

	Stoichiometric coefficient	Mass of compound (g)	Mass Carbon (g)	Total (g)
REACTANTS				
Coal	1	12	8.51	
NH_3	0.056	0.72	-	
O_2	0.55	12.50	-	**25.22**
PRODUCTS				
H^+	0.02	0.02	-	
H_2O	0.012	0.15	-	
CO_2	0.50	15.62	4.26	
Biomass	0.38	6.64	3.24	
SO_4^{2-}	0.01	0.68	-	
Propionic acid	0.12	2.1	1.03	**25.21**

Table 5.7: Carbon mass balance of solubilised coal in the stirred tank slurry bioreactor.

	Coal	Biomass	Liquid products	CO_2
Mass compound produced (g)	**-12**			**0.74**
Mass Carbon Produced (g)	**-8.51**	**7.77**	**0.531**	**0.21**
Overall mass	**-8.51**	**+8.51**		

5.5 QUANTIFICATION OF YIELD

The estimated biomass in Section 5.3.3 was used to evaluate the process yield of the coal biosolubilisation reaction, shown in Table 5.8. The sample calculation is given in Appendix H. The experimental process yields determined were 0.18 g biomass g $coal^{-1}$, 0.02 g propionic acid g $coal^{-1}$ and 0.002 g phenolic compounds g $coal^{-1}$. The low yields of all products except CO_2 measured in this study indicate that a large fraction of the coal undergoes complete oxidation to CO_2; hence significant improvement to the process to enable accumulation of organic intermediates is required before rigorous kinetic study is valuable.

Table 5.8: Process yield parameters for the coal biosolubilisation process.

Yield coefficient	Theoretical Yield ($g\ g^{-1}$)	Experimental Yield (gg^{-1})
$Y_{X/Coal}$	0.55	0.18
$Y_{X/O2}$	0.53	0.05
$Y_{X/NH3}$	9.82	
$Y_{X/CO2}$	0.42	3.0
$Y_{propronic\ acid/coal}$	0.31	0.02
$Y_{phenol/coal}$	0.33	0.002

5.6 THE ROLE OF EXTRACELLULAR ENZYMES AND THE FUNGAL CELL IN COAL SOLUBILISATION AND DEGRADATION OF HIGH MOLECULAR WEIGHT ORGANIC COMPOUNDS

In order to establish whether the organic products of coal biosolubilisation are taken up by fungal cells or further degraded by extracellular enzymes, coal biosolubilisation was carried out initially with fungal biomass for 8 days. The fungal cells were then removed by vacuum filtration in a sterile environment and fresh coal was added to the supernatant to determine the effect of extracellular enzymes present in the cell free supernatant. The composition of phenolic compounds in solution was monitored to detect whether there was further production or degradation. This was compared with the continued incubation in the presence of fungal biomass.

The release of phenolics from coal in both the presence and absence of fungal biomass is presented in Figure 5.9. Similar profiles were obtained in each instance. These suggest that cell-associated and extracellular enzymes are not involved in the degradation or the production of phenolic compounds. There was a higher coal weight loss when the fungal culture was used for coal biolubilisation. The coal weight loss was 7.2% and 0.7 % in the fungal and cell free cultures respectively. This suggests that contact is needed between the fungal culture and the coal particle for efficient coal solubilisation.

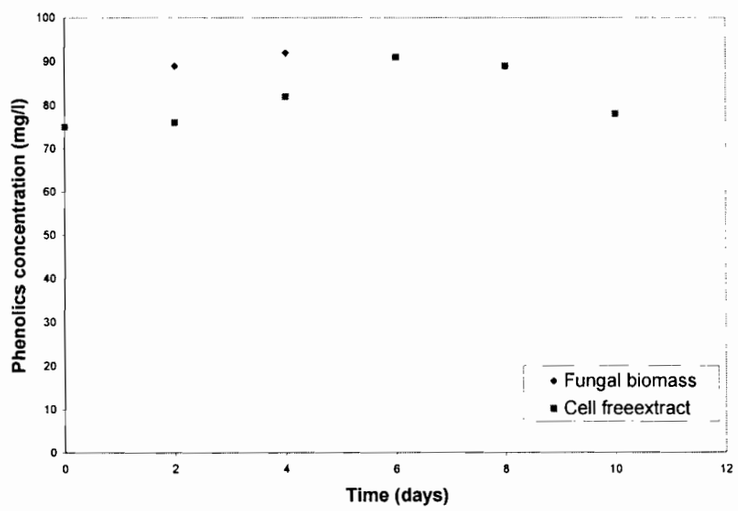

Figure 5.9: The change in concentration of phenolic compounds from coal in the presence or absence of fungal biomass at 5 % (w/v) coal loading and 28°C.

5.7 CHAPTER SUMMARY AND CONCLUSIONS

In this chapter, the role of fungi and their extracellular enzymes in coal solubilisation and degradation of organic products was investigated. This study has shown that extracellular enzymes and fungal biomass are not responsible for the release or degradation of soluble phenolics. There was no significant difference in the phenolic concentration in cell free and whole cell culture of coal.

The maximum phenolic concentration observed was 106 mg l^{-1} while the TOC concentration was 528 mg l^{-1} after 2 weeks of incubation. The maximum change in phenolic concentration of some 30 mg l^{-1} supported that these were not primary products of coal sooubilisation. An HPLC analysis on the resulting solution of coal biosolubilisation showed the presence of organic acids. The concentration of the organic acids identified were 35 mg l^{-1} and 176 mg l^{-1} for acetic acid and propionic acid respectively. The presence of additional unidentified organic compounds was also observed and supported by the TOC concentration. Further more, the highest CPR was 0.05 mmole l^{-1} hr^{-1}which was 20-fold less than CPR value predicted from stoichiometry for complete mineralisation of the coal solubilised to CO_2 .

The use of an indirect method for the estimation of the growth and metabolism of fungal biomass by measuring CO_2 evolution and O_2 consumption using an off–gas analyser was investigated. Growth yield coefficients and maintenance coefficients, based on CO_2 and O_2 in the off-gas were calculated from growth of the fungus under the same conditions using the non-coal carbon source glucose. These data were used to determine the stoichiometric coefficients for biomass growth, enabling the biomass production rate to be quantified in terms of CO_2 production rate and O_2 consumption rate. The estimated biomass produced from cultivation with 5% (w/v), calculated in terms of CO_2 production rate and O_2 consumption rate were 2.3 g l^{-1} and 2.1 g l^{-1} respectively. The estimated biomass production was used to evaluate product yield. Experimental product yields of 0.18 g biomass coal g^{-1}, 0.02 g propionic acid coal g^{-1} and 0.002 g phenolic g^{-1} compounds were determined. The performance of the coal solubilisation process was determined by comparing the maximum stoichiometric yield with experimental yield.

The experimental process yield for propionic acid and phenolic were 12 % and 0.6% of the theoretical values, indicating that production of these value-added products may not be economically feasible.

CHAPTER 6
REACTOR CONFIGURATION

6.1 INTRODUCTION

The proposed bioreactor configuration for coal bioprocessing comprises a multi-phase interacting system in which there is a particulate solid phase consisting of coal particles, a liquid phase comprised of nutrients, a biomass phase of suspended catalyst and solubilised products, and a gas phase containing reactants such as oxygen or products such as CO_2 (Scott, 1990). In order to investigate different bioreactor configurations, coal biosolubilisation was carried out in a stirred aerated slurry bioreactor, a fixed bed bioreactor and a fluidised bed bioreactor. The stirred aerated bioreactor and fluidised bioreactor represent slurry reactor systems enabling a comparative study. Direct comparison between these and the fixed bed bioreactor could not be made since small coal particles (150-300 and 600-850 μm) required for the slurry reactor systems cannot be used in the fixed bed bioreactor due to the large pressure drop. Earlier results in this study have shown that particle size is the most important operating variable in coal biosolubilisation (Section 4.1.3), hence direct comparison of rate and extent of solubilisation is inappropriate. However key data are presented to allow feasibility of the packed bed system to be assessed for later comparison in terms of compromise between biosolubilisation rate, efficiency, energy input and communition required.

6.2 SLURRY SYSTEMS

Slurry bioreactors are used in many industrial processes such as catalytic reactions, coal conversion (Andrews and Noah, 1997; Scott *et al.* 1994; Hulston *et al.* 1996), waste water treatment (Sokol, 2001) soil bioremediation and mineral bioprocessing (Ryan *et al.* 1991, Bailey and Hansford, 1993; Nemati *et al.* 2000). Different configurations of these slurry reactor systems are the stirred tank, the airlift reactor (Chisti and Jauregui-Haza, 2002) and the fluidised bed bioreactors (Andrews and Noah 1997, Garcia-Ochoa *et al.* 1997, 1999). In this study two different slurry bioreactor configurations were used, namely an aerated stirred tank slurry bioreactor and a fluidised bed bioreactor.

6.2.1 Aerated stirred tank slurry bioreactor

Stirred tank reactors are the most common reactor for biological systems (Doran, 1995). Stirred tank reactors are characterised by ability for high power input (P/V), a good mass transfer coefficient (K_La) and oxygen transfer rate (OTR). In addition, there is good suspension and the reactor is well mixed. Coal biosolubilisation was investigated in the stirred tank slurry bioreactor in order to assess its advantages and disadvantages and to enable a comparative study with the fluidised bed bioreactor. The stirred tank reactor is described in Section 3.2.1 and conditions under which it was operated are described in Section 3.6.1. A 5% (w/v) loading of coal particles of 600-850 μm diameter was treated in an aerated reactor agitated with a pitch bladed turbine. While, it is recognised that a smaller particle size fraction (150-300μm) resulted in higher coal biosolubilisation (Section 4.3.1), size fraction of 600-850 μm was used as standard particle size throughout this study.

6.2.1.1 Coal solubilisation

The time profile of absorbance of the supernatant at 450 nm for coal biosolubilisation at a 5% (w/v) coal loading is presented in Figure 6.1. An increase in absorbance from 0.116 on day 2 to 0.176 on day 14 at 450nm was noted. This is similar to the increase from 0.121 to 0.174 in shake flask experiments over the same period. The average rate of solubilisation for both slurry reactors using the same conditions is reported in Table 6.1. While the rates are of the same order of magnitude, the increased rate in the stirred tank reactor is consistent with effective mass transfer.

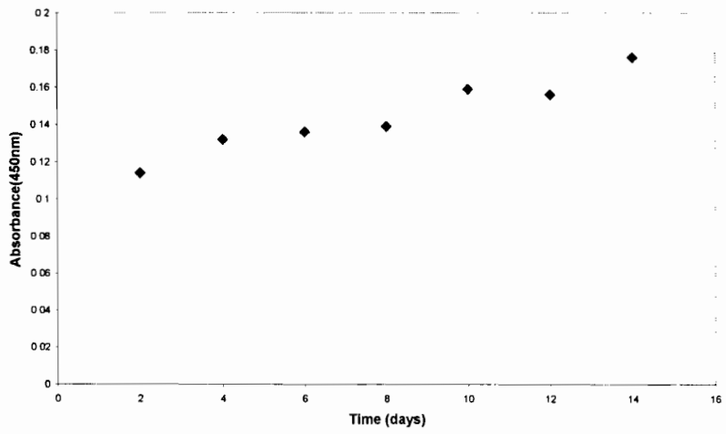

Figure 6.1: Coal biosolubilisation in an aerated stirred tank slurry bioreactor at 5 %(w/v) coal loading of size distribution 600-850 μm, 28^{0}C and 560 rpm.

Table 6.1: Rate of coal biosolubilisation in shake flask and STR at 5% (w/v) coal loading and 600-850 μm particle size fraction.

Bioreactor	Rate (Absorbance day^{-1})
STR	0.005
Shake flask	0.004

Coal biosolubilisation in a slurry bioreactor and shake flask at 5% (w/v) coal loading and 650-850 μm size fractions for both systems was measured by the decrease in dry weight after 14 days of incubation relative to the initial coal weight. The data are presented in Table 6.2. The efficiency of coal biosolubilisation in the slurry reactor was three times higher than in the shake flask. This is postulated to result from improved mass transfer and suspension in the stirred tank reactor.

Table 6.2: Coal weight loss in shake flask and the aerated stirred tank bioreactor

Reactor	Initial coal weight (g)		Final coal weight (g)		% Coal weight loss		
	Sample1	Sample2	Sample1	Sample2	Sample1	Sample2	Avg
Slurry reactor	50.0	50.0	37.9	38.0	24.1	24.1	24.1
Shake flask	7.50	7.50	6.85	6.98	8.67	6.94	7.88

6.2.1.2 Production of phenolic compounds

The total phenolic concentration in solution is shown as a function of time at 5 % (w/v) coal loading in Figure 6.2 (data previously presented in Figure 5.6). There was a decrease in phenolic concentration after day 10. It decreased to a value not much more than that measured on day 0. This further suggests that there was no production of phenolics in this process.

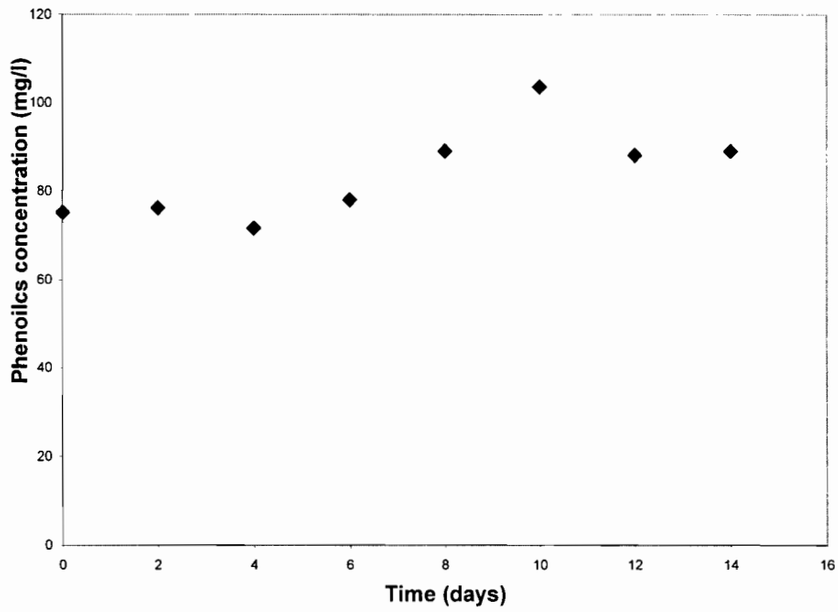

Figure 6.2: Total phenolic concentration in an aerated tank stirred slurry bioreactor at 5 % (w/v) coal loading, 28^{0}C, 560 rpm and 600-850 μm.

6.2.1.3 Total organic carbon

Coal solubilisation may lead to an increase in total organic carbon in solution as this provides a compound analysis of aromatic products, volatile fatty acids and other organic compounds formed. Alternatively coal may be completely oxidised to CO_2. The total organic carbon concentration as a function of time is illustrated in Figure 6.3 (same data previously presented in Figure 5.7). The TOC increased from 350 mg l^{-1} on addition of coal to 1700 mg l^{-1} by day 2, and then decreased to 350 mg l^{-1} day on 4 whereafter it stabilised at 600-700 mg l^{-1}. This suggests that there was both a release of volatile material from coal and the degradation of soluble carbon. On stabilisation of TOC at 600-700 mg l^{-1}, it is postulated that either the production and consumption of soluble organic carbon compounds cease, or that the rate of solubilisation of coal and oxidation of soluble carbon compounds to CO_2 is equal.

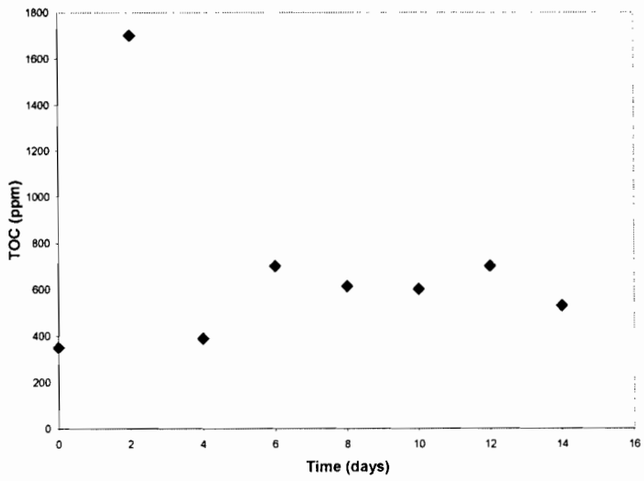

Figure 6.3: Total organic carbon concentration in an aerated stirred tank slurry bioreactor at 5 % (w/v) coal loading, 28^{0}C, 560 rpm and 600-850 μm.

6.2.1.4 pH measurement

The pH profile obtained during coal solubilisation in a stirred aerated slurry bioreactor is represented in Figure 6.4. The highest rate of increase in pH was found between the 2nd and 4th day after addition of coal. Subsequently, the increase in pH was marginal.

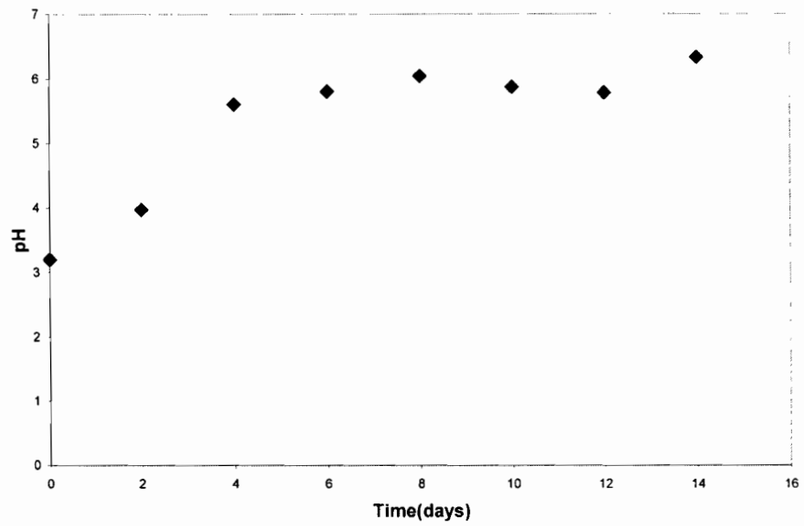

Figure 6.4: pH measurement of fungal coal biosolubilisation in an aerated stirred tank slurry bioreactor at 5% (w/v) loading of 600-850 μm coal.

6.2.1.5 Volumetric mass transfer coefficient

Adequate mass transfer is required in any bioprocess operation. Oxygen transfer is particularly important in aerobic processes owing to its sparing solubility. The oxygen transfer rate (OTR) is a function of the volumetric transfer coefficient and the concentration driving force. It is typically manipulated through manipulating K_La. The K_La is a function of power input, superficial gas velocity and the physical properties of the liquid. Increase in power input (proportional to the cube of agitation rate) and superficial gas velocity lead to an increase in K_La. However, an increase in agitation can lead to an increase in shear rate. Further, introduction of air influences the power draw of agitation at a particular aeration rate (Bailey and Ollis 1986).

Coal biosolubilisation was carried out in a stirred tank slurry bioreactor with working volume of 1.0 litre. Complete suspension of the coal fraction determined visually in the absence of air with a particle size distribution in the range 650 to 800 μm diameter was achieved at an agitation rate of 560 rpm. The air flow rate was set at 350 ml min^{-1}. The power requirement for agitation for this reactor was calculated from Equation 6.1 to be 0.42 W.

$$P = N_P \rho_L N^3 D_i^5 \qquad \textbf{Equation 6.1}$$

where N_p is the power number = 1.3 (Source : Blanch and Clarke,1997)

ϱ_L is the density of the fluid = 1.3 g cm^{-3} (Determined experimentally)

N is the rotation speed = 560 rpm

D_i is the diameter of the impeller = 5 cm

$$k_L a = k\, u_s^{\alpha} \left(\frac{P_g}{V} \right)^{\beta} \qquad \textbf{Equation 2.12}$$

The mass-transfer coefficient K_La can be estimated from the general correlation of the form in Equation 2.12. The values of k, α and β used are 0.02, 0.4 and 0.475, reported by Moo-Young and Blanch in 1981 for various agitators used in non-coalescing fluids, and illustrated earlier in Table 2.9. The estimated K_La value was 0.0144 s^{-1}. The detailed calculation is shown in Appendix E.

In order to check if there was oxygen limitation in the system (i.e., OTR ≤ OUR), the maximum oxygen transfer rate $(OTR)_{max}$ was calculated from Equation 6.2 to be 0.101 mg l^{-1} s^{-1}.

$OTR_{max} = K_L a^* C_{sat}$ **Equation 6.2**

where $K_L a$ is 0.0144 s^{-1} and C_{sat} is 7 mg l^{-1}. The experimental oxygen utilisation rate that was reported in Figure 5.5 was 3.8 mmol l^{-1} h^{-1} equivalent to 0.03 mg l^{-1} s^{-1}. This result suggests that there was no oxygen limitation in the process.

Adequate mixing and mass transfer may lead to cell damage because of the formation of shear fields in the fluid (Illing and Harrison, 1996; Scholtz *et al.* 1997; Lamaignere, 2003). Shear rate is a measure of spatial variation in local velocity of the fluid. The shear rate and shear stress are linearly related in Equation 6.3.

$\tau = \mu_L \gamma$ **Equation 6.3**

where γ is the shear rate

μ_L is the apparent viscosity = 0.0013 Ns m^{-2}

τ is the shear stress

Equation 6.3 only holds for Newtonian fluids. Newtonian fluids exhibit viscosities that are independent of the shear rate. Apparent viscosity measurement at different shear rates of the fluid showed that the fluid was Newtonian. The experimental procedure and results are presented in Appendix F.

The shear rate at the impeller can be related to agitation rate, according to Equation 6.4.

$\gamma = NK$ **Equation 6.4**

where the proportionality constant K depends on the impeller geometry. In this case where a pitch blade was used, K= 10 (Nagata, 1975) at a rotational speed, N, of 560 rpm. The impeller tip speed is also a useful indication for correlating cell damage. It may be evaluated from Equation 6.5:

Tip speed= πND **Equation 6.5**

The shear rate calculated from Equation 6.3 is 93 s^{-1} and was used to calculate shear stress in Equation 6.3. The shear stress was 0.12 N/m^{-2}. The tip speed is 1.47 ms^{-1}. The shear stress in this reaction is less than the maximum shear stress of 8 x 10^7 N m^{-2} reported by Mersmann *et al.* (1990) required to disrupt *Saccharomyces cerevisiae.* The tip speed of 1.47m s^{-1} and an aeration rate of 0.35 l min^{-1} in the stirred tank reactor is less than tip speed of 2.76 m $s^{-1}$and an aeration rate of 3.2 l min^{-1} reported by Toma *et al.* (1991) to inhibit the growth of *Saccharomyces cerevisiae.* They also reported that a lower tip speed of 0.52 m $s^{-1}$and aeration rate of 0.35 l min^{-1} inhibited the growth of *Trichoderma reesei.* The critical difference between this study and those reported by Mersmann *et al.* (1990) and Toma *et al.* (1991) was the absence of solid particles. For solid systems, Pearce (1993) observed the growth inhibition of *thiobacilli* in the presence of 2 %(v/v) pyrite at tip speed of 2.6 m s^{-1} for a 6-bladed Rushton turbine, while at impeller speed of 1.4 m s^{-1} was not detrimental to the cells. Furthermore, Lamaignere (2003) observed that optimum growth of *Saccharomyces cerevisiae* occurred in the presence of 1% volume of suspended solids in a 1 litre slurry reactor agitated at 600 rpm. Cell damage was reported at 2% solids and at 600rpm. No cell growth was observed at 5% solid loading. The duration for both studies was shorter than our study which was carried out for 14 days. The duration of the study of Pearce (1993) was 90 hours while Lamaignere (2003) was 30 hours. This indicates that there was cell damage at a lower speed (N) when solid particles are present. Also fungi are more sensitive to shear damage at lower N values (Toma *et al.* 1991).

6.2.2 Fluidised bed bioreactor

The fluidised bed bioreactor has wide application such as in the catalytic cracking of hydrocarbons, catalytic partial oxidation, gasification of coal and the roasting of sulphides (Kunii and Levenspiel, 1977). The use of a liquid fluidised-bed reactor is expected to be effective in coal solubilisation due to efficient mass transport, ease of gas disengagement and amenability of continuous operation (Kaufman *et al.* 1995). The fluidised bed bioreactor has been used for coal liquefaction previously (Scott *et al.* 1994; Asif *et al.* 1993), however a comparative study of coal biosolubilisation in fluidised bed bioreactor with other reactor configurations such as the aerated stirred slurry bioreactor and the fixed bed bioreactor has not been reported. In addition, reactor parameters such as the overall gas hold-up and the volumetric gas-liquid mass transfer coefficient, K_La of the fluidised bed bioreactor used in coal biosolubilisation have not been reported in the literature.

6.2.2.1 Hydrodynamic behaviour of coal biosolubilisation in the fluidised bed bioreactor

The efficient design, operation and scale up of a slurry fluidised bed bioreactor require detailed knowledge of the hydrodynamic behaviour of the slurry system. In this study, the overall gas hold-up parameter was estimated for coal solubilisation in the fluidised bed bioreactor. The three phases included air, growth medium and coal particles of size fraction of 150-300 μm at coal loading at 5 % and 10 % (w/v) and 600-850 μm at 5 % coal loading. While the 600-850 μm size fractions was used as the standard particle size, studies at the smaller particle size was included to ensure complete fluidisation. The latter was not obtained with larger fraction. Air was used as the fluidising medium and the superficial air velocity was varied from 0.43 to 3.15 cm s^{-1}. The static liquid (slurry) height ranged from 2.4 m to 3.2 m.

The onset of fluidisation of the coal-liquid system occurred when the gas superficial velocity was 0.4 cm s^{-1} and 1.2 cm s^{-1} for 150-300 μm and 600-850 μm size fractions respectively. The experimental minimum fluidisation velocity was close to the theoretical minimum fluidisation velocity calculated from Equation 2.5. This is shown in Table 6.3. The physical properties of fluidising medium (air) and coal particles are tabulated in Appendix G. The shape factor for a sub bituminous coal was taken from the literature (Kunii and Levenspiel, 1977). The voidage was determined experimentally measuring the static height of the bed and the height of the after the bed expansion. The average particle diameter was estimated by the evaluation of the geometric mean of each particle size fraction.

$$U_{mf} = \frac{d^2 p}{150\mu}(\rho_s - \rho)g\frac{\varepsilon^3{}_{mf}\Phi^2 s}{1-\varepsilon_{mf}} \qquad \textbf{Equation 2.5}$$

where U_{mf} = minimum fluidisation velocity, cm s^{-1}

d_p = average particle diameter, cm

ρ_s = particle density of fluidising solids, g cm^{-3}

ρ = density of fluidising medium, g cm^{-3}

μ = viscosity of fluidising medium, g cm^{-1} s^{-1}

g = acceleration of gravity cm s^{-2}

ε_{mf} = minimum fluidised bed voidage

Φ_s =shape factor

Table 6.3: Comparison of theoretical and experimental minimum fluidisation velocity

Particle size	Minimum fluidisation velocity	
	Measured	**Calculated**
150-300 μm	0.4 cm s^{-1}	0.39 cm s^{-1}
600-850 μm	1.2 cm s^{-1}	1.9 cm s^{-1}

When gas velocity was increased to 1.06 cm s^{-1}, using a particle size fraction range of 150-300 μm sufficient turbulence was generated in the bed for it to become a bubbling fluidised bed. Visualisation of the flow pattern was not possible when the reactor was operated at either low or higher gas velocity owing to the black colour of coal particles. When the gas flow was turned off, three distinct layers were observed: biomass, liquid and coal particles. Due to the difference in density, the biomass formed the upper phase, a clear liquid layer in the middle phase and at the bottom were sedimented coal particles. This observation illustrates that the fungal biomass did not adhere to the coal under these operating conditions.

The efficiency of gas-liquid mass transfer depends to a large extent on the characteristics of bubble in the liquid medium. The volume fraction of gas–phase in the gas liquid (or slurry) dispersion is known as the gas holdup or gas void fraction (Chisti, 1989). Gas hold-up can be used to determine the residence time of gas in the liquid and the gas–liquid interfacial area available for mass transfer (Zhang *et al.* 2003). For a given volume of gas, more interfacial area is provided if the gas is dispersed into small bubbles rather large ones. Small bubbles stay in the liquid longer, allowing more time for oxygen to dissolve. Small bubbles create high gas hold-up which lead to a high oxygen transfer.

Gas hold up was measured by the volume expansion method as described by Chisti (1989). The overall gas hold up (ε) is expressed in Equation 6.5.

$$\varepsilon = \frac{V_G}{V_G + V_L} \qquad \textbf{Equation 6.5}$$

where V_G = gas volume in the reactor

V_L= liquid (or slurry) volume in the reactor

The fractional gas hold up increased linearly with an increase in superficial gas velocity as shown in Figure 6.5. The increase in gas hold up was due to the increase in the number of bubbles resulting from increased gas velocity (Zhang *et al.* 2003). At higher superficial gas velocity, the rise in gas hold up was not steep. Similar results have been reported by Garcia-Ochoa *et al.* (1997) and Choi *et al.* (1996). There was marginal decrease in overall gas hold-up when the solid loading was increased from 5 %(w/v) to 10 % (w/v). Similar results have been reported by Choi *et al.* (1996) and Zhang *et al.* (2003). The solid systems reported by these studies are glass beads and quartz sands. The magnitude of decrease in the system that had glass beads reported by Choi *et al.* (1996) was marginal (1%) on increasing solids from 0 to 5% (v/v). The magnitude of decrease in the system containing quartz sand reported by Zhang *et al.* (2003) was also marginal (4%) on increasing solids from 10-15 %(v/v). The extent of the marginal decrease in the gas hold up in this study was about 1%.

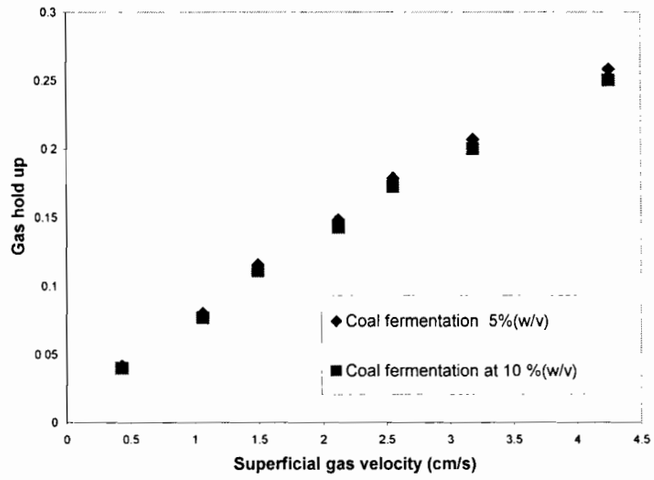

Figure 6.5: Effect of solid loading and superficial gas velocity on the overall gas hold-up in the fluidised bed bioreactor. Experiments was carried out using 150-300 μm particle size fraction.

6.2.2.2 Gas-liquid mass transfer

In order to investigate the importance of oxygen transfer during coal biosolubilisation in the fluidised bed bioreactor, the volumetric gas-liquid mass transfer coefficient K_La was measured. The experimental method and data are reported in Appendix C2. The effect of superficial gas velocity and solids loading on K_La is shown in Table 6.4. The results indicate that an increase in superficial gas velocity resulted in an increase in transfer K_La and an increase in solid loading resulted in a decrease in K_La. These results support the findings of Derksen *et al.* (1999). They observed a 40 % decrease in K_La when silica was increased from 0 to 15 % (v/v) loading.

Table 6.4: The effect of superficial gas velocity and solid loading on K_La in the fluidised bed bioreactor for 150-300 μm.

Coal loading (w/v)	Superficial velocity (cm s^{-1})	K_La (s^{-1})
5%	0.43	0.010
	0.64	0.012
10%	0.64	0.006

6.2.2.3 Coal biosolubilisation

Coal weight loss data at different coal size fractions is represented in Table 6.5. High reduction in mass of coal for the particle size fraction of 150-300 μm was not entirely due to coal dissolution but partly a result of elutriation on bed expansion. No significant elutriation from the bed at a particle size fraction of 600-850 μm was noted because the superficial gas velocity of 0.64 cm s^{-1} did not produce sufficient bed expansion. The results indicate a major constraint for this type of reactor when fine particles are used. Theoretically, elutriatrion of solid particles increases when there is an increase in gas velocity, gas viscosity, vessel diameter and cconcentration of fine particles. It decreases when there is an increase in disengaging height and particle density. It is advisable to operate the bed at the minimum fluidisation velocity to reduce elutriation.

Table 6.5: Coal biosolubilisation measured as percentage decrease in dry weight related to the initial coal weight for different coal size fractions in the fluidised bed bioreactor at 5%(w/v).

Particle size fraction (μm)	Superficial velocity (cm s^{-1})	Initial coal weight (g)	Final coal weight (g)	Coal weight loss (%)
150-300	0.64	100	48.5	51.5
600-850	1.2	100	90	10

6.2.2.4 Phenolic concentration

Concentration of total phenolics in solution as a function of time at different coal size fractions is presented in Figure 6.6. The phenolic concentration during the course of coal biosolubilisation for 150-300 μm and 600-850 μm size fractions were similar. These results further corroborate earlier results in shake flask experiments which showed that coal loading and particle size fraction did not affect production of phenolic compounds and release of phenolic compounds into the liquid medium on biosolubilisation of coal was negligible.

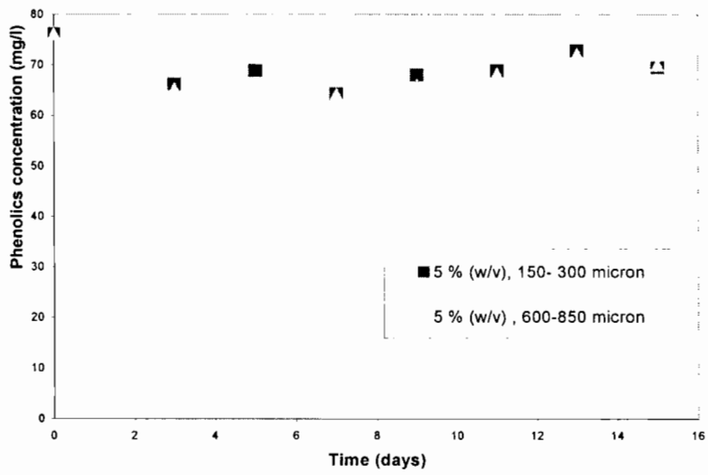

Figure 6.6: Phenolics concentration for different coal size fraction in the fluidised bed bioreactor at 5% (w/v) coal loading

6.2.2.5 pH measurement

Figure 6.7 represents measurement of pH as function of time of two different coal size fractions. A higher pH value was initially observed for the smaller particle size fraction of 150-300 μm due to higher rate of dissolution. However on day 10 of coal biosolubilisation, there was no difference in pH.

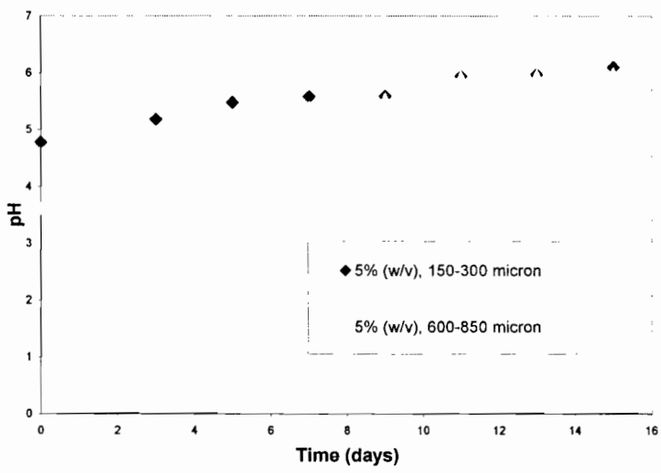

Figure 6.7: pH for different coal size fraction in the fluidised bed bioreactor

6.2.2.6 Comparative study of coal biosolubilisation in different slurry systems

Earlier results from this study have shown that particle size fraction is the key operating variable in coal biosolubilisation. Coal biosolubilisation was carried out in an aerated stirred tank slurry reactor at 5 % (w/v) and a particle size fraction of 600-850 μm. The aeration rate was at 350 ml l^{-1} and the impeller speed was 560 rpm. Coal biosolubilisation was carried out in the fluidised bed bioreactor at 5 % (w/v) and particle size fraction of 600-850 μm. The aeration rate was 5 l min^{-1}. Table 6.6 shows the decrease in mass of coal loaded during coal biosolubilisation for the different slurry bioreactor systems. The quantity of initial coal that was solubilised in the aerated stirred tank slurry bioreactor was higher than that of the fluidised bed bioreactor. Furthermore, coal solubilisation (% coal weight loss) obtained in aerated stirred tank slurry bioreactor was greater than reported by Holker and Hofer in 2002. They obtained a coal weight loss of 9.3% in a 25-litre Airmix II solid state bioreactor. The particle size fraction used in their study was 1-10 mm. There was no agitation in the Airmix II solid state bioreactor. The high coal weight

loss obtained in this study may be as result of increased suspension and improved mass transfer by the increase in agitation rate impeller (560 rpm) and the use of smaller particle size of coal.

Table 6.6: Coal biosolubilisation measured as percentage decrease in dry weight related to the initial coal weight for different slurry bioreactor system.

Slurry bioreactor systems	Particle size (µm)	Coal loading (w/v)	Initial coal weight (g)	Final coal weight (g)	% Coal weight loss
Aerated stirred tank slurry bioreactor	600-850	5	50	37.9	24.1
Fluidised bed bioreactor	600-850	5	100	90	10

6.3 THE FIXED BED BIOREACTOR

Coal biosolubilisation studies were carried out in the packed bed bioreactor as described in Section 3.6.3. The packed bed bioreactor was used to minimise damage to fungal cells and investigate the possibility of using bigger particles sizes (2-4 mm), thereby requiring less communition.

6.3.1 Reactor hydrodynamics

Flow behaviour of gases or liquid in reactors is determined by residence time distribution i.e. the distribution of time which fluid elements spend within a reactor. The mean residence time of fluid in the bed is given in Equation 6.6:

$$\bar{t} = \frac{\varepsilon_f L_f}{\upsilon_o} = \frac{volume\ \ of\ void\ space\ in\ the\ bed}{volumetric\ feed\ rate\ of\ gas}$$ **Equation 6.6**

where

$\bar{t}$ = mean residence time (s)

ε_f = voidage

l_f = volume of the bed (m^3)

v_o = volumetric feed rate ($m^3\ s^{-1}$)

The residence time distribution was determined by using the step tracer input technique. A concentrated sodium chloride (NaCl) solution was applied to the top of the packed bed and the conductivity of the tracer at the outlet of the reactor measured. The calculated mean residence time at a flow rate of 33 ml min^{-1} was 3.5 minutes. The short residence time may limit degradation of soluble phenolic compounds in the packed bed. The tracer test was carried out separately from the solubilisation test.

On running the reactor, in the presence of fungi; the bed porosity had become reduced after 2 days. This was caused by the presence of the growing fungal culture. The feed rate was reduced to prevent build up of fluid at the top of the bed. The decrease in feed rate caused an increase in the residence time of the liquid feed. This is illustrated in Table 6.7.

Table 6.7: Flow rate as function of residence time in the packed bed bioreactor.

Days	Liquid flow rate (ml min^{-1})	Residence time (min)
1	33	3.1
3	22.83	4.4
4	12.05	8.3

6.3.2 Coal solubilisation

Figure 6.8 represents absorbance at 450 nm in the packed bed bioreactor as a function of time. An increase in absorbance occurred from 0.10 on day 1 to 0.14 on day 5. Thereafter there was a decrease in absorbance to an approximately constant value of 0.12

from day 7 to 14. The initial increase in absorbance observed was not due coal biosolubilisation; rather it was due to the introduction of growth medium (without glucose) on day 2, 3, and 4. The coal weight loss data also supports this observation as after 14 days of biosolubilisation, only 0.5% coal weight loss was observed.

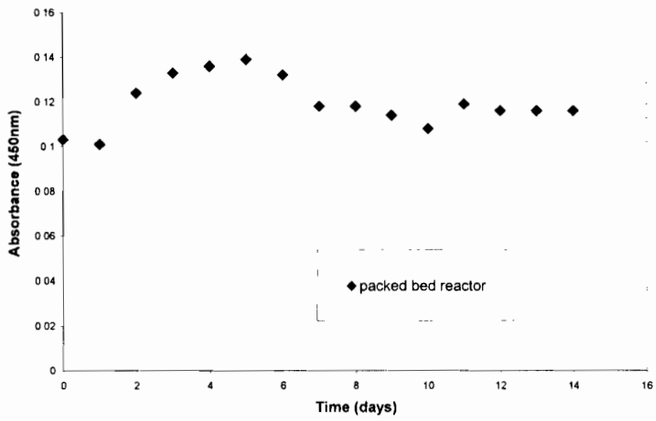

Figure 6.8: Coal biosolubilisation in the packed bed bioreactor.

On comparing coal weight loss across different particle size and different reactor systems, data presented in Figure 6.9 support that particle size fraction is the key operating variable in coal biosolubilisation. A decrease in particle size leads to an increase in coal weight loss. Stirred tank reactor showed the highest coal weight loss, when 600-850μm size fraction was used. The need to use a larger particle size in the packed bed reduces the release rates obtained with this system.

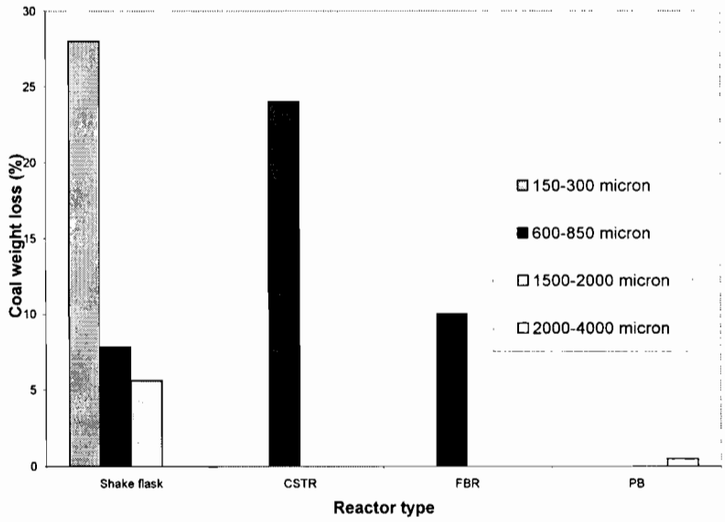

Figure 6.9: Direct comparison of coal biosolubilisation in different reactor systems using different particle size.

6.3.3 pH measurement

The time profile of pH measurement in the packed bed bioreactor is illustrated in Figure 6.10. An increase in pH from about 4 to 6 was noted when the growth medium was trickled down the reactor. However there was no commensurate increase in coal solubilisation in terms of coal weight loss.

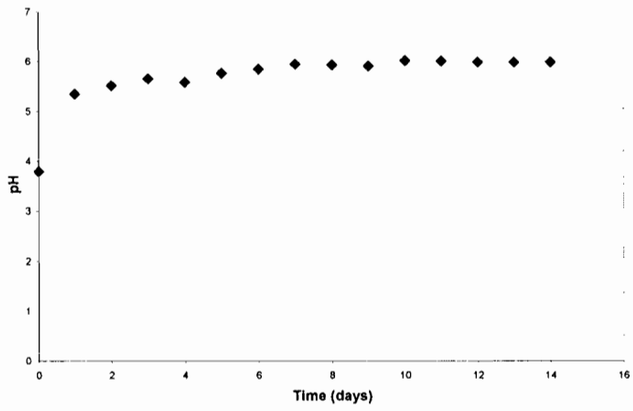

Figure 6.10: pH measurement in the packed bed bioreactor.

There was still microbial activity in the fixed bed bioreactor after 14 days of coal solubilisation. A greenish colouration of the *Trichoderma atroviride* ES 11 fungal biomass was observed at the end of the experiment run (14 days). This indicated a stationary phase of growth. This is a characteristic of fungal growth (Prescott, 1993). However, there was problem of clogging of the packed bed by the fungal biomass. This reduced bed porosity and subsequently led to reduction in the feed rate. The reduction in feed rate lead increase in residence time and reduction in recycle ratio. Reduction in recycle ratio may lead to decrease gas-liquid mass transfer. Owing to these operational difficulties and the need for fungal contact with the coal reported in Section 5.6, a detailed study of the packed bed reactor was not undertaken.

6.4 CHAPTER SUMMARY AND CONCLUSIONS

In this study, a comparison of coal solubilisation in the stirred tank slurry reactor and fluidised bed bioreactor was made in order to assess advantages and shortcomings of these reactor configurations. Coal particle size fractions used in the slurry bioreactor system were 150-300 μm and 600-850 μm. Direct comparison between these and the fixed bed bioreactor could not be carried out since these small particles result in a very large pressure drop across the fixed bed reactor. A particle size fraction of 2.0-4.0 mm was used in the packed bioreactor.

Coal solubilisation was carried out in a stirred tank slurry bioreactor at 5 % (w/v) and a particle size fraction of 600-850 μm. The supernatant showed a maximum absorbance of 0.180 at 450 nm. Dry weight analysis showed a coal weight loss of 24 %. There was an increase in pH from 3.8 to 6.2. Complete mixing of coal particles and fungal biomass was obtained at 560 rpm. The estimated volumetric mass transfer coefficient (K_La) value was 0.09 s^{-1}. The estimated oxygen transfer rate (OTR) was 0.03 mg l^{-1} s^{-1}. On comparing the estimated OTR value and the OUR value reported in Section 6.2.1.5, there was no oxygen limitation in the stirred tank bioreactor.

In the fluidised bed slurry bioreactor, coal solubilisation was carried out at two coal size fractions, 150-300 μm at 5 % and 10 % coal loading and 600-850 μm at 5 % (w/v) coal loading. The smaller particle size was included to ensure complete fluidisation. The agitation and mixing of the coal particles was done by aeration only. An increase in particle size required an increase in superficial gas velocity for efficient suspension of particles to occur. The minimum fluidisation velocity was 0.4 cm s^{-1} and 1.2 cm s^{-1} for 150-300 μm and 600-850 μm respectively. There was also considerable elutriation of coal particles from the bed when using the 150-300 μm coal size fractions. However, for 600-850 μm there was not enough turbulence to create good mixing at a superficial gas velocity of 0.64 cm^{-1} because the minimum fluidisation velocity was 1.2 cm^{-1}. This may explain the low coal weight loss of 10% for this size fraction. Higher coal weight loss observed in the stirred tank slurry bioreactor in comparison to the fluidised bed slurry bioreactor at 5% (w/v) coal loading and 600-850 μm coal fractions may be due to increased mass transfer and mixing.

The overall gas hold-up in the fluidised bed slurry bioreactor increased when there was an increase in superficial gas velocity. There was a marginal decrease in the overall gas hold-up where there was an increase in coal loading. There was an increase in the gas-liquid mass transfer due to an increase in the superficial gas velocity from 0.43 cm^{-1} to 0.64 cm^{-1} at 5% (w/v) coal loading and a particle size fraction distribution of 150-300 μm in the fluidised bed bioreactor, but a decrease in mass transfer on increasing the coal loading.

The analysis of supernatant from coal solubilisation in the packed bed bioreactor showed no increase in absorbance due to coal solubilisation and the gravimetric coal measurement showed a 0.5% coal weight loss. This limited solubilisation was due to large coal particle size fraction (2-4mm) used. There was no correlation between increase in pH and coal weight loss. This is in agreement with Larboda *et al.* (1997) and Holker *et al.* (1995).

Minimal or no damage to the microbial cell after 14 days of coal solubilisation in the packed bed reactor was noted. The fungal biomass showed green colouration which signified stationary phase of the growth cycle (Prescott, 1993). The presence of fungi in the packed bed resulted in it occupying the void volume on its growth, thereby reducing bed porosity. This caused a high pressure drop across the bed or channelling and maldistributioin of the liquid phase.

The overall conclusion is that a good mass transfer environment is needed for coal solubilisation in a slurry bioreactor. This was illustrated by the improved solubilisation in the STR over the shake flask or incompletely fluidised bed. There were practical problems with operation of a fluidised bed with fine particles, such as elutriation of coal particles. The fixed-bed reactor suffers from several shortcomings related to the minimum particle size and the impact that this has on the rate of reaction, and to fungal accumulation which leads to clogging and increased pressure drop. It can be concluded that the packed bed is an unsuitable reactor for use in the presence of fungi cells; it can only be used for treatment of the coal by cell free extracts.

CHAPTER 7: CONCLUSIONS AND RECOMMENDATIONS

7.1 SCOPE OF STUDY

The under-utilisation of low rank coal for electricity generation, transportation and metallurgical processes by coal conversion technologies is due to its physical properties e.g. low calorific value, high moisture and sulphur content. However, the reserves of low rank coal are substantial, accounting for 47 % of the overall coal reserves (Faison, 1993). Microbial solubilisation of low rank coal at ambient temperature and pressure has been demonstrated (Scott *et al.* 1986). Biosolubilisation of low rank coal has been reported to lead to valuable oxidised products. These products can further be used as substrates in the biotransformation process for the production of value added compounds such as antioxidants. The remaining unsolubilised coal fractions, which are enriched in aliphatic compounds and have low water and ash content, can be used as a clean and cost effective energy source (Holker and Hofer, 2002).

In this study, the key variables that affect coal biosolubilisation were investigated through a factorial experiment. Coal loading and particle size fraction were studied to determine optimum conditions for coal biosolubilisation. A mass balance approach based on off-gas analysis for the quantification of fungal biomass was developed. The estimated biomass was further used for the evaluation of product yield. Coal biosolubilisation was investigated in a stirred tank bioreactor, a fluidised bed bioreactor and a fixed bed bioreactor. The advantages and shortcomings of each of these reactor configurations were assessed.

7.2 CONCLUSIONS DRAWN

In order to assess the outputs of the thesis, the appropriate conclusions around each objective should be identified. This is addressed below.

The first objective of the thesis was to investigate the role of fungal biomass and extracellular enzymes in both coal biosolubilisation and subsequent degradation of phenolics intermediates. The key questions centred on this objective are:

- What contact is needed between the fungus and the coal for efficient biosolubilisation and depolymerisation?
- Is further decomposition or degradation of the soluble polyphenolic products attributed to extracellular enzymes or is it a whole cell process?

It was shown that there was a higher degree of coal biosolubilisation in the fungal culture than in the cell free-culture containing extracellular enzymes. The extent of coal biosolubilisation in the presence of fungi was 7.2 % (measured by coal weight loss) in comparison to 0.7 % in the cell free culture. This suggests that contact is needed between the fungal biomass and the coal particle for efficient coal biosolubilisation. In both cases, the release of phenolic compounds was negligible. This suggests that neither the fungal cell nor the extracellular enzymes are responsible for the release of phenolic products. Further, to prevent product degradation, a reactor configuration is required to remove soluble products from the fungi on their formation. The study showed that soluble products such as organic acids were further metabolised by fungi in the stirred tank bioreactor.

The second objective centred on identifying key operating variables influencing coal biosolubilisation. Here the key question was:

- What are the key operating variables influencing the coal biosolubilisation process and what are their preferred values?

The key operating variables that influence coal biosolubilisation in the slurry bioreactor were shown to be coal loading and particle size. Concurrently they affect the surface area available for coal biosolubilisation. Under the factorial conditions of 5 to 10% solids loading and particle size in the range 600 to 2000 μm, 5% loading and a size range of 600-850 μm gave the greatest extent of coal solubilisation. An increase in solids loading led to inhibition of the fungal culture of *Trichoderma atroviride* (ES11) by fragmentation of the fungal mycelium. A decrease in particle size fraction, extending the range studied to 150 to 300 μm, led to an increase in the degree of coal solubilisation. The highest degree of coal solubilisation obtained in this study was at 150-300 μm. It is expected that further size reduction below 150 μm diameter will further enhance solubilisation but will be limited economically. To confirm the hypotheses that coal biosolubilisation is enhanced by increased availability of coal surface area, coal biosolubilisation was shown to increase by 4-fold when the particle size fraction was decreased from 600-850 to 150-300 μm. The extent of solubilisation of coal at 150-300 μm characterised by a surface specific area of 2.17 $cm^2 g^{-1}$ was 28 % measured as coal weight loss. This can be compared with a 7.8% coal weight loss at 600-850 μm diameter (0.54 $cm^2 g^{-1}$).

The third objective of the thesis was to compare the stirred tank slurry bioreactor, fluidised bed bioreactor and fixed bed bioreactor configuration for the fungal biosolubilisation of coal. It was shown that coal biosolubilisation requires a good mass transfer environment in a slurry bioreactor as illustrated by the improved solubilisation in the STR over the shake flask or incompletely fluidised bed. There are practical problems with operation of a fluidised bed with fine particles, such as elutriation of coal particles. The fixed-bed reactor suffers from several shortcomings related to the minimum particle size and its impact on the rate of reaction, and to fungal accumulation which leads to clogging and increased pressure drop. It can be concluded that the packed bed is an unsuitable reactor for use in the presence of fungi cells; it can only be used for treatment of the coal by cell free extracts.

The fourth objective of the thesis was to provide methodology by which to quantify fungal growth and biomass formation in the slurry reactor system. In order to facilitate kinetic analysis, a stoichiometric approach based on off-gas analysis can be used to quantify biomass growth in the presence of coal. This methodology has been developed and applied in the slurry STR. The study showed that a stoichiometric approach based on off-gas analysis can be used to quantify biomass growth in the presence of coal. The estimated biomass formation in terms of CO_2 production rate and O_2 consumption rate were 2.3 g l^{-1} and 2.1 g l^{-1} respectively at a 5% (w/v) loading of coal particles of 600-850 μm particle size fraction in the stirred tank reactor. These biomass production rates were based on the stoichiometric analysis of biomass formation from glucose. Refinement is recommended to use a stoichiometric analysis based on carbon source better representing coal, such as humic acid.

The fifth objective was to provide process kinetic data on the biosolubilisation and biodegradation of coal for bioreactor design. Basic kinetic data for growth of *Trichoderma atroviride* on soluble carbon source has been provided through this study; however, the low extent and low rate of solubilisation measured in this work, as well as the significant degradation of soluble intermediates to CO_2, indicate that significant process improvement is required before it is of value to complete a rigorous kinetic study. In the current process, coal solubilisation remains limited (10-25%) and the dominant product results from complete oxidation to CO_2. Optimisation of the accumulation of complex intermediates is desirable.

Overall Conclusion

Biosolubilisation of un-treated low rank coal by *Trichoderma atroviride* (ES 11) is limited. The resulting products are biomass, soluble organic products and CO_2. The soluble products accumulated include organic acids and are not predominantly phenolics. Negligible release of phenolics was observed. These soluble products are further metabolised by the fungi to CO_2. For efficient coal biosolubilisation, contact between the fungal biomass and the coal particle is required through provision of a slurry bioreactor environment. Key operating variables in this environment are solids loading and particle size.

7.3 RECOMMENDATIONS

Based on these findings to date as well as the recognised shortcomings in the study and the understanding generated, the following are recommended areas of further study:

- While the use of growth yield from glucose provided an overall estimation of biomass formed through off-gas analysis, it introduced some error in the estimation of biomass on coal owing to potential change in microbial metabolic pathways on changing the carbon source. It is recommended that the method be refined through the use of growth yield data from a similar substrate such as humic acid.
- The study has highlighted the need for more detailed analyses of the soluble organic product spectrum produced, allo wing a more comprehensive carbon balance to be carried out.
- Following characterisation of the product spectrum, it will be possible to undertake a study of key metabolic pathways involved, providing information to propose operating conditions that favour product accumulation.
- While it has been shown that a slurry bioreactor configuration is required for coal biosolubilisation, optimisation of both the STR and fluidised bed reactor configuration is still required. Further research should be carried out in expanded bed height in a fluidised bed bioreactor to address the problem of elutriation of fine particles.
- The study has shown that particle size is a key operating variable but further work is required to determine the optimum particle size fraction. Also it is

necessary to assess the compromise between the milling cost and the extraction benefit.

- An effort should be made to confirm the rate of release of soluble carbon and the rate of oxidation of the soluble carbon to CO_2.
- Novel process development strategies are required to maximise the formation of soluble organic compounds and minimise their further degradation to CO_2.
- Coal solubilisation should be investigated in a bubble-column because it can overcome the problem of shear in a stirred tank reactor, the problem of fine-particles in a fluidised bed reactor and the problem of biomass blockage in a packed bed reactor.

REFERENCES

Achi OK (1993). Studies on the microbial degradation of Nigerian preoxidised sub bituminous coal. *International Biodeterioration and Biodegradation,* **31**, 293-303.

Andrews GF (1991). Mass and energy balance constraints on the biological production of chemicals from coal. *Fuel,* **70**, 585-589.

Andrews GF and Noah KS (1997). The slurry-column coal beneficiation process. *Fuel Processing Technology,* **52**, 247-266.

Asif M, Petersen JN, Scott TC and Cosgrove JM (1993). Hydrodynamic studies of an advanced fluidised bed bioreactor for direct coal liquefaction. *Applied Biochemical Biotechnology,* **39/40,** 535-547.

Bailey JE and Ollis DF (1986). *Biochemical Engineering Fundamentals.* McGraw-Hill, New York.

Bailey AD and Hansford GS (1993). Factors affecting bio-oxidation of sulfide minerals at high concentrations of solid: A review. *Biotechnology and Bioengineering,* **42,** 1164-1174.

Blanch HW and Clarke DS (1997). *Biochemical Engineering.* Marcel Dekker, New York.

Box GEP, Hunter WG and Hunter JS (1978). *Statistics for Experimenters—An Introduction to Design, Data Analysis and Model Building,* John Wiley & Sons, New York.

Box J. D. (1983). Investigation of the Folin-Ciocalteau phenol reagent for the determination of polyphenolic substances in natural waters. *Water Research,* **17**, 511-525.

Brand D, Pandey A, Rodriguez-Leon JA, Roussos S, Brand I and Soccol CR (1999). Packed bed column fermenter and kinetic modeling for upgrading the nutritional quality of coffee husk in solid state fermentation. *Biotechnology Progress,* **17,** 1065-1070.

Breed AW, Dempers CJ, Searby GE, Gardner MN, Rawlings DE and Hansford GS (1999). The effect of temperature on the continuous ferrous-iron oxidation kinetics of a predominantly *Leptospirillum ferroxidans* culture. *Biotechnology and Bioengineering,* **65,** 44-53.

Burton SG (2003). Laccases and phenol oxidases in organic synthesis: A review. *Current Organic Chemistry,* **7,** 1317-1331.

Chisti Y and Jauregui-Haza UJ (2002). Oxygen transfer and mixing in mechanically agitated airlift bioreactors. *Biochemical Engineering Journal,* **10**, 143-153.

Choi KH, Chisti Y and Moo-Young M (1996). Comparative evaluation of hydrodynamic and gas-liquid mass transfer characteristics in bubble column and airlift slurry reactors. *The Chemical Engineering Journal*, **62,** 223-229.

Cohen MS and Gabriele PD (1982). Degradation of coal by fungi *Polyporus* and *Poria Monticolar. Applied and Environmental Microbiology,* **44,** 23-47.

Cohen ST, Bowers WC, Aronson H, Gray ET (1987). Cell-free solubilisation of coal by *Polyporus veriscolor. Applied and Environmental Microbiology,* **58**, 2840-2843.

Cohen ST, Bowers WC, Gray ET, Feldmann KA (1990). Isolation and identification of the coal-solubilisation agent produced by *Trametes versicolor. Applied and Environmental Microbiology*, **56**, 3285-3290.

Cox PW and Thomas CR (1992). Classification and measurement of fungal pellets by automated image analysis. *Biotechnology and Bioengineering*, **39,** 845-952.

Cowan D (2004). Personal communication.

Crawford DL and Gupta RK (1991). Influence of cultural parameters on the depolymerisation of soluble lignite coal polymer by *Pseudomonas cepaci* DLC-07. *Resources Conservation and Recycling*, **5**, 245-254.

de Kock SH, Barnard P and du Plessis CD (2004). Oxygen and carbon dioxide kinetic challenges for thermophilic mineral bioleaching processes. *Biochemical Society Transactions*, **32**, 273-275.

Derksen JJ, Buist K, van Weert G and Reuter MA (1999). Oxygen transfer in agitated silica and pyrite slurries. *Minerals Engineering,* **13,** 25-36.

Desgranges C, Vergoignan C, Georges M and Durand A (1991). Biomass estimation in solid state fermentation. II On line measurements. *Applied Microbiology and Biotechnology*, **35,** 206- 209.

Doran PM (1995). *Bioprocess Engineering Principles.* Academic press, London.

Drossou M (1986). The kinetics of the bioleaching of a refractory gold-bearing pyrite. MSc thesis, University of Cape Town.

Dunford HB (1991). Horseradish peroxidase: structure and kinetic properties. In *Peroxidases in Chemistry and Biology* (Everse J., Everse K.E., Gisham M.B. Eds) pp.1-24 Boca Raton , FL: CRC Press.

Elliot M.A. (1981). *Chemistry of Coal Utilisation*, 2nd supplementary volume, John Wiley and Sons, New York.

Faison RD (1991). Biological coal conversions. *Critical Reviews of Biotechnology*, **11**, 347-356.
Faison BD (1993). The chemistry of low rank coal and its relationship to biochemical mechanism of coal biotransformation. In *Microbial transformation of low rank coals.* Crawford Dl (Ed) CRC Press. Boca Raton. Pp 1-26.

Fakoussa RM (1981). *Kohle als substrat fur microorganism: Untersuchugen zur Mikrobellien Umsetzung nativer Steinkohle.* Ph.D. thesis, University of Bonn, Germany. Translated as: *Coal as a substrate for the microorganism's investigations of the microbial decomposition of untreated hard coal,* Prepared for U.S Department Of Energy, Pittsburgh Energy Technology Center, 1987.

Fakoussa RM (1988). Production of water–soluble coal substances by partial microbial liquefaction of untreated hard coal. *Resource Conservation and Recycling,* **1,** 251-260.

Fakoussa RM (1990). Microbiological treatment of German hard coal. In *Bioprocessing and Biotreatment of Coal* (Wise, D.L., Ed.), pp 95-107, Marcel Dekker. New York.

Fakoussa RM (1994). The influence of different chelators on the solubilisation/ Liquefaction of different pretreated and natural lignites. *Fuel Processing Technology*, **40** 183-192.

Fakoussa RM and Hofrichter M (1999). Biotechnology and microbiology of coal degradation. *Applied Microbiology and Biotechnology,* **52**, 25-40.

Fakoussa RM and Frost P (1999). *In vivo*-decolorisation of coal derived humic acids by laccase- excreting fungus *Trametes versicolor. Applied Microbiology and Biotechnology,* **52**, 60-65.

Fuchtenbusch B and Steinbuchel A (1999). Biosynthesis of polyhydroxyalkanoates from low-rank coal liquefaction products by *Pseudomonas oleovorans* and *Rhodococcus rubber Applied Microbiology and Biotechnology,* **52,** 91-95.

Garcia Ochoa J, Khalfet R, Poncin S, Morin D and Wild G (1997). Hydrodynamics and mass transfer in a suspended solid bubble column with poly dispersed high density particles. *Chemical Engineering Science*, **52,** 3827-3834.

Garcia Ochoa J, Poncin S, Morin D and Wild G (1999). Bioleaching of mineral ores in a suspended solid bubble column. In *Proceedings of International Biohydrometallurgy Symposium* Madrid, Spain, June 1999, 631-641.

Gokacy CF, Kolankaya N and Dilek FB (2001). Microbial solubilisation of lignite. *Fuel* **80**, 1421-1433.

Gupta RK, Spiker JK and Crawford DL (1988). Biotransformation of coal by ligninolytic *Streptomyces. Canadian Journal of Microbiology,* **34,** 667-676.

Hagan CW (1989). Energy technology R&D: what could make a difference? *Oak Ridge National Laboratory Rep.*, 6541/v1, 166.

Harrison STL, Sissing A, Raja S, Pearce SJA, Lamaignere V and Nemati M (2003). Solids loading in the biotech slurry reactor: mechanisms through which particulate parameters influence slurry bioreactor performance. In biohydrometallurgy: a sustainable technology in evolution. *Proceedings of the 15th International Biohydrometallurgy Symposium*, pp 359-375.

Hodek W (1994). The chemical structure of coal in regard of microbiological degradation. *Fuel Processing Technology*, **40**, 369-378.

Hofrichter M and Fritsche W (1996). Depolymerisation of low rank coal by extra cellular fungal enzyme systems **I**. Screening for low rank coal depolymerising activities. *Applied Microbiology and Biotechnology,* **46**, 220-225.

Hofrichter M, Bubltiz F and Fristsche W (1997). Fungal attack on coal. II. Solubilisation of low rank coal by filamentous fungi. *Fuel Processing Technology,* **52**, 55-64.

Hofrichter M and Fritsche W (1997). Depolymerisation of low rank coal by extracellular fungal enzyme systems III. *In vitro* depolymerisation of coal humic acids by crude preparation of manganese peroxidase from white–rot fungus *Nematoloma Frowdii* B19. *Applied Microbiology and Biotechnology,* **47**, 419-424.

Hofrichter M, Vares T, Schreiber K, Galkin S, Sipila J and Hatakka A (1998). Mineralisation of synthetic lignin (DHP) by manganese peroxides from *Nematoloma Frowardii* and *Phelia radiate. Journal of Biotechnology*, **67**, 217-228.

Hofrichter M and Fakoussa RM (2001). Microbial degradation and modification of coal. In *Biopolymers: Lignin, Humic Substances and Coal* (Hofrichter M and Steinbuchel A., Ed), pp 393- 429. Wiley-Vch, Germany.

Holker U, Fakoussa RM, and Hofer M (1995). Growth substrates control the ability of *Fusarium oxyporium* to solubilise low-rank coal. *Applied Microbiology and Biotechnology,* **44**, 351-355.

Holker U, Ludwig S, Scheel T, Hofer M (1999a). Mechanisms of coal solubilisation by *Trichoderma atroviride* and *Fusarium oxysporium. Applied Microbiology and Biotechnology*, **52,** 57-59.

Holker U, Ludwig S, Scheel T, Hofer M, Polsakiewicz M and Schinke-kissing S (1999b). Coal as inductor of esterases in the deuteromycete *Trichoderma atroviride. Proceedings of 5th International Symposium on Biological Processing of Fossil Fuels*, 26-29th Sept.1999, Madrid, Spain.

Holker U and Hofer M (2002). Solid substrate fermentation of lignite by the coal-solubilizing mould, *Trichoderma atroviride,* in a new type of bioreactor. *Biotechnology Letters*, **24,** 1643-1645.

Hulston CKJ, Redlich PJ, Jackson WR and Larkins FP (1996). The effect of tubular reactor orientation on conversion of coal to liquid products. *Fuel,* **75,** 43-45.

Kaufman EN, Petersen JN, Wang Y and Little MH (1995). Experimental and numerical characterisation of liquid fluidized bed of coal particles. *Chemical Engineering Science,* **50,** 3703-3714.

Kirk-Othmer (1964). *Encyclopedia of Chemical Technology.* Second edition, Vol 2, John Wiley and Sons Inc. New York.

Klein J, Catcheside DEA, Fakoussa RM, and Fritsche W (1999). Biological processing of fossil fuels. *Applied Microbiology and Biotechnology,* **52,** 2-15.

Koutinas A.A., Wang R. and Webb C. (2003a). Estimation of fungal growth complex, heterogeneous culture. *Biochemical Engineering Journal*, **14**, 93-100.

Koutinas A.A., Wang R. Kookos I.K. and Webb C. (2003b). Kinetic parameters of *Aspergillus awamori* in submerged cultivations on whole wheat flour under oxygen limiting conditions. *Biochemical Engineering Journal*, **16**, 23-34.

Kunii D and Levenspiel O (1977). *Fluidisation Engineering.* Melbourne, Fla.: Robert E. Krieger Publishing.

Lamaignere V (2003). Effect of hydrodynamic stress on growing *Saccharomyces cerevisiae* in a slurry reactor. MSc dissertation, University of Cape Town.

Larboda F, Monistrol IF, Luna N and Fernandez M (1997). Study of the mechanisms by which microorganisms solubilise and/or liquefy Spanish coals. *Fuel Processing Technology,* **52,** 95-107.

Larboda F, Monistrol IF, Luna N and Fernandez M (1999). Processes of liquefaction / solubilisation of Spanish coals by microorganisms. *Applied Microbiology and Biotechnology,* **52**, 49-56.

Levenspiel O (1972). *Chemical Reaction Engineering.* Wiley, New York.

Luedeking R. and Piret EL (1959). A kinetic study of the lactic acid fermentation. *Journal of Biochemical Microbiology Technology Engineering,* 1, 393.

Linek V, Vacek V and Benes P (1987). A critical review and experimental verification of the correct use of the dynamic method for the determination of oxygen transfer in aerated agitated vessels to water, electrolyte solutions and viscous liquids. *Chemical Engineering Journal,* **36,** 26-28.

Mohebby B (2005). Attenuated total infrared spectroscopy of white-rot decayed beech wood. *International Biodeterioration and Biodegradation*, **55,** 247-251.

Mersmann A, Schneider G, Voit H and Wenzig E (1990). Selection and design of aerobic bioreactors. *Chemical Engineering Technology*, **13,** 357-370.

Miller GL (1959). Use of dinitrosalicylic acid reagent for determination of reducing sugar. *Analytical Chemistry,* **31,** 426.

Moo-Young M and Blanch HW (1981). Design of biochemical reactors. Mass transfer criteria for simple and complex systems. *Advances in Biochemical Engineering,* **19,** 1-69.

Nagata S (1975). *Mixing: Principles and Application.* Kodansha, Tokyo.

Nemati M, Lowenadler J and Harrison STL (2000). Particle size fraction in bioleaching of pyrite by acidophilic thermophile *Sulfolobus metallicus (BC). Applied Microbiology Biotechnology,* **53,** 173-179.

Nemati M, and Harrison STL (2000). Effects of solid on thermophilic bioleaching of sulphide minerals. *Journal of Chemical Technology and Biotechnology,* **75,** 526-532.

Nyirenda J (2003). An introduction to comparative statistics and experimental design course note, CHE530Z, University of Cape Town.

Odier E, Mozuch MD, Kalyanaraman B and Kirk TK (1988). Ligninase-mediated phenoxy radical formation and polymerisation unaffected by cellobiose: quinone oxidoreductase. *Biochemie,* **70,** 847-852.

Oguz H, Brehm A, and Deckwer W (1987). Gas–liquid mass transfer in sparged agitated slurries. *Chemical Engineering Science*, **42**, 1815-1822.

Ospiowicz B, Jablonski L, Siewinski, Jasienko S and Rymkiewicz A (1994). Biodegradation of hard coal and its organic extract by selected microorganisms. *Fuel,* **73,** 1858-1862.

Osborne DG (1988). *Coal Preparation Technology* Volume 1. Alden Press, Oxford.

Paul EA and Clark (1996). *Soil and Biochemistry.* Pp148-153, 2nd Edition, Academic Press, London.

Pearce SJA (1993). The disruption of microorganisms due to agitation in slurries of fine particles. MSc Thesis. University of Cape Town.

Perry RH and Green DW (1984). "Chapter 9: Energy Utilisation, Conversation and Resource Conservation" In *Perry's Chemical Engineers' Handbook.* 6th edition, McGraw-Hill, Singapore.

Polman JK, Miller KS, Stoner DL and Breckenridge CR (1994). Solubilisation of bituminous and lignite coals by chemically and biologically synthesized surfactants. *Journal of Chemical Technology Biotechnology*, **61**, 11-17.

Prescott LM, Harley JP and Klein DA (1993). *Microbiology*: 2nd Edition, Wm. C. Brown Publishers. London.

Quigley DR, Wey JE, Breckenridge CR and Stoner D (1988). The influence of pH on biological solubilization of oxidised low rank coal. *Resources Conservation and Recycling,* **1**, 163-174.

Quigley D, Ward B, Crawford DL, Hatcher HJ and Dugan PR, (1989a). Evidence that microbially produced alkaline materials are involved in coal biosolubilisation. *Applied Biochemical Biotechnology,* **21**, 753-763.

Quigley DR, Dugan PR and Breckenridge CR (1989b). Effects of multivalent cations on low rank coal solubility in alkaline solutions and microbial cultures. *Energy Fuels,* **3,** 571-763.

Ralph JP and Catcheside DEA (1993). Action of aerobic microorganisms on the macromolecular fraction of lignite. *Fuel,* **72**, 1679-1686.

Ralph JP and Catcheside DEA (1994) Decolourisation and depolymerisation of Solubilised low rank-coal by the white-rot basidiomycete *Phanerochae chrysosporium. Applied Microbiology and Biotechnology,* **42**, 536-542.

Ralph JP and Catcheside DEA (1997). Transformations of low rank coal by *Phanerochaete chrysosporium* and other wood-rot fungi. *Fuel Processing Technology,* **52,** 73-93.

Ralph JP and Catcheside DEA (1999). Transformation of macromolecules from brown coal by lignin peroxidase. *Applied Microbiology and Biotechnology,* **52,** 70-77.

Rao TC (1977). Mineral crushing and grinding circuits. Page 98, (Edited by Lynch AJ). Elsevier, Amsterdam.

Rawlings DE, Dew D and du Plessis CD (2003). Biomineralisation of metal-containing ores and concentrates. *Trends in Biotechnology,* **21**, 38-44.

Rheinbraun, (2000). 'Lignite Worldwide' 'Hard Coal Worldwide' and Lignite in Europe. Article published on Rheinbraun's Internet site (www.rheinbraun.de) by Rheinbraun Information, August, 2000.

Rogoff MH, Wender I and Anderson RB (1962). Microbiology of coal, U.S. Dept. Interior Bureau of Mines Information Circ. No. 8075.

Rushton JH Costich EW and Everett HJ (1950). Power characteristics of mixing impellers. Part I. *Chemical Engineering Progress,* **46**, 395-404.

Rushton JH Costich EW and Everett HJ (1950). Power characteristics of mixing impellers. Part II. *Chemical Engineering Progress,* **46**, 464-476.

Ryan JR, Loher RC and Rucker E (1991). Bioremediation of organic contaminated soils. *Journal* of *Hazardous Materials*, **28,** 159-169.

Sales FG, Maranhao LCA and Pereira JAF (2005). Experimental dynamic evaluation of three-phase reactors. *Brazilian Journal of Chemical Engineering*, **22,** 443-452.

Scholtz NJ, Pandit AB and Harrison STL (1997). The effect of microbial cell disruption. In *Proceedings of 4th International Conference on Bioreactor and Bioprocess Fluid Dynamics,* Edinburgh Scotland. pp 199-215.

Scholtz NJ. (1998). The effect of non-biological particulates on microbial cell disruption in a slurry bioreactor. PhD thesis, University of Cape Town.

Scott CD, Strandberg GW and Lewis SN (1986). Microbial solubilisation of coal *Biotechnology Progress,* **2,** 131-139.

Scott CD (1990). Advanced bioreactor concept for coal bioprocessing. *Resources, Conversation and Recycling,* **3,** 125-135.
Scott CD, Woodward AC and Scott TC (1994). Mechanisms and effect of using chemical modified reducing enzymes to enhance the conversion of coal to liquids. *Fuel Processing Technology,* **40**, 319-32.

Sissing A and Harrison S T L (2003). Thermophilic mineral bioleaching performance: a compromise between maximising mineral loading and maximising microbial growth and activity. *SAIMM Journal,* March 2003, 1-4.

Sokol W (2001). Operating parameters for gas-liquid–solid fluidised bed bioreactor with a low density biomass support. *Biochemical Engineering Journal,* **8,** 203-212.

Steffen K, Hofrichter M and Hatakka A (2000). Mineralisation of 14 C-labelled synthetic lignin and ligninolytic enzyme activities of litter-decomposing basidiomycete fungi. *Applied Microbiology and Biotechnology,* **54**, 819-825.

Stewart DL, Thomas BL, Bean RM and Fredrickson JK (1990). Colonisation and degradation of oxidised bituminous and lignite colas by fungi. *Journal of Industrial Microbiology* 6, 53-59.

Strandberg GW and Lewis SN (1987). Solubilisation of coal by extracellular product from *Streptomyces setonii* 75Vi2. *Journal of Industrial Microbiology*, **1**, 371-376.

Temp U, Meyralm H and Eggert C (1999). Extracellular phenol oxidase patterns during depolymerisation of low rank coal by three basidiomycetes. *Biotechnology Letters*, **21,** 281-287.

Tien M and Kirk TK (1984). Lignin peroxidase of *Phanerochate chrysosporium. Methods in Enzymology*, **161**, 238-249.

Toma MK, Ruklisha MP, Vangas JJ, Zeltina MO, Liete MP, Galinina NL, Viesturs UE and Tengerdy RP (1991). Inhibition of microbial growth and metabolism by excess turbulence. *Biotechnology and Bioengineering*, **38,** 552- 556.

Torzilli AP and Isbister JD (1994). Comparison of coal solubilisation by bacteria and fungi. *Biodegradation*, **5,** 55-62.

Tsai SC (1982). *Fundamentals of coal beneficiation and utilisation.* Elsevier, New York.

Van't Riet K (1979). Review of measuring methods and results in non-viscous gas-liquid mass transfer in stirred vessels. *Industrial Engineering Chemical Process Development,* **18,** 357-364.

Viniegra-Gonazalez G, Saucedo-Castaneda G, Lopez-Isunza F and Favela–Torres (1993). Symmetric branching model for kinetics of mycelial growth. *Biotechnology and Bioengineering,* **42**, 1-10.

Viniegra-Gonazalez G, Larralde-Corona C and Lopez-Isunza F (1994). A new approach for modeling the kinetics of mycelial growth. In: Galindo E and Ramirez O (Eds) *Advances in Bioprocess Engineering,* Kluver Academic Publishers, and Amsterdam.

Ward B (1985). Lignite-degrading fungi isolated from a weathered outcrop. *System Applied Microbiology*, **6,** 236-238.

Ward B (1993). Quantitative measurements of coal solubilisation. *Biotechnology Techniques*, **7,** 213- 216.

Willmann G and Fakoussa RM (1997a). Biological bleaching of water-soluble coal macromolecules by a basidiomycete strain. *Applied Microbiology and Biotechnology,* **47,** 95-101.

Willmann G and Fakoussa RM (1997b). Extracellular oxidative enzymes of coal attacking fungi. *Fuel Processing Technology*, **52,** 27-41.

Wilson BW. In: *Biological treatment of coals workshop*, 23-25 June 1986, Proceedings, 1986: 114.

World Coal Institute (2005). What is coal? [Online]. Available from: http//www.worldcoal.org/assets_cm/files/PDF/whatiscoal. pdf [Accessed 10 November 2005]

Wondrack L, Szanto M and Wood W (1989). Depolymerisation of water soluble coal polymer from sub bituminous coal and lignite by lignin peroxidase. *Applied Biochemical Biotechnology* **20/21**, 765-780.

Zhang K, Zhao Y and Zhang B (2003). Gas holdup characteristics in a tapered bubble column. *International Journal of Chemical Reactor Engineering,* **1,** 1-7.

Ziegenhagen D and Hofrichter M (1998). Degradation of humic acids by manganese peroxidase from the white rot fungus *Clitocybula dusenii. Journal of Basic Microbiology,* **38,** 289-299.

APPENDIX A: DESCRIPTION OF ANALYTICAL PROCEDURES

A.1 ABSORBANCE

3 ml of the supernatant were used for absorbance measurements. Absorbance was read at 450 nm with a UV-Vis spectrophotometer, using plastic cuvette filled with distilled water as blank.

A.2 TOTAL DISSOLVED SOLIDS

Apparatus:

- Three dry weight eppendorf tubes
- 1mL pipetman
- 4 decimal place balance

Method

1 Weigh empty dry tubes to 4 decimal places

2 Add 1 ml of supernatant to each dry weight tube.

3 Dry the tubes in an oven at 80^0C for 24 hours.

4 Weigh the tubes. The TDSS is the difference in mass between the tubes containing the dry TDSS and the tubes alone, divided by the volume used.

A.3 COAL WEIGHT LOSS

Method

1. Decant the supernatant from the flask or reactor, remove spent biomass by washing.
2. Dry the coal samples in an oven at 80^0C for 48 hours
3. Weigh the dry coal samples.

A.4 DRY BIOMASS CONCENTRATION

Apparatus

- Vacuum filter
- 0.45μm membrane Filter
- Oven

Method

- Weigh the filter paper
- Filter 5ml of cell suspension using vacuum filter
- Dry filter paper containing biomass at 80^{0}C for 2 days
- Reweigh the dried filter paper.

A.5 pH MEASUREMENT

Apparatus

- pH meter
- Distilled water
- 5ml sample bottle

Method

- 5ml of the supernatant was placed in the in the sample bottle. The pH meter was calibrated for a range of pH 4-7 before use.

A.6 GLUCOSE CONCENTRATION

Apparatus

- UV-VIS spectrophotometer
- 4ml plastic cuvettes
- Test tubes
- Water bath

The composition of Dinitrosalicyclic acid (DNS) reagent is shown below

Chemical	Amount
3,5 Dinitrosalicyclic acid	10.6g
NaOH	19.8g
Rochelle salts (Na K Tartrate)	306g
Phenol	7.6g
Na- metabisulphate	8.3g
Distilled water	1416ml

Method

Standard calibration curve is first obtained by

- Dissolve 1 g of glucose in a 10 ml volumetric flask with distilled water
- Pipette out 0, 10, 20, 40, 60 80 and 100µl into 10 ml volumetric flasks.
- Bring the volume up to 10 ml with distilled water
- Add 200µl of the standard glucose solution into a test tube and 600µl DNS. Do in triplicate
- Boil rapidly in a water bath at 100^0C for 5minutes and cool in ice.
- Add 3200 µl distilled water
- Measure the absorbance against the blank(distilled water) at 510nm

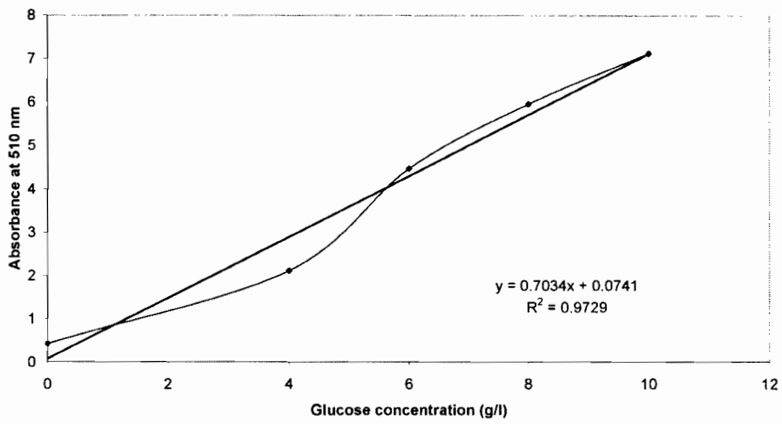

Figure: A.6 Calibration curve of glucose analysis

Table A .6: Reproducibility of glucose analysis

Sample no	Glucose concentration (g/l)
1	6.61
2	6.98
3	6.99
Average	6.86
Standard deviation	0.22
Coefficient of variance (%)	3.16

A.7 PHENOLIC CONCENTRATION

Apparatus

- UV-VIS spectrophotometer
- 4ml plastic cuvettes

Reagents

Reagent A: Folin-Ciocalteau phenol reagent (Sigma Chemical Company, Catalogue no. F9252). The Folin-Ciocalteau phenol reagent contains an active constituent called phosphomolybdic-tungstic mixed acid.

Reagent B: Dissolve 100 g $Na_2 C0_3$ in 1 litre

Method

- Add 1 ml of sample to a 100 ml volumetric flask
- Add 16 ml of distilled water , then 2.5 ml Folin–Ciocalteau phenol reagent
- Mix for 30 seconds
- Add 15 ml sodium carbonate and mix well
- Make up to the 100ml mark with distilled water
- Allow the mixture to stand for 60 minutes.
- The absorbance is then measured at 725nm.

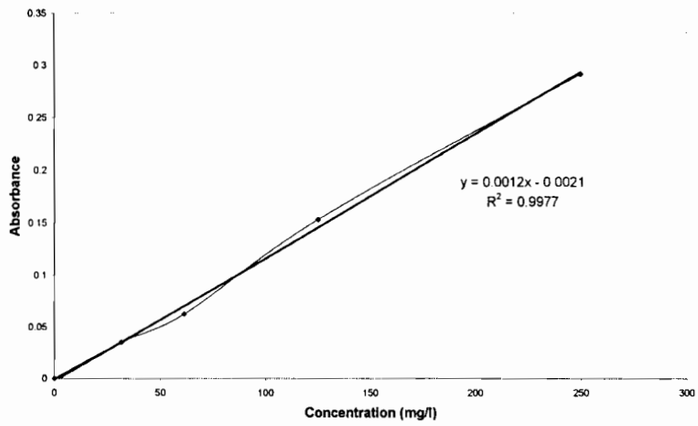

Figure A.7 Calibration curve for phenol analysis

Table A .7 Reproducibility of Phenolic concentration

Sample no	Phenolic concentration (mg/l)
1	90.72
2	89.18
3	90.17
Average	90.24
Standard deviation	0.46
Coefficient of variation (%)	0.51

A.8 TOTAL ORGANIC CARBON

Method

- Acidification(to between pH 1-3) of sample with 0.1M perchloric acid and filtered prior to injection
- Injection of 1000µl sample into the SGE ANATOC II TOC analyzer
- The concentration of carbon is then calculated from the volume.

Table A .8 Reproducibility of total organic carbon (TOC)

Sample	TOC (mg/l)
1	220
2	208
3	212
Average	213.13
Standard deviation	6.11
Coefficient of variance (%)	2.86

APPENDIX B: CALCULATION OF CARBON PRODUCTION RATE (CPR)

Carbon dioxide balance

In- out + formation – consumption =accumulation

$$\frac{F_{in}}{V}\left(Y_{C0_2}\right)_{in} - \frac{F_{out}}{V}\left(Y_{CO_2}\right)_{out} + 0 - CPR = 0 \text{ ----------1}$$

The flow rate of the off-gas, F_{out}, can be calculated from a nitrogen balance in gas phase

$$\frac{F_{in}}{V}\left(Y_{N_2}\right)_{in} - \frac{F_{out}}{V}\left(Y_{N_2}\right)_{out} = 0 \text{ ----------2}$$

$$\left(Y_{N_2}\right)_{out} = 1 - \left(Y_{0_2}\right)_{out} - \left(Y_{CO_2}\right)_{out} \text{ ----------3}$$

Using Equation 3 to substitute for Y_{N2} in Equation 2

$$F_{out} = \frac{F_{in}\left(Y_{N_2}\right)_{in}}{1 - \left(Y_{O_2}\right)_{out} - \left(Y_{CO_2}\right)_{out}} \text{ ----------4}$$

Substituting for F_{out} in Equation 1 by Equation 4 yields

$$\text{CPR} = \frac{F_{in}}{V}\left[\left(Y_{CO_2}\right)_{in} - \frac{\left(Y_{N_2}\right)_{in}\left(Y_{CO_2}\right)_{out}}{1 - \left(Y_{O_2}\right)_{out} - \left(Y_{CO_2}\right)_{out}}\right] \text{ ----------5}$$

APPENDIX C

APPENDIX C1: OVERALL GAS HOLDUP (VOLUME EXPANSION TECHNIQUE)

In the volume method, the measurement of unaerated, static liquid height (h_L) and the height of the gas-liquid dispersion (h_D) upon aeration were used to calculate the overall gas holdup (ε)

$$\varepsilon = \frac{h_D - h_L}{h_D}$$

APPENDIX C2: OVERALL VOLUMETRIC MASS TRANSFER COEFFICIENT

The volumetric mass transfer coefficient K_La in the bioreactor was determined using "gassing-out" method (Chisti, 1989). Nitrogen gas was used to get rid of the dissolved oxygen in the culture.

Procedure:

1. The dissolved oxygen was first calibrated at the required temperature. This was done by first sparging with N_2 gas and then air sparged and left to equilibrate until saturation value (C_{sat}) was obtained.
2. Turn off supply and start N_2 sparging
3. Monitor the time profile of the dissolved oxygen concentration
4. When the dissolved oxygen dropped to 21% of air saturation, stop N_2 sparging
5. Start air sparging
6. The increase in dissolved oxygen concentration is monitored with time until saturation value of oxygen is reached.

The K_La was calculated from the slope of ln (1-E) as function of time during aeration. This is illustrated in Figure C1 and Equation C1.

$$-\ln (1-E) = K_L a_L (t-t_0) \qquad \textbf{C 1}$$

where E, is expressed as

$$E = \frac{C - C_0}{C^* - C}$$

where

C^* = is the saturation dissolved oxygen concentration

C_0 = the initial dissolved oxygen concentration

C = the dissolved oxygen concentration at time t

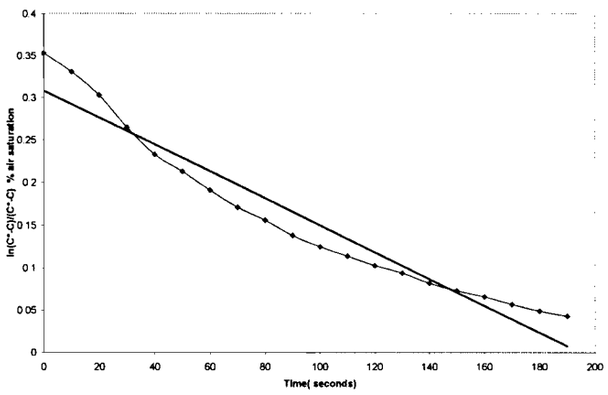

Figure C1: Determination of $K_L a$ by the gassing-in and gassing out technique

APPENDIX D: RAW DATA OF FACTORIAL EXPERIMENT IN SHAKE FLASK CONDITION

APPENDIX D1: COAL WEIGHT LOSS DATA

Coal balance	Initial wt	Final	Coal weigh loss	% Conversion
Coal loading	(g)	(g)		(g)
5%, 600-850μm	7.5	6.8	0.7	9.3
10%,600-850μm	15	13.9645	1.0355	7.0
5%, 1500-2000μm	7.5	7.0665	0.4335	5.78
10%,1500-2000μm	15	14.2	0.8	5.3

APPENDIX D2: ABSORBANCE

5 %(w/v) Coal loading and 600-850μm particle size fraction

Time	Absorbance(450nm)			
Days	Sample 1	Sample 2	Sample 3	Average
0	0.095	0.095	0.095	0.095
2	0.120	0.121	0.121	0.121
4	0.143	0.143	0.143	0.143
6	0.140	0.140	0.139	0.139
8	0.155	0.156	0.156	0.155
10	0.139	0.139	0.139	0.139
12	0.159	0.159	0.160	0.159
14	0.176	0.174	0.174	0.175

10 %(w/v) Coal loading and 600-850μm particle size fraction

Time	Absorbance (450nm)			
Days	Sample 1	Sample 2	Sample 3	Average
0	0.095	0.095	0.095	0.095
2	0.112	0.113	0.110	0.112
4	0.138	0.138	0.138	0.138
6	0.156	0.156	0.156	0.156
8	0.138	0.139	0.139	0.139
10	0.142	0.142	0.142	0.142
12	0.147	0.147	0.147	0.147
14	0.151	0.151	0.151	0.151

5 %(w/v) Coal loading and 1500-2000μm particle size fraction

Time	Absorbance(450nm)			
Days	Sample 1	Sample2	Sample3	Average
0	0.094	0.093	0.094	0.094
2	0.108	0.109	0.108	0.108
4	0.124	0.122	0.124	0.123
6	0.129	0.129	0.126	0.128
8	0.140	0.140	0.139	0.140
10	0.128	0.125	0.128	0.127
12	0.143	0.140	0.143	0.142
14	0.151	0.149	0.151	0.150

10 %(w/v) Coal loading and 1500-2000μm particle size fraction

Time	Absorbance(450nm)			
Days	Sample 1	Sample2	Sample3	Average
0	0.094	0.094	0.092	0.093
2	0.123	0.120	0.123	0.122
4	0.138	0.138	0.138	0.138
6	0.126	0.126	0.124	0.125
8	0.141	0.142	0.142	0.142
10	0.130	0.132	0.132	0.131
12	0.136	0.137	0.137	0.136
14	0.134	0.134	0.134	0.134

Control: 5 %(w/v) Coal loading and 600-850μm particle size fraction in distilled water

Time	Absorbance(450nm)			
Days	**Sample 1**	**Sample2**	**Sample3**	**Average**
0	0.084	0.084	0.084	0.084
2	0.126	0.125	0.126	0.126
4	0.096	0.096	0.096	0.096
6	0.106	0.106	0.106	0.106
8	0.130	0.130	0.130	0.130
10	0.073	0.073	0.073	0.073
12	0.084	0.084	0.084	0.084
14	0.079	0.079	0.079	0.079

Control: Fungal culture without coal

Time	Absorbance(450nm)			
Days	**Sample 1**	**Sample2**	**Sample3**	**Average**
0	0.088	0.088	0.088	0.088
2	0.124	0.124	0.124	0.124
4	0.121	0.121	0.121	0.121
6	0.109	0.109	0.109	0.109
8	0.137	0.137	0.137	0.137
10	0.120	0.120	0.120	0.120
12	0.128	0.128	0.128	0.128
14	0.144	0.144	0.144	0.144

Control: Growth medium only

Time	Absorbance(450nm)			
Days	**Sample 1**	**Sample2**	**Sample3**	**Average**
Days	Sample 1	Sample2	Sample3	Average
0	0.083	0.083	0.083	0.083
2	0.088	0.088	0.088	0.088
4	0.082	0.082	0.082	0.082
6	0.085	0.085	0.085	0.085
8	0.085	0.085	0.085	0.085
10	0.085	0.085	0.085	0.085
12	0.085	0.085	0.085	0.085
14	0.085	0.085	0.085	0.085

APPENDIX D3: PHENOLIC CONCENTRATION

5 %(w/v) Coal loading and 600-850μm particle size fraction

Time	Phenolic concentration (mg l^{-1})			
Days	**Sample 1**	**Sample 2**	**Sample 3**	**Average**
0	90.72	90.70	90.73	90.72
2	90.72	89.18	90.17	90.02
4	80.72	80.73	80.73	80.73
6	83.45	83.46	83.46	83.46
8	90.73	90.73	90.73	90.73
10	84.36	84.37	84.33	84.35
12	82.55	82.55	82.55	82.55
14	86.18	86.18	86.18	86.18

10 %(w/v) Coal loading and 600-850μm particle size fraction

Time	Phenolic concentration (mg l^{-1})			
Days	**Sample 1**	**Sample 2**	**Sample 3**	**Average**
0	90.72	90.70	90.73	90.72
2	97.09	97.10	97.15	97.12
4	82.55	82.55	82.55	82.55
6	85.27	83.37	85.27	85.27
8	79.82	79.83	79.82	79.82
10	78.91	78.91	78.91	78.91
12	77.75	77.09	77.25	77.36
14	79.81	79.88	79.82	79.84

5 %(w/v) Coal loading and 1500-2000μm particle size fraction

Time	Phenolic concentration (mg l^{-1})			
Days	**Sample 1**	**Sample 2**	**Sample 3**	**Average**
0	89.50	88.55	89.00	89.35
2	93.54	93.45	93.45	93.48
4	85.30	85.30	85.30	85.30
6	82.55	82.55	82.55	82.55
8	81.63	81.15	80.25	81.01
10	90.12	90.27	90.27	90.22
12	78.00	78.00	78.00	78.00
14	79.00	78.90	78.90	78.93

10 %(w/v) Coal loading and 1500-2000 µm particle size fraction

Time	Phenolic concentration (mg l^{-1})			
Days	**Sample 1**	**Sample 2**	**Sample 3**	**Average**
0	90.00	90.00	90.00	90.00
2	91.64	91.25	90.25	91.05
4	85.23	85.27	86.30	85.6
6	82.55	82.55	82.55	82.55
8	86.20	86.68	86.18	86.35
10	81.64	81.64	81.65	81.64
12	81.65	81.56	82.67	81.96
14	75.30	75.20	75.27	75.26

Control: 5 %(w/v) Coal loading and 600-850 µm particle size fraction in distilled water

Time	Phenolic concentration (mg l^{-1})			
Days	**Sample 1**	**Sample 2**	**Sample 3**	**Average**
0	59.00	58.00	59.00	58.33
2	58.00	58.00	58.00	58.00
4	54.00	55.00	57.00	55.33
6	68.90	68.00	68.00	68.30
8	65.27	65.50	65.00	65.26
10	58.90	58.20	58.30	58.45
12	56.18	58.35	58.00	58.17
14	62.54	62.30	62.50	62.45

Control: Fungal culture without coal

Time	Phenolic concentration (mg l^{-1})			
Days	**Sample 1**	**Sample 2**	**Sample 3**	**Average**
0	78.60	78.60	78.60	78.60
2	78.60	78.60	78.60	78.60
4	78.60	78.60	78.60	78.60
6	78.60	78.60	78.60	78.60
8	78.60	78.60	78.60	78.60
10	78.60	78.60	78.60	78.60
12	78.60	78.60	78.60	78.60
14	78.60	78.60	78.60	78.60

APPENDIX D4: pH

5 %(w/v) Coal loading and 600-850µm particle size fraction

Time	pH			
Days	**Sample 1**	**Sample 2**	**Sample 3**	**Average**
0	3.89	3.85	3.88	3.87
2	4.43	4.45	4.45	4.44
4	5.48	5.48	5.50	5.49
6	6.95	6.96	6.96	6.96
8	7.12	7.11	7.11	7.11
10	7.11	7.11	7.11	7.11
12	7.03	7.03	7.03	7.03
14	7.03	7.03	7.03	7.03

10 %(w/v) Coal loading and 600-850µm particle size fraction

Time	pH			
Days	**Sample 1**	**Sample 2**	**Sample 3**	**Average**
0	3.98	3.99	3.99	3.99
2	4.78	4.80	4.78	4.79
4	5.57	5.57	5.57	5.57
6	5.79	5.80	5.80	5.80
8	7.23	7.25	7.23	7.24
10	7.32	7.32	7.32	7.32
12	7.34	7.34	7.34	7.34
14	7.22	7.22	7.22	7.22

5 %(w/v) Coal loading and 1500-2000µm particle size fraction

Time	pH			
Days	**Sample 1**	**Sample 2**	**Sample 3**	**Average**
0	3.52	3.50	3.50	3.51
2	4.19	4.19	4.19	4.19
4	4.72	4.72	4.72	4.72
6	5.25	5.23	5.20	5.23
8	6.17	6.17	6.17	6.17
10	7.02	7.02	7.02	7.02
12	7.00	7.00	7.02	7.01
14	6.95	6.93	6.93	6.94

10 %(w/v) Coal loading and 1500-2000µm particle size fraction

Time	pH			
Days	**Sample 1**	**Sample 2**	**Sample 3**	**Average**
0	3.64	3.65	3.65	3.65
2	4.15	4.16	4.17	4.16
4	5.10	5.06	5.10	5.09
6	5.40	5.45	5.40	5.42
8	6.85	6.85	6.85	6.85
10	6.97	6.97	6.97	6.97
12	7.04	7.04	7.04	7.04
14	6.97	6.97	6.97	6.97

Control: 5 %(w/v) Coal loading and 600-850µm particle size fraction in distilled water

Time	pH			
Days	**Sample 1**	**Sample 2**	**Sample 3**	**Average**
0	3.46	3.50	3.46	3.47
2	3.60	3.60	3.60	3.60
4	4.10	4.00	4.10	4.07
6	5.52	5.52	5.52	5.52
8	7.58	7.60	7.60	7.59
10	7.90	7.88	7.88	7.89
12	7.90	7.90	7.90	7.90
14	7.19	7.19	7.19	7.19

Control: Fungal culture without coal

Time	pH			
Days	**Sample 1**	**Sample 2**	**Sample 3**	**Average**
0	2.93	2.93	2.93	2.93
2	2.96	2.96	2.96	2.96
4	2.58	2.58	2.58	2.58
6	3.99	3.95	3.95	3.96
8	4.54	4.55	4.55	4.55
10	5.75	5.70	5.70	5.72
12	5.50	5.50	5.50	5.50
14	5.88	5.88	5.88	5.88

APPENDIX D5: TOC

5 %(w/v) Coal loading and 600-850 µm particle size fraction

Time	TOC (mg l^{-1})			
Days	**Sample 1**	**Sample 2**	**Sample 3**	**Average**
0	250	247	249	249
2	602	600	595	599
4	292	289	286	289
6	280	285	290	285
8	266	270	276	271
10	276	279	270	275
12	308	307	312	309
14	315	312	322	316

10 %(w/v) Coal loading and 600-850 µm particle size fraction

Time	TOC (mg l^{-1})			
Days	**Sample 1**	**Sample 2**	**Sample 3**	**Average**
0	250	250	248	249
2	1004	995	1005	1001
4	300	295	296	297
6	296	299	300	299
8	304	306	300	304
10	206	200	210	205
12	286	300	285	290
14	244	250	240	245

5 %(w/v) Coal loading and 1500-2000 µm particle size fraction

Time	TOC (mg l^{-1})			
Days	**Sample 1**	**Sample 2**	**Sample 3**	**Average**
0	250	243	253	249
2	1000	1005	995	1000
4	240	240	245	243
6	234	240	241	240
8	248	244	240	244
10	344	348	344	345
12	224	221	216	220
14	312	320	320	317

10 %(w/v) Coal loading and 1500-2000 µm particle size fraction

Time	TOC (mg l^{-1})			
Days	**Sample 1**	**Sample 2**	**Sample 3**	**Average**
0	250	251	259	253
2	330	330	335	332
4	250	250	250	250
6	286	282	288	285
8	264	260	265	263
10	268	268	269	268
12	290	295	290	292
14	240	240	240	240

Control: 5 %(w/v) Coal loading and 600-850µm particle size fraction in distilled water

Time	TOC (mg l^{-1})			
Days	**Sample 1**	**Sample 2**	**Sample 3**	**Average**
0	56	58	55	56
2	60	63	62	62
4	96	99	99	98
6	68	66	69	68
8	94	95	95	95
10	30	30	30	30
12	36	37	39	37
14	26	27	26	26

Control: Fungal culture without coal

Time	TOC (mg l^{-1})			
Days	**Sample 1**	**Sample 2**	**Sample 3**	**Average**
0	250	250	250	250
2	306	310	306	307
4	228	230	230	229
6	238	241	238	239
8	216	216	216	216
10	208	208	208	208
12	220	222	220	221
14	222	222	222	222

Control: Coal in sterile medium

	TOC (mg l^{-1})			
Days	**Sample 1**	**Sample 2**	**Sample 3**	**Average**
0	1700	1700	1700	1700
2	1570	1570	1570	1570
4	1540	1550	1540	1543
6	1675	1675	1675	1675
8	1672	1670	1670	1671
10	1670	1670	1670	1670
12	1674	1670	1674	1673
14	1671	1671	1671	1671

Control: Growth medium

	TOC (mg l^{-1})			
Days	**Sample 1**	**Sample 2**	**Sample 3**	**Average**
0	1850	1850	1850	1850
2	1760	1760	1760	1760
4	1845	1845	1845	1845
6	1710	1715	1715	1715
8	1725	1720	1725	1725
10	1725	1725	1725	1725
12	1725	1725	1725	1725
14	1714	1714	1714	1714

APPENDIX D6: TOTAL DISSOLVED SOLIDS

5 %(w/v) Coal loading and 600-850µm particle size fraction

	TDSS (mg l^{-1})			
Days	**Sample 1**	**Sample 2**	**Sample 3**	**Average**
0	8.5	8.8	9.2	8.8
2	10.3	11.0	10.7	10.7
4	11.8	12.5	11.2	11.8
6	13.2	12.8	13.7	13.2
8	12.9	12.2	11.4	12.2
10	10.2	10.7	11.4	10.8
12	11.9	11.4	10.8	11.4
14	12.9	12.5	11.8	12.4

5 %(w/v) Coal loading and 600-850 μm particle size fraction

	TDSS (mg l^{-1})			
Days	**Sample 1**	**Sample 2**	**Sample 3**	**Average**
0	8.5	9.0	8.0	8.5
2	9.8	9.9	10.3	10.0
4	11.9	12.5	10.7	11.7
6	13.6	12.6	13.0	13.1
8	12.9	12.7	12.4	12.7
10	11.2	10.6	11.7	11.2
12	10.9	10.1	11.5	11.8
14	13.5	13.7	13.8	13.7

5 %(w/v) Coal loading and 1500-2000 μm particle size fraction

	TDSS (mg l^{-1})			
Days	**Sample 1**	**Sample 2**	**Sample 3**	**Average**
0	8.5	8.8	8.6	8.6
2	10.2	9.9	10.7	10.3
4	10.9	11.0	10.5	10.8
6	14.6	14.0	15.3	14.6
8	13.9	14.7	12.9	13.8
10	11.9	12.7	11.4	12.0
12	12.6	12.9	12.7	12.7
14	13.4	12.9	13.9	13.4

10 %(w/v) Coal loading and 1500-2000 μm particle size fraction

	TDSS (mg l^{-1})			
Days	**Sample 1**	**Sample 2**	**Sample 3**	**Average**
0	8.5	8.7	8.4	8.5
2	12.7	12.0	13.0	12.6
4	11.1	11.9	10.7	11.2
6	13.2	13.5	14.0	13.6
8	12.6	12.9	12.5	12.7
10	10.6	11.0	10.2	10.6
12	10.2	10.6	10.3	10.4
14	9.7	9.9	9.5	9.7

Control: 5 %(w/v) Coal loading and 600-850 μm particle size fraction in distilled water

	TDSS (mg l^{-1})			
Days	**Sample 1**	**Sample 2**	**Sample 3**	**Average**
0	0.2	0.2	0.2	0.2
2	1.2	1.2	1.2	1.2
4	0.8	0.8	0.8	0.8
6	3.2	3.4	3.2	3.3
8	0.0	0.0	0.0	0.0
10	0.0	0.0	0.0	0.0
12	0.0	0.0	0.0	0.0
14	0.0	0.0	0.0	0.0

Control: Fungal culture without coal

	TDSS (mg l^{-1})			
Days	**Sample 1**	**Sample 2**	**Sample 3**	**Average**
0	8.5	8.5	8.7	8.6
2	9.5	9.5	9.2	9.4
4	9.3	9.4	9.3	9.3
6	10.0	10.8	9.5	10.1
8	9.7	9.0	9.0	9.2
10	12.7	12.5	12.7	12.7
12	5.2	5.2	5.6	5.3
14	10.9	11.4	10.9	11.3

APPENDIX E: ESTIMATION OF MASS TRANSFER COEFFICIENT FOR THE STIRRED TANK REACTOR

$$k_L a = k\, u_s^{\alpha} \left(\frac{P_g}{V}\right)^{\beta}$$

The values of k, α *and* β used are 0.02, 0.4 and 0.475.

P (Ungassed power) is 0.42 W. The ungassed power was calculated from Equation 6.1 in Section 6.2.1.5.

Gassed power (P_g) was estimated from the relationship between P_g/P and the aeration number Na (Q/NDi^3) in Figure 8.9 in Bailey and Ollis (1986). The aeration number was 6.2×10^2 and the ratio of gassed power to ungassed power read from the graph was 0.5. The gassed power is 0.21W equating to 215 W/m^3 and the calculation is shown below

$P_g = 0.5 * 0.42 = 0.21W$

$$u_s = \frac{Q}{A} =$$

$0.350\ d\ m^3$	4	1 min
$min\ 1000\ dm^3$	$3.14 * 0.1^2\ m^2$	60 s

$= 0.0007430\ m\ s^{-1}$

The $k_L a$ is

0.02	$0.0007430^{0.4}$ m	$215^{0.475}$
	s	

$$k_L a = 0.02 * 0.0007430^{0.4} (0.21)^{0.475}$$

$= 0.0144\ s^{-1}$

The maximum oxygen transfer rate (OTR_{max}) is 0.101 mg l^{-1} s^{-1}. This is shown below:

$OTR_{max} = K_L a ** C_{sat} = 0.0144\ s^{-1} * 7\ mg\ l^{-1}$

where $K_L a$ is $0.0144\ s^{-1}$ and C_{sat} is $7\ mg\ l^{-1}$.

APPENDIX F: VISCOSITY MEASUREMENT OF THE COAL–WATER-FUNGAL SYSTEM.

The apparent viscosity of the system was measured by using the Z1-DIN viscometer of PHYSICA RHEOLAB MC1 at 25^0C. The viscometer uses coaxial cylinders to determine the shear stress and viscosity as the shear rate changes. The system used in this study is the DIN 54453 rotor system. This sensor consists of a cup and a rotor with an annulus spacing of 0.50 mm. The shear stress is recorded at each shear rate and the apparent viscosity calculated. The range of shear rate used was between 178 to 500 s^{-1}. To prevent settling, the data was collected within 120 seconds. Data are presented in Table F1 and illustrate that viscosity does not change as a function of shear rate, illustrating its Newtonian behaviour.

Table F1: Viscosity measurement of coal–water-fungal system.

Measurement Points	Shear Rate (S^{-1})	Shear Stress (Pa)	Viscosity (mPa s)	Speed (min^{-1})	Torque (μNm)
1	178	0.20	1.15	35.8	168
2	193	0.23	1.19	38.8	188
3	209	0.26	1.24	42.0	213
4	226	0.29	1.29	45.4	239
5	245	0.32	1.30	49.2	261
6	265	0.34	1.28	53.3	278
7	287	0.36	1.27	57.7	299
8	311	0.39	1.26	62.4	322
9	336	0.42	1.26	67.6	348
10	364	0.46	1.25	73.2	375
11	394	0.50	1.25	79.2	406
12	420	0.54	1.27	84.5	440
13	462	0.57	1.24	92.9	470
14	500	0.62	1.24	101	511

APPENDIX G: ESTIMATION OF MINIMUM FLUIDISATION IN FLUIDISED BED BIOREACTOR

$$U_{mf} = \frac{d^2 p}{150\mu}(\rho_s - \rho)g\frac{\varepsilon^3{}_{mf}\Phi^2 s}{1-\varepsilon_{mf}}$$

d_p = average particle diameter, is 212μm and 848μm

ρ_s= particle density of fluidising solids is 1.0 g/cm^3

ρ = density of fluidising medium, air, is 0.0012 g/cm^3

μ = viscosity of fluidising medium is 0.0013 g/cm s

g = acceleration of gravity is 980 cm/s^2

ε_{mf}= minimum fluidised bed voidage is 0.55

Φ_s =shape factor 0.63 (Source: Kunni and Levenspeil, 1977 Shape factor for bituminous coal).

For d_p 212μm = U_{mf} = 0.37 cms^{-1}

848μm = U_{mf} = 1.9 cms^{-1}

APPENDIX H: SAMPLE CALCULATION FOR PROCESS YIELD

Theoretical yield calculated on a mass basis

Stoichiometric ratios were taken from Equation 5.3

$Y_{X/Coal}$ =

0.38 mol biomass	24.6g biomass	mol coal
mol coal	mol biomass	16.92 g coal

=0.55 g biomass g coal $^{-1}$

$Y_{X/O2}$=

0.38 mol biomass	24.6g biomass	mol O_2
0.55mol O_2	mol biomass	32 g O_2

=0.53 g biomass g O_2^{-1}

$Y_{X/NH3}$=

0.38 mol biomass	24.6g biomass	mol NH_3
0.056 mol NH_3	mol biomass	17 g NH_3

=9.82 g biomass g NH_3^{-1}

$Y_{X/CO2}$=

0.38 mol biomass	24.6g biomass	mol CO_2
0.50 mol CO_2	mol biomass	44 g CO_2

=0.42 g biomass g CO_2^{-1}

0.21 mol propionic acid	24.56 propionic acid	mol coal
mol coal	mol propionic acid	16.92 g coal

= 0.31 g Propionic acid g coal $^{-1}$

For Phenolics, the stoichiometric ratio was taken from the equation below

Coal ⟶ biomass and propionic acid

$$CH_{0.8}O_{0.22}N_{0.02}S_{0.01} + 0.42\ O_2 + 0.028\ NH_3 \rightarrow$$
$$0.02\ H^+ + 0.036\ H_2O + 0.40\ CO_2 + 0.24\ CH_{1.8}O_{0.5}N_{0.2} + 0.01\ SO_4^{2-} + 0.06 C_6H_5OH$$

$Y_{phenol/coal=}$ =

0.06 mol phenolic	94 phenolic	mol coal
mol coal	mol phenol	16.92 g coal

=0.33 g Phenolic g coal $^{-1}$

Experimentally Yield

Average biomass estimated was (2.3+ 2.1)/2 = 2.2 g l^{-1} (Reported in Section 5.3.3)

Cumulative amount of O_2 used =

4 mmol O_2	32g O_2	24h*14
l .h	1000mmol O_2	

=43g/l

Cumulative amount of CO_2 used =

0.05mmol CO_2	44g CO_2	24h*14
l .h	1000mol CO_2	

= 0.74 g /l

Propionic acid produced =176 mg l^{-1} (From Table 5.4)

Concentration of phenolic accumulated =18 mg l^{-1} (From Figure 5.6)

Mass of coal solubilised = 12 g l^{-1} (From Table 5.5)

$Y_{X/Coal}$ =

$$\frac{\text{2.2 g biomass}}{\text{12 g coal}}$$

= 0.18 g biomass g $coal^{-1}$

$Y_{X/O2}$=

$$\frac{\text{2.2 g biomass}}{\text{43 g } O_2}$$

=0.05 g biomass g O_2^{-1}

$Y_{X/CO2}$=

$$\frac{\text{2.2 g biomass}}{\text{0.74 g } CO_2}$$

=3.0 g biomass g CO_2^{-1}

$Y_{propionic\ acid/coal}$ =

$$\frac{\text{0.176 g propionic acid}}{\text{12 g coal}}$$

= 0.02g propionic acid g $coal^{-1}$

$Y_{phenol/coal=}$ =

$$\frac{\text{0.018 g phenolic}}{\text{12 g coal}}$$

=0.002g phenolic g $coal^{-1}$

APPENDIX I: SAMPLE CALCULATION FOR EXPERIMENTAL YIELD COEFFICIENTS FOR GROWTH ON GLUCOSE

The biomass yield coefficients for the growth phase, stationary phase as well as the overall biomass yield coefficient were calculated from the quotient of the biomass formed by the product of the average instantaneous oxygen consumption rate or carbon dioxide production rate and time i.e.

$$Y_{X/O_2} = \frac{biomass\ formed}{average\ instantaneous\ OUR/CPR * time}$$

OXYGEN

Overall biomass yield coefficient (0-110h), based on oxygen consumption (average instantaneous)

Change in biomass = 5.42 g (From Figure 5.1)

Average oxygen consumption rate = 3 mmol/h (From the Table JI on page167)

Average oxygen consumption = average O_2 consumption rate * time of consumption

$$\frac{3\ mmol}{h} \mid 110h \mid \frac{32g\ O_2}{1000mmol}$$

$=10.56\ g\ O_2$

$$\text{Overall biomass yield coefficient} = \frac{biomass\ formed}{O_2\ consumption} = 5.42/10.56$$

$= 0.51\ g\ biomass\ g\ O_2^{-1}$

Biomass yield coefficient for growth phase (0-72h), based on oxygen consumption (average instantaneous)

Change in biomass = 5.6 g (From Figure 5.1)

Average oxygen consumption

$$\frac{3\ mmol}{h} \mid 72h \mid \frac{32g\ O_2}{1000mmol}$$

$=6.9\ g\ O_2$ (From the Table JI on page167)

Growth yield coefficient = $\frac{biomass\ formed}{O_2\ consumption}$ = 5.6/6.9

= 0.81 g biomass g O_2^{1}

CARBON DIOXIDE

Overall biomass yield coefficient (0-110 h), based on carbon dioxide production (average instantaneous)

Change in biomass = 5.42 g (From Figure 5.1)

Average carbon dioxide consumption =

$$\frac{3.1\ mmol}{h} \left| \begin{matrix} 110h \\ \end{matrix} \right. \frac{44g\ O_2}{1000mmol}$$

=15.01 g CO_2 (From the Table J2 on page167)

Overall biomass yield coefficient= $\frac{biomass\ formed}{CO_2\ production}$ =5.42/15.01

= 0.36 g biomass g CO_2^{-1}

Biomass yield coefficient for growth phase (0-72h), based on oxygen consumption (average instantaneous)

Change in biomass = 5.6g (From Figure 5.1)

Average carbon dioxide consumption=

$$\frac{3.1\ mmol}{h} \left| \begin{matrix} 72h \\ \end{matrix} \right. \frac{44g\ O_2}{1000mmol}$$

=9.82g CO_2 (From the Table J2 on page167)

Growth yield coefficient= $\frac{biomass\ formed}{CO_2\ production}$ = 5.6/9.82 = 0.57 g biomass g CO_2^{-1}

APPENDIX J: RAW DATA FOR OXYGEN UTILISATION AND CO_2 PRODUCTION ON FUNGAL GROWTH ON GLUCOSE IN THE STR

Table J1: Raw data for oxygen utilisation on fungal growth on glucose in the stirred tank slurry bioreactor.

Time(Hours)	Glucose (g/l)	O_2 measured(mmol/h)	Biomass measured (g/l)
0	10	3	0.2
24	5.3	3	1.5
48	1.9	3	3.8
72	0.53	3	5.6
96	0.33	3	5.6
110	0.12	3	5.4

Table J2: Raw data for CO_2 production on fungal growth on glucose in the stirred tank slurry bioreactor

Time(Hours)	Glucose (g/l)	CO_2 measured(mmol/h)	Biomass measured (g/l)
0	10	4	0.2
24	5.3	4	1.5
48	1.9	1.5	3.8
72	0.53	3	5.6
96	0.33	3	5.6
110	0.12	3	5.4